

ISTANBUL TECHNICAL UNIVERSITY ★ INFORMATICS INSTITUTE

**CIRCULARLY POLARIZED ARRAY ANTENNA DESIGN WITH EMPHASIS
TO ENHANCE THE ANTENNA PERFORMANCE
FOR C-BAND APPLICATIONS**

Ph.D. THESIS

Saeid KARAMZADEH

Department of Communication Systems

Satellite Communication and Remote Sensing Programme

DECEMBER 2015

ISTANBUL TECHNICAL UNIVERSITY ★ INFORMATICS INSTITUTE

**CIRCULARLY POLARIZED ARRAY ANTENNA DESIGN WITH EMPHASIS
TO ENHANCE THE ANTENNA PERFORMANCE
FOR C-BAND APPLICATIONS**

Ph.D. THESIS

**Saeid KARAMZADEH
(705142002)**

Department of Communication Systems

Satellite Communication and Remote Sensing Programme

Thesis Advisor: Assoc. Prof. Dr. Mesut KARTAL

DECEMBER 2015

İSTANBUL TEKNİK ÜNİVERSİTESİ ★ BİLİŞİM ENSTİTÜSÜ

**C-BANDI UYGULAMALARI İÇİN ANTEN PERFORMANSINI GELİŞTİREN
DAİRESEL POLARİZASYONLU DİZİ ANTEN TASARIMI**

DOKTORA TEZİ

**Saeid KARAMZADEH
(705142002)**

İletişim Sistemleri Anabilim Dalı

Uydu Haberleşmesi ve Uzaktan Algılama Programı

Tez Danışmanı: Doç. Dr. Mesut KARTAL

ARALIK 2015

Saeid Karamzadeh, a **Ph.D.** student of ITU Informatics Institute student ID 705142002, successfully defended the **thesis** entitled “**CIRCULARLY POLARIZED ARRAY ANTENNA DESIGN WITH EMPHASIS TO ENHANCE THE ANTENNA PERFORMANCE FOR C-BAND APPLICATIONS**”, which he prepared after fulfilling the requirements specified in the associated legislations, before the jury whose signatures are below.

Thesis Advisor : **Assoc. Prof. Dr. Mesut KARTAL**

İstanbul Technical University

Jury Members : **Prof. Dr. Sedef Kent PINAR**

İstanbul Technical University

Asisst. Prof. Dr. Hamid TORPİ

Yıldız Technical University

Assoc. Prof. Dr. Serkan ŞİMŞEK

İstanbul Technical University

Prof. Dr. Osman Nuri UÇAN

İstanbu Aydın University

Date of Submission : 30 November 2015

Date of Defense : 18 December 2015

FOREWORD

In an endeavor to successfully complete my thesis, I received assistance from many people and I take this opportunity to thank those who have helped me along the way to achieve this success.

I am grateful to my research advisor, Assoc. Prof. Dr. Mesut Kartal for his guidance and continuous support throughout my thesis. His patience and knowledge have been invaluable throughout my research and I express my deep sense of gratitude to him.

I am indebted to my parents for always encouraging me and standing by my side. I would like to special thanks to my spouse, dear Semra Kocaaslan Karamzadeh for encouraging and supporting me anytime and anywhere. Many thanks to my friend Vahid Rafii for any technical and mental support.

December 2015

Saeid KARAMZADEH

TABLE OF CONTENTS

	<u>Page</u>
FOREWORD	vii
TABLE OF CONTENTS	ix
ABBREVIATIONS	xii
LIST OF TABLES	xiv
LIST OF FIGURES	xvi
SUMMARY	xvii
ÖZET	xix
1. INTRODUCTION	1
1.1 Antenna Parameters	2
1.1.1 Input impedance	2
1.1.2 Reflection Coefficient, Return Loss and Voltage Standing Wave Ratio	3
1.1.3 Radiation Patterns	4
1.1.4 Directivity, Gain and Efficiency	5
1.1.5 Linear Polarization, Circular Polarization and Axial Ratio	5
1.1.6 Bandwidth and Resonant Frequency	8
1.1.7 Methods of design CP antenna	8
1.2 Broadband Circularly Polarized Antennas.....	10
1.2.1 Slot Loading	10
1.2.2 Broadband Coupler	11
1.2.3 Ring Slot with a Broadband Coupler	13
1.2.4 Circular/Square Slot with an L-Shaped Feed.....	14
1.2.5 Grounded Strip	16
1.3 Array Design	20
1.3.1 Sequential Rotation	20
1.3.2 Single-Feed Patch.....	21
1.3.4 Dual-Feed Patch	23
1.3.5 Multi-Band CP Patch Antenna Arrays	25
1.3.6 High-Efficiency CP Patch Arrays at the Ku Band and Above.....	27
1.3.7 CP Array with Reconfigurable Beams	31
1.3.8 Beam-Switching CP Array using Butler Matrix Network	32
2. PUBLISHED WORKS	37
2.1 Circularly Polarized Square Slot Antenna Using Crooked T-Shape Technique	37
2.1.1 Abstract	37
2.1.2 Introduction	37
2.1.3 Antenna configuration.....	39
2.1.4 Experimental results and discussion	39
2.1.5 Conclusion	45
2.2 Compact UWB CP Square Slot Antenna with Two Corner Connected by a Strip Line	47
2.2.1 Abstract	47

2.2.2 Introduction	47
2.2.3 Antenna design	48
2.2.4 Results and discussions	50
2.2.5 Conclusion.....	52
2.3 Circularly Polarized Slot Antenna Array with Sequentially Rotated Feed Network for Broadband Application	54
2.3.1 Abstract	54
2.3.2 Introduction	54
2.3.3 Single Element design	56
2.3.4 Feed Network design.....	58
2.3.5 Experimental results and discussion	60
2.3.6 Conclusion.....	64
2.4 Circularly Polarized Array Antenna with Cascade Feed Network for Broadband Application in C-Band	66
2.4.1 Abstract	66
2.4.2 Introduction	66
2.4.3 Antenna elements	67
2.4.4 Feed Network and CPSSAA configuration.....	67
2.4.5 Results and discussion.....	68
2.4.6 Conclusion.....	69
2.5 Circularly Polarized MIMO Tapered Slot Antenna Array for C-Band Application	71
2.5.1 Abstract	71
2.5.2 Introduction	71
2.5.3 Single element	72
2.5.4 Feed Network and MIMO array configuration	74
2.5.5 Result and discussion	74
2.5.6 Conclusion.....	76
2.6 Modified Circularly Polarized Beam Steering Array Antenna by Utilized Broadband Coupler and 4×4 Butler Matrix.....	77
2.6.1 Abstract	77
2.6.2 Introduction	77
2.6.3 Single element	79
2.6.4 Branch line coupler	81
2.6.7 Butler matrix feed network	83
2.6.8 Result and discussion	85
2.6.9 Conclusion.....	88
2.7 Circularly Polarized 1×4 Square Slot Array Antenna by Utilizing Compacted Modified Butler Matrix and Branch Line Coupler.....	90
2.7.1 Abstract	90
2.7.2 Introduction	90
2.7.3 Single element	92
2.7.4 Branch line coupler	95
2.7.5 Butler Matrix Feed Network	97
2.7.6 Result and discussion	99
2.7.7 Conclusion.....	101
3. CONCLUSIONS AND RECOMMENDATIONS.....	103
REFERENCES	105
CURRICULUM VITAE	109

ABBREVIATIONS

AR	: Axial Ratio
BW	: Band width
CP	: Circularly Polarized
CPSS	: Circularly Polarized Square Slot
CPW	: Co-Planer Waveguide
DSB	: Direct Broadcasting Service
GNSS	: Global Navigation Satellite Systems
LHCP	: Left-Hand Circular Polarization
LP	: Linear Polarize
RFID	: Radio Frequency Identification
RHCP	: Right-Hand Circular Polarization
UWB	: Ultra Wide Band
WiMAX	: Worldwide Interoperability for Microwave Access
WLAN	: Wireless Local Area Networks
WPAN	: Wireless Personal Area Networks

LIST OF TABLES

	<u>Page</u>
Table 1.1: Comparison Of The Radiation Performance Between Single Antenna Element And Its -----	23
Table 1.2: Meaning Of The Ports Shown In Figure 1.24 -----	32
Table 1.3: The Phase Of Output Signal When Different Ports Are Excited-----	33

LIST OF FIGURES

	<u>Page</u>
Figure 1.1: Basic operations of a transmit antenna -----	2
Figure 1.2: A directional radiation pattern in the elevation plane -----	4
Figure 1.3: Omni-directional pattern-----	5
Figure 1.4: Polarization ellipse traced at a certain position as a function of time ----	7
Figure 1.5: Dual-Feed CP square patch antenna -----	8
Figure 1.6: Singly fed CP circular patch antenna with a 90° hybrid-----	9
Figure 1.7: CP single feed square and circular patches -----	9
Figure 1.8: Geometry of a slot-loaded patch antenna -----	10
Figure 1.9: Geometry of the aperture-coupled CP patch antenna using a three-stub branch-line coupler -----	12
Figure 1.10: Geometry of the dual L-probe fed circular patch antenna -----	12
Figure 1.11: Geometry of the quadruple L-probe fed circular patch antenna-----	13
Figure 1.12: Geometry of a ring slot antenna with a hybrid coupler -----	14
Figure 1.13: Geometry of a microstrip-fed CP slot antenna-----	15
Figure 1.14: Simulated and measured return loss for the slot antenna-----	16
Figure 1.15: Simulated and measured AR for the slot antenna -----	16
Figure 1.16: Geometry of a CPW-fed CP slot antenna with a T-shaped strip protruding the ground -----	17
Figure 1.17: Geometry of a square slot antenna with a lightning-shaped feedline and inverted-L grounded strips -----	19
Figure 1.18: Configuration of the conventional CP patch antenna array using sequential rotated LP patch elements -----	21
Figure. 1.19: Geometry of the wideband stacked CP antenna array-----	22
Figure 1.20: Configuration of the dual-feed slot-coupling CP patch. The Figure in the left shows the detailed view of the patch with two feed lines and the Figure on the right presents the overall structure of this CP patch	24
Figure 1.21: The layout of the 2×2 sequentially rotated CP array -----	24
Figure 1.22: Side, top and back view of the dual band CP antenna array for RFID reader application -----	26
Figure 1.23: Measured and simulated S_{11} , axial ratio of the dual band CP antenna array for RFID reader application -----	26
Figure 1.24: Geometry of the single radiation element and configuration of the subarray -----	28
Figure 1.25: Configuration of the full array using the double sequential rotation technique -----	28
Figure 1.26: Measured S_{11} and AR bandwidth of the array using the double sequential rotation technique-----	29
Figure 1.27: The switch feed network for the switch-beam antenna array -----	30
Figure 1.28: Measured radiation patterns and AR bandwidth of the antenna array with different sets of excitation phase -----	31
Figure 1.29: Circuit model of the branchline coupler -----	32

CIRCULARLY POLARIZED ARRAY ANTENNA DESIGN WITH EMPHASIS TO ENHANCE THE ANTENNA PERFORMANCE FOR C-BAND APPLICATIONS

SUMMARY

The C band is a name given to certain portions of the electromagnetic spectrum, including wavelengths of microwaves that are used for long-distance radio telecommunications. The IEEE C-band (4 to 8 GHz) and its slight variations contain frequency ranges that are used for many satellite communications transmissions, some Wi-Fi devices, some cordless telephones, and some weather radar systems. For satellite communications, the microwave frequencies of the C-band perform better under adverse weather conditions in comparison with the Ku band (11.2 GHz to 14.5 GHz) microwave frequencies used by other communication satellites.

The increasing demands for more capacity and higher data rate in wireless systems have led to the development of broadband CP antennas. During recent decades, a variety of broadband CP antennas have been proposed for applications in mobile satellite communications, WLAN, DBS, RFID, GNSS, space communications and wireless power transmission systems.

The CP antenna is very effective in combating multi-path interferences or fading . The reflected radio signal from the ground or other objects will result in a reversal of polarization, that is, right-hand circular polarization (RHCP) reflections show left-hand circular polarization (LHCP). A RHCP antenna will have a rejection of a reflected signal which is LHCP, thus reducing the multi-path interferences from the reflected signals. The second advantage is that CP antenna is able to reduce the 'Faraday rotation' effect due to the ionosphere. The Faraday rotation effect causes a significant signal loss (about 3 dB or more) if linearly polarized signals are employed. The CP antenna is immune to this problem, thus the CP antenna is widely used for space telemetry applications of satellites, space probes and ballistic missiles to transmit or receive signals that have undergone Faraday rotation by travelling through the ionosphere.

Another advantage of using CP antennas is that no strict orientation between transmitting and receiving antennas is required. This is different from linearly polarized antennas which are subject to polarization mismatch losses if arbitrary polarization misalignment occurs between transmitting and receiving antennas. This is useful for mobile satellite communications where it is difficult to maintain a constant antenna orientation. With CP, the strength of the received signals is fairly constant regardless of the antenna orientation. These advantages make CP antennas very attractive for many wireless systems.

For a circularly polarized microstrip antenna, both axial ratio and impedance bandwidths need considerations. Use the array antenna is a recognized methods to increase axial ratio bandwidth and gain of circularly polarized antenna. for better result in increase the impedance bandwidth and decrease the array mutual coupling prepare feed network have to design too.

In this thesis, with attention to advantage of CP antenna and C-band application as mentioned above, will be tried to generate a CP array antenna by broadband feed network and antenna element. In order to achieve mentioned CP array antenna, three aspects will be considered. In first step (aspect 1), will be focused on feed network. For this purpose, will be employed broadband microwave components such as broadband power divider, broadband hybrid coupler and broadband phase shifter instead of equal narrowband component that hitherto, have been utilized. Use of broadband CP antenna element with high gain will be the second priority. To achieve broadband CP element, use of slot antenna and in order to attain high gain element, use of cavity back structure are recommended. In this case, the single element must be changed polarization diversity because the feed network will be able to change polarization diversity and for this purpose, polarization of element and feed network should be coordinated. In third step (aspect 3), method of location element in array such as distance between element, mutual coupling between them and feed network will be significant. Also, communicate between feeding in array feed network and antenna elements, in order to impedance matching and power transfer, have important role.

Thus, In order to achieve the above mentioned goals antennas were created as follows: a 3 dB axial-ratio of the CPSSA extends to approximately 2 GHz. The CPSSA was designed to operate over the frequency range between 3 and 11.1 GHz corresponding to an impedance bandwidth of 115% for $VSWR < 2$. Acceptable agreement between the simulation and measured results validates the proposed design (section 2.1). And then a compact size of $20 \times 20 \text{ mm}^2$ CPSSA in section 2.2 is reported. The measured impedance bandwidth is as large as 11050 MHz (2950–14000 MHz) or about 130.38% with respect to the center frequency. The measured 3-dB AR is 3373 MHz (35.7%) from 3729 to 7102 MHz and the average measured gain of CPSSA is almost 3.5 dBi in the operating band. In order to attain array antenna by broadband CP antenna elements in section 2.3 and 2.4 two type of antenna with novel methods in designing feed network are reported. In first case a array antenna which feed by sequentially rotated feed network is mentioned. the 3 dB axial-ratio bandwidth of the this array antenna extends to approximately 1.3 GHz and was designed to operate over the frequency range between 4.5 and 6.4 GHz corresponding to an impedance bandwidth of 34.86% for $VSWR < 2$ (section 2.3). in section 2.4 by modified feed network and array elements the characteristics of array was improved. The reported array consists of 2×2 CPSSA elements and is fed by a novel feeding network consisting of the circuit strip-line couplers and delay lines. The feeding technique is applied to the 2×2 antenna array to increasing the axial ratio (AR) bandwidth. The measured impedance bandwidth for $VSWR < 2$ is around 78.5% (3.4 – 7.8 GHz) and 3dB axial-ratio bandwidth is about 35.7% (4.6–6.6 GHz) and average 14.2 dBic gain over the 3 dB ARBW. In final, in order to investigate of broadband feeding network and elements on array antenna, two type of array with capable to change polarization and pattern diversity are reported (sections 2.5-2.7). for example in section 2.5, a array antenna by changing to polarization diversity by broadband vivaldi antenna is reported and in section 2.6, a beam steering array antenna composed of a broadband circularly polarized square slot antenna and a novel Butler matrix feed network designed with a broadband branch line coupler is introduced. The Results show that a compact and its improvements are discussed. In this work a broadband double box coupler with impedance bandwidth over 5 - 7.4 GHz frequency and the phase error less than 3 degree is employed. Also the measured impedance bandwidth of the proposed beam steering array antenna is 39% (from 4.7GHz to 7 GHz).

C-BANDI UYGULAMALARI İÇİN ANTEN PERFORMASINI GELİŞTİREN DAİRESEL POLARİZASYONLU DİZİ ANTEN TASARIMI

ÖZET

Günümüzde alıcı, verici sistemlerinde iletişimin kaliteli olması için anten tasarımı çok önem taşımaktadır. Antenin bir devrimi sayılan Mikroşerit antenler birçok özelliklere sahip oldukları için kablosuz haberleşme, radar ve uydu haberleşmesinde kullanım alanı bulmuştur. Kolay üretilebilmesi, boyut olarak az yer kaplaması bu özelliklerdendir. Bunların yanı sıra, dar bantlı olması ve yüksek kazançta sahip olmaması bu antenin dezavantajlarından. Bu sorunların çözümü olarak, dizi antenler önerilir. Dizi antenler tasarıma bağlı olarak, daha fazla bant genişliğine ve kazançta sahiptirler. Birden fazla antenin yan yana veya farklı kombinasyonlarla bir araya gelmesi birkaç yan etkiye de sebep olacaktır. Antenlerin birbiriyle etkileşimleri ve daha büyük boyuta sahip olmaları, dizilerin dezavantajlarıdır. Tasarım açısından, antenlerin dizilişinin yanısıra, besleme tipleri de önem taşımaktadır. Kaynaktan gelen gücü doğru paylaşmak ve istenilen zaman ve faz gecikmesini yaratmak besleme şebekesinin görevlerindedir. Dolayısıyla, iyi tasarlanmış besleme şebekesi dizi anteniyle birlikte iyi bir performans doğuracaktır. Dizi antenler yüksek kazançta sahip oldukları için, uydu haberleşmesi, DSB (Direct Broadcasting Service), WLAN (Wireless Local Area Networks) ve uzay haberleşmesi gibi birçok uygulamada kullanılmaktadır.

Uydu haberleşmesi, WLAN, DBS, GNSS (Global Navigation Satellite Systems), RFID (Radio Frequency Identification), WPAN (Wireless Personal Area Networks) GNSS, WiMAX (Worldwide Interoperability for Microwave Access) ve kablosuz haberleşme gibi uygulamalarda doğrusal polarizasyon yerine dairesel polarizasyonlu antenler tercih edilir. Bunun sebebi, dairesel polarizasyonunun sağladığı avantajlardır. Bu avantajların birkaç tanesi aşağıdaki gibidir. Alıcı ve verici antenler dairesel polarizasyonlu olduğu takdirde doğrusal polarizasyonlu antenler gibi ilk ayarlara ihtiyaç duymayacaktır. Dairesel polarizasyonlu anten kullanarak polarizasyon uyumsuzluk kayıpları da önlenmiş olur. Dairesel polarizasyonlu antenler kullanarak çok yönlü etkileşimler ve kayıplar da önlenir. Sağ dairesel polarizasyonlu işaret (Right-Hand Circular Polarization (RHCP)) vericiden gönderiliyorsa, ortamdan alıcıya doğru yansıyan işaret sol polarizasyonlu olduğu için (left-hand circular polarization (LHCP)) girişim önlenecektir. Ayrıca uydu haberleşmesinde karşılaştığımız Faraday rotasyonu kaybını da giderme kabiliyetine sahiptir.

Uydu haberleşmesi, mikrodalga radyo haberleşmesi ve radar gibi uygulamalar C bandında çalışmaları için tasarlamak istediğimiz antenin C bandında olması planlanmaktadır. C bandı IEEE tarafından 4 GHz'den den 8 GHz aralığına kadar tanımlanmıştır. Bu bantta çalışmanın avantajları, birçok alana uygun olmasıdır. Örneğin hava tahmini uydularında Ku bandı yerine C bandı kullandığımız da yağmur zayıflaması (Rain Fade) denilen kayıpları oldukça azaltabiliriz.

Bu çalışmada C bandı için uygun dairesel polarizasyonlu dizi antenler tasarlanıp performansını artırmak için yöntemler sunulacaktır. Tasarım esnasında ilk olarak, dizi

antenin bant genişliği ve kazancı üzerinde çalışılacaktır. Bunun için önce dairesel anten elemanının tasarım metotları tartışılıp performansı artırılacaktır. Uygun bir anten tasarlandıktan sonra, antenin dizilişi ve besleme şebekesi üzerinde çalışılıp Butler matrisi gibi yeni besleme şebekeleri sunulacaktır.

Bu amaçlara ulaşma yolunda, izlenilecek adımlar aşağıdaki gibidir. CPSSA tasarımının 3 dB axial-ratio, 2 GHz e kadar yükseltilmiştir. CPSSA 3 le 11.1 GHz aralığında çalışacak şekilde tasarlanıp empedans bant genişliği 115 % e ulaşmıştır. Simülasyon ve gerçek model sonuçları yeterince uyumlu olduğu tespit edilmiştir (2.1 bölüm). 2.2. bölümdeyse, anten elemanının boyutu 20×20 mm² olarak tasarlanmıştır. Bu anten için ölçülen empedans bant genişliği 11050 MHz (2950–14000 MHz) 3-dB AR içse 3373 MHz (35.7%) 3729 den 7102 MHz ve ortalama kazanç 3.5 dBi elde edilmiştir. 2.3 ve 2.4 bölümlerinde dizi antenler için yeni besleme şebekeleri tasarlanmıştır. 2.3 de olan dizi antenin 3 dB axial-ratio bant genişliği 1.3 GHz e ulaşmıştır. 2.4 te ise, dizi antenin besleme şebekesi geliştirilmiştir. 2×2 dizi antenin empedans bant genişliği 78.5% ve 3dB axial-ratio bant genişliği 35.7% e ulaşmıştır. Ortalama 14.2 dBic kazanç sağlanmıştır. Son bölümlerde (2.5 – 2.7) geniş bantlı performans almak üzere, iki yeni dizi anten tasarlanmıştır. Bu yapılar, polarizasyon çevirme özelliklerine de sahiptir. 2.5 de bu özellik bir Vivaldi anteni kullanarak sağlanmıştır. 2.6. bölümle özgün Butler matrisiyle dizi anten tasarlanmıştır. Çalışmaların tüm detayları ve sonuçları sunulacaktır.

1. INTRODUCTION

Circularly polarized (CP) antennas are a type of antenna with circular polarization. Due to the features of circular polarization, CP antennas have several important advantages compared to antennas using linear polarizations, and are becoming a key technology for various wireless systems including satellite communications, mobile communications, global navigation satellite systems (GNSS), wireless sensors, radio frequency identification (RFID), wireless power transmission, wireless local area networks (WLAN), wireless personal area networks (WPAN), Worldwide Interoperability for Microwave Access (WiMAX) and Direct Broadcasting Service (DBS) television reception systems. Lots of progress in research and development have been made during recent years. The CP antenna is very effective in combating multi-path interferences or fading [1, 2]. The reflected radio signal from the ground or other objects will result in a reversal of polarization, that is, right-hand circular polarization (RHCP) reflections show left-hand circular polarization (LHCP). A RHCP antenna will have a rejection of a reflected signal which is LHCP, thus reducing the multi-path interferences from the reflected signals. The second advantage is that CP antenna is able to reduce the 'Faraday rotation' effect due to the ionosphere [3, 4]. The Faraday rotation effect causes a significant signal loss (about 3 dB or more) if linearly polarized signals are employed. The CP antenna is immune to this problem, thus the CP antenna is widely used for space telemetry applications of satellites, space probes and ballistic missiles to transmit or receive signals that have undergone Faraday rotation by travelling through the ionosphere. Another advantage of using CP antennas is that no strict orientation between transmitting and receiving antennas is required. This is different from linearly polarized antennas, which are subject to polarization mismatch losses if arbitrary polarization misalignment occurs between transmitting and receiving antennas. This is useful for mobile satellite communications where it is difficult to maintain a constant antenna orientation. With CP, the strength of the received signals is constant regardless of the antenna orientation. These advantages make CP antennas very attractive for many wireless systems.

1.1 Antenna Parameters

An antenna is a device which can receive or/and transmit radio signals. As a receiving device, it can collect the radio signals from free space and convert them from electromagnetic waves (in the free space) into guided waves in transmission lines; as a transmitting device, it can transmit radio signals to free space by converting the guided waves in transmission lines into the electromagnetic waves in the free space. In some cases, an antenna can serve both functions of receive and transmit. Figure 1.1 depicts the basic operation of a transmit antenna. As shown, the information (voice, image or data) is processed in a radio transmitter and then the output signal from the transmitter propagates along the transmission lines before finally being radiated by the antenna. The antenna converts the guided-wave signals in the transmission lines into electromagnetic waves in the free space. The operation of a receive antenna follows a reverse process, that is, collecting the radio signals by converting the electromagnetic waves in free space into guided-wave signals in the transmission lines, which are then fed into radio receivers.

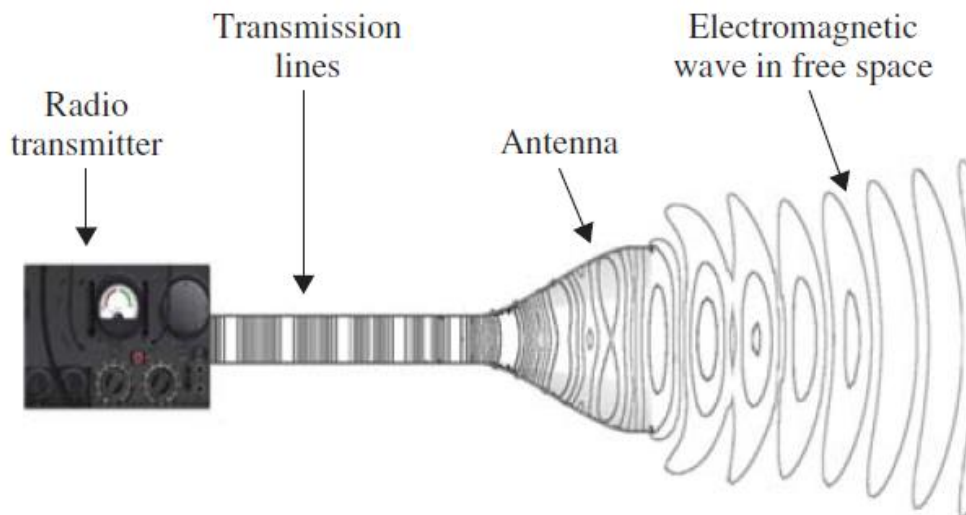


Figure 1.1: Basic operations of a transmit antenna.

1.1.1 Input impedance

The input impedance Z_{in} is defined as the impedance presented by an antenna at its feed point, or the ratio of the voltage to current at the feed point [5]. The input impedance is usually a complex number which is also frequency dependent. It can be expressed as:

$$Z_{in} = R_{in} + jX_{in} \quad (1.1)$$

The real part of the impedance, R_{in} , includes the radiation resistance R_r of the antenna and the loss resistance R_L . R_r relates to the power radiated by the antenna, and R_L relates to the power dissipated in the antenna due to losses in dielectric materials, antenna conductor losses, and so on.

1.1.2 Reflection Coefficient, Return Loss and Voltage Standing Wave Ratio

The antenna input impedance needs to be matched with the characteristic impedance of the transmission line connected to the feed point of the antenna. Usually a 50 Ω cable is used to feed the antenna. Thus the antenna input impedance needs to be equal to 50 Ω , otherwise there will be an impedance mismatch at the antenna feed point. In the case of impedance mismatch, there will be signal reflections, that is, some of signals fed to the antenna will be reflected back to the signal sources.

The reflection coefficient Γ denotes the ratio of the reflected wave voltage to the incident wave voltage [5]. The reflection coefficient at the feed point of the antenna can be related to the antenna input impedance by the following equation:

$$\Gamma = \frac{Z_{in} - Z_0}{Z_{in} + Z_0} \quad (1.2)$$

Here, Z_{in} and Z_0 denote the input impedance of the antenna, and the characteristic impedance of the transmission line connected to the antenna feed point, respectively. As shown in equation (1.2), the reflection coefficient is zero if Z_{in} is equal to Z_0 .

Return loss (in dB) is defined as:

$$RL = -20 \log |\Gamma| \quad (1.3)$$

For a well-designed antenna, the required return loss should usually be at least 10 dB, though some antennas on small mobile terminals can only achieve about 6 dB. Voltage Standing Wave Ratio (VSWR) is the ratio of the maximum voltage V_{max} to the minimum voltage V_{min} on the transmission line. It is defined as:

$$VSWR = \frac{|V_{max}|}{|V_{min}|} = \frac{1 + \Gamma}{1 - \Gamma} \quad (1.4)$$

1.1.3 Radiation Patterns

The radiation pattern of the antenna illustrates the distribution of radiated power in the space [6–9]. It can be plotted in a spherical coordinate system as the radiated power versus the elevation angle (θ) or the azimuth angle (φ). Figure 1.2 shows a radiation pattern plotted as the radiated power versus the elevation angle (θ). As shown, the radiation pattern has a few lobes. The main lobe is the lobe containing the majority of radiated power. The lobe radiating towards the backward direction is the back lobe. Usually there will also be a few other small lobes called the side lobes. The 3-dB beamwidth indicated in the Figure refers to the angular range between two points where the radiated power is half the maximum radiated power. Figure 1.2 shows the radiation pattern in the elevation plane. There is also the radiation pattern in the azimuth plane, which can be plotted as the radiated power versus the azimuth angle (φ). The antenna pattern can be isotropic, directional or omni-directional. An isotropic pattern is uniform in all directions, which does not exist in reality. The pattern in Figure 1.2 is directional. As shown in Figure 1.2, the majority of radiated power is focused at one direction and the maximum radiation is along the z axis. An omni-directional pattern is donut-shaped, as shown in Figure 1.3.

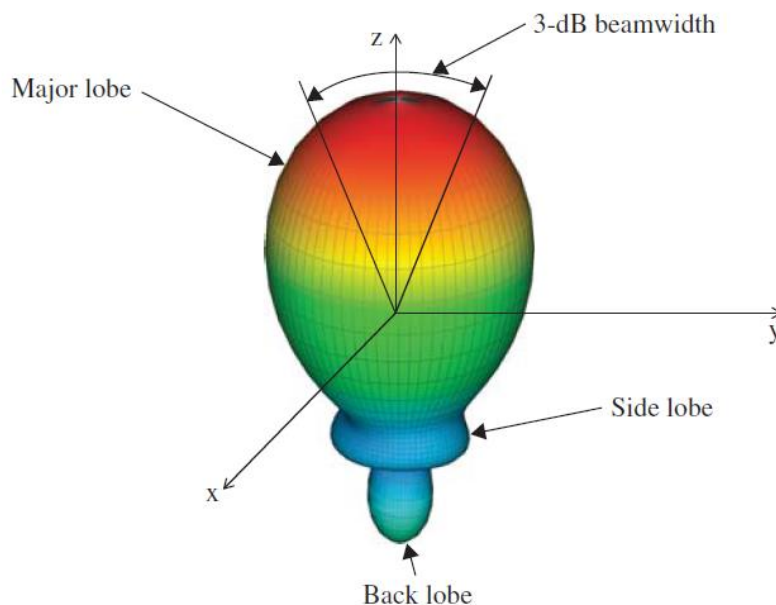


Figure 1.2: A directional radiation pattern in the elevation plane.

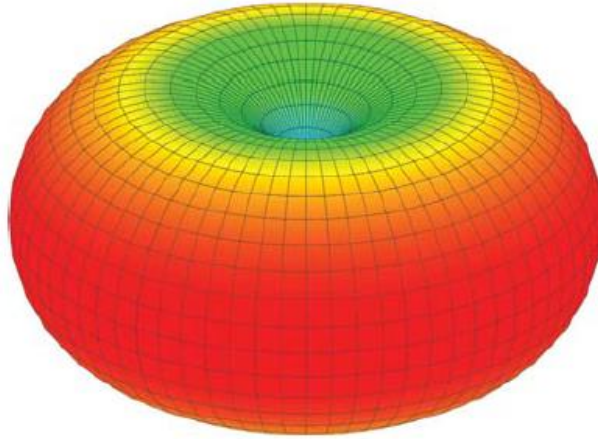


Figure 1.3: Omni-directional pattern.

1.1.4 Directivity, Gain and Efficiency

A practical antenna usually radiates in certain directions. The directivity, $D(\theta, \varphi)$, is defined as the radiated power per unit solid angle compared to what would be received by an isotropic radiator [6–9]. It could be calculated by

$$D(\theta, \varphi) = \frac{r^2 \cdot \frac{1}{2} \text{Re}[E \times H^*]}{\frac{P_{rad}}{4\pi}} = \frac{2\pi r^2 \cdot \text{Re}[E \times H^*]}{P_{rad}} \quad (1.5)$$

where E , H , r and P_{rad} denote the peak value of electric field, the peak value of magnetic field, the distance between the source and test point, and the radiated power from the antenna, respectively. It is also assumed that the test point is in the far field region of the antenna, which means the distance $r > \frac{2D^2}{\lambda}$ [6–9]. Here D is the maximum dimension of the antenna and λ is the wavelength. The gain of the antenna is similar as the directivity though it includes the efficiency η of the antenna, since some power will be lost in the antenna.

$$G(\theta, \varphi) = \eta \cdot D(\theta, \varphi) \quad (1.6)$$

Both directivity and gain are normally expressed in dB. It is common practice to write the antenna gain in dBi, which means that it is defined relative to an isotropic radiator.

1.1.5 Linear Polarization, Circular Polarization and Axial Ratio

Polarization of an antenna is related to the orientations of electric fields radiated by the antenna. Assuming a half-wavelength dipole is vertically oriented above the Earth, it

will produce radiated fields in the far field and the radiated electric fields will be dominated by $E(\theta, \varphi)$. In this case, the polarization of the dipole is called vertical polarization. On the other hand, if a half-wavelength dipole is horizontally oriented above the Earth, the radiated electric fields of the antenna will be dominated by $E(\theta, \varphi)$ in the far field. The polarization of the antenna is then called horizontal polarization. Both vertical and horizontal polarizations are linear polarizations. Linearly polarized antennas are commonly used in terrestrial wireless communications. To produce circular polarization, two orthogonal components of electric fields in the far field region are required [6–10]. The electrical field radiated by an antenna can be written as

$$\vec{E}(\theta, \varphi) = \vec{\theta}E_{\theta}(\theta, \varphi)e^{j\phi_1} + \vec{\varphi}E_{\varphi}(\theta, \varphi)e^{j\phi_2} \quad (1.7)$$

Here $E_{\theta}(\theta, \varphi)$ and $E_{\varphi}(\theta, \varphi)$ denote the magnitudes of electric field components in the far field of the antenna. ϕ_1 and ϕ_2 denote the phase shift of each field component. Circular polarization can be achieved only if the total electric field has two orthogonal components which have the same magnitudes and a 90 phase difference between the two components. That is

$$E_{\theta}(\theta, \varphi) = E_{\varphi}(\theta, \varphi)$$

$$\phi_2 - \phi_1 = \pm\pi/2 \quad (1.8)$$

For a circularly polarized wave, the electric field vector at a given point in space traced as a function of time is a circle. The sense of rotation can be determined by observing the direction of the field's temporal rotation as the wave is viewed along the direction of wave propagation: if the field rotation is clockwise, the wave is RHCP; if the field rotation is anti-clockwise, the wave is LHCP. In reality, it is impossible to achieve a perfect circular polarization, thus the curve traced at a given position as a function of time is usually an ellipse, as shown in Figure 1.4. Lines a and b denote the major axis and the minor axis of polarization ellipse, respectively. The ratio of the major axis to the minor axis of the ellipse is termed as the axial ratio (AR) [6–10].

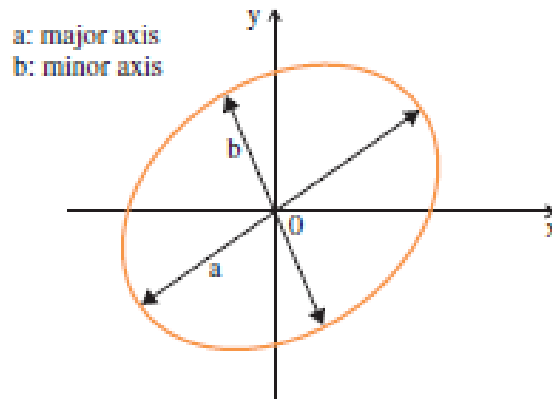


Figure 1.4: Polarization ellipse traced at a certain position as a function of time.

$$AR = a/b \quad (1.9)$$

AR is a key parameter for measuring the circular polarization. Usually AR is required to be below 3 dB for a CP antenna.

1.1.6 Bandwidth and Resonant Frequency

Usually an antenna is designed to operate within a specified frequency range. The bandwidth of an antenna is usually determined by the frequency range within which the key parameter of the antenna satisfies a certain requirement, for example, minimum return loss of 10 dB. At the resonant frequency of an antenna, the antenna input impedance is purely resistive. Often the resonant frequency is chosen as the centre of the frequency bandwidth of an antenna. The bandwidth of an antenna can be calculated by using the upper and lower edges of the achieved frequency range:

$$BW = \frac{f_2 - f_1}{f_0} \times 100 \quad (1.10)$$

where f_1 is the lower edge of the achieved frequency range,

f_2 is the upper edge of the achieved frequency range, and

f_0 is the center frequency of the range.

Note that this definition is for antennas with a bandwidth below 100%. For antenna bandwidths over 100%, the bandwidth can be calculated using the ratio between the

upper and lower edge of frequencies. For a linearly polarized antenna, the input impedance is usually the most sensitive parameter compared to other antenna parameters such as radiation patterns, gain and polarization. Thus the bandwidth of a linearly polarized antenna is often referred to as the ‘impedance bandwidth’, but it can also be to do with other parameters such as radiation patterns, gain and polarization. When evaluating the bandwidth of CP antennas, one must check both the impedance bandwidth and the bandwidth of AR, that is, the frequency range within which the AR is below 3dB. A good impedance matching does not necessarily lead to a good gain or a low AR value. The impedance bandwidth of an antenna can be broadened using suitable impedance matching networks, while the AR bandwidth can be broadened by using a broadband phase shifter network [5].

1.1.7 Methods of Design CP antenna

CP waves can be generated by exciting two spatially orthogonal LP waves that are in phase quadrature and have equal amplitudes. Hence, the designs may require dual feeding or power divider, which increases the size and complexity. For example, a square patch can generate a CP wave by feeding two edges of the square as shown in Figure 1.5. Alternatively, a 90° hybrid can be used in a conjunction with a single feeding for a circular patch at two orthogonal points as illustrated in Figure 1.6. For wide band CP radiation, four feeding ports may be used with 0, 90, 180 and 270 phase differences.

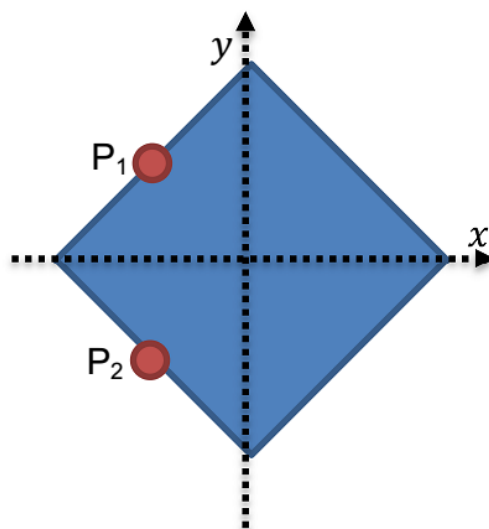


Figure 1.5: Dual-Feed CP square patch antenna.

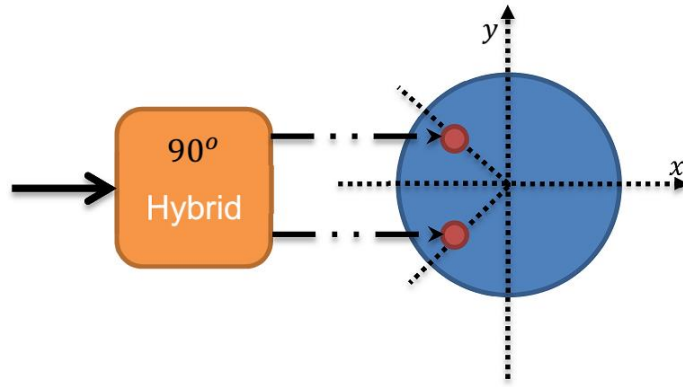


Figure 1.6: Singly fed CP circular patch antenna with a 90° hybrid.

Another method to generate CP waves is by introducing perturbation in the antenna. The small perturbation has to be with the right amount at the desired frequency to produce two orthogonally polarized components with the same amplitude and a 90° phase difference. An example of such method is the truncated square patch shown in Figure 1.7(a) or a circular patch with two opposing edges with notches as can be seen in Figure 1.7(b) [10].

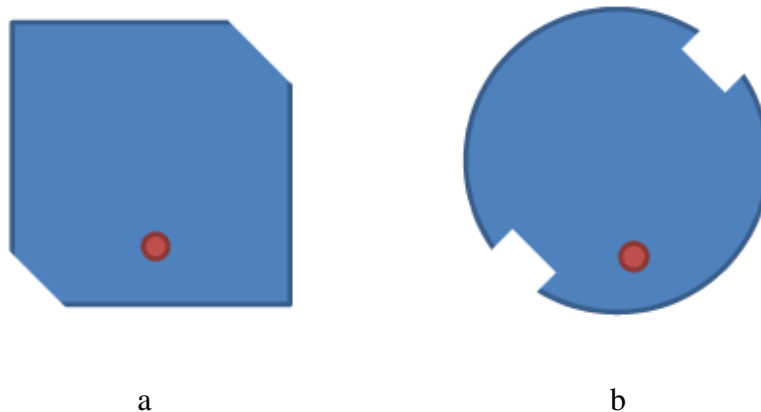


Figure 1.7: CP single feed square and circular patches.

1.2 Broadband Circularly Polarized Antennas

1.2.1 Slot Loading

The broadband CP antennas utilizing a thick air substrate are bulky and thus not suitable for compact-size electronic systems. An alternative method for achieving a single-feed broadband CP patch antenna is the use of slot loading. Figure 1.8 presents the configuration of a slot-loaded patch antenna. The probe-fed patch with a width of

W and a length of L is printed on a substrate with a thickness of h. Two connected slots are inserted in the square patch. The physical dimensions of the slots are L_1 , W_1 , L_2 , W_2 and T, as illustrated in Figure 1.8. When connected to each other, the two slots translate into two distinct resonant frequencies close to each other, leading to a wide frequency band. Circular polarization can be obtained when selecting proper values of the parameters for the slots. Two cases with different substrates (Rohacell foam and Duroid 5880) have been studied in this design [11]. The optimized parameters in the case of using Rohacell with a relative permittivity of $\epsilon_r = 1$ are: $L = 21$ mm, $W = 21.2$ mm, $s_1 = 4.5$ mm, $s_2 = 5.6$ mm, $s_3 = 3.5$ mm, $s_4 = 4.5$ mm, $s_5 = 5.6$ mm, $d = 3.6$ mm, $s_6 = 3$ mm, $s_7 = 6.5$ mm and $h = 3.0$ mm. The simulated and measured impedance bandwidths ($|S_{11}| \leq -10$ dB) are 11.9% (5.14–5.79 GHz) and 11.8% (5.17–5.82 GHz), respectively, which are much broader than the impedance bandwidth of the same antenna without slot loading (4.2%). When the Duroid 5880 substrate ($\epsilon_r = 2.2$) is applied in the design, the optimized parameters of the antenna are: $L = 14.8$ mm, $W = 14.8$ mm, $s_1 = 2.95$ mm, $s_2 = 3.65$ mm, $s_3 = 2.45$ mm, $s_4 = 2.95$ mm, $s_5 = 3.65$ mm, $d = 2.84$ mm, $s_6 = 2.1$ mm, $s_7 = 5.0$ mm and $h = 3.175$ mm. It is noticed that, the antenna size is significantly reduced when Duroid 5880 substrate is used. The measured operating frequency of the antenna is decreased by about 90MHz compared to the simulated result, which is probably owing to the tolerance limitation of the dielectric material. The measured impedance bandwidth ($|S_{11}| \leq -10$ dB) is 11.6%. It is also noted that, when using Rohacell foam, the AR is less than 3 dB only within a small frequency range, while the 3-dB AR bandwidth can reach 8% when the Duroid 5880 substrate is utilized.

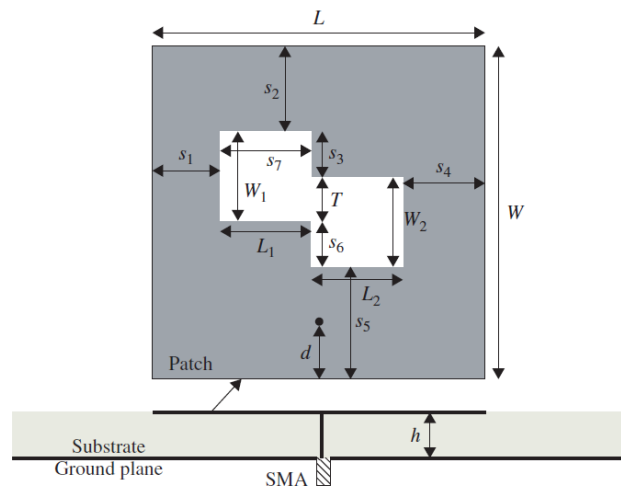


Figure 1.8: Geometry of a slot-loaded patch antenna [11].

1.2.2 Broadband Coupler

The bandwidth of CP patch antennas can be further increased by using a broadband coupler. Figure 1.9 presents the configuration of such an aperture-coupled CP patch antenna fed by a three-stub hybrid coupler [12]. Compared to a two-stub branch-line coupler which has a bandwidth of around 25%, the bandwidth of a three-stub branch-line coupler can go up to 40%. The hybrid coupler is printed on one side of the lower 0.813-mm-thick RO4003 substrate ($\epsilon_r = 3.38$, $\tan \delta = 0.002$). The characteristic impedance of the two wider parallel strips and the inner shunt strip is $Z_2 = 35.4 \Omega$. The outer shunt strip has a characteristic impedance of $Z_5 = 120.8 \Omega$ and the characteristic impedance of all other lines is $Z_1 = Z_3 = Z_4 = 50 \Omega$. Port 2 is terminated with a 50Ω resistor to absorb the reflected power. Two rectangular slots with a width of 1.88mm are embedded in the square ground plane with a side length of l_1 on the opposite side and separately perpendicular to the feed strip of the hybrid coupler.

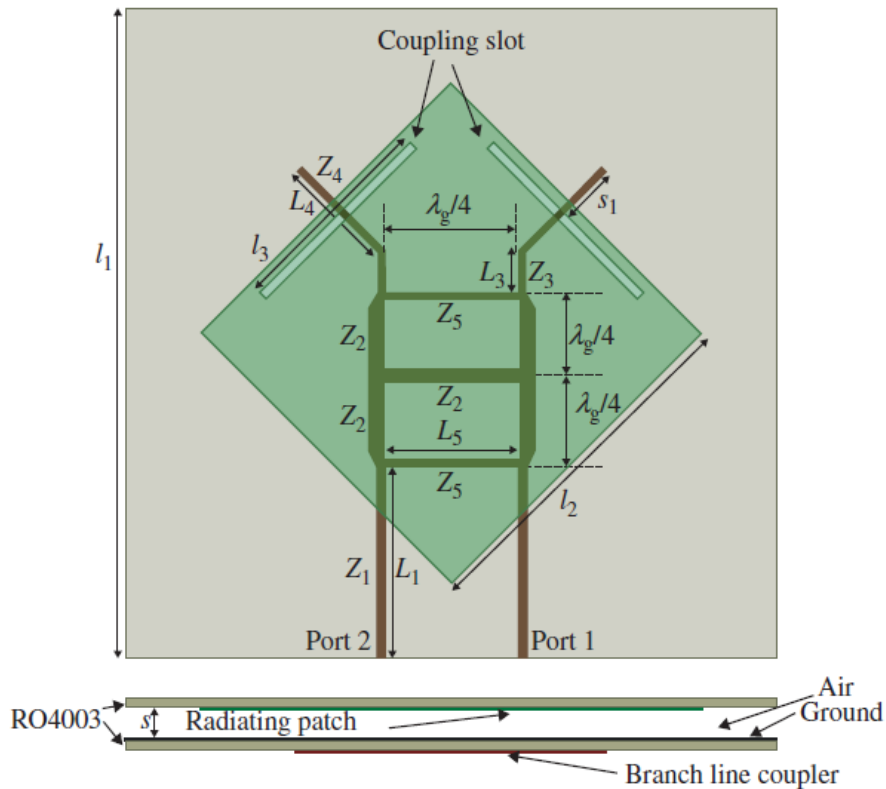


Figure 1.9: Geometry of the aperture-coupled CP patch antenna using a three-stub branch-line coupler [12].

The square radiating patch is printed on the bottom side of the upper substrate. The energy is coupled to the square radiating patch through the slots. Two dielectric substrates are connected by some plastic posts. The optimized values of the dimensions are: $L_1 = 31.4$ mm, $L_3 = 10$ mm, $L_4 = 26.5$ mm, $L_5 = 30.38$ mm, $s_1 = 12.15$ mm, $l_1 = 156$ mm, $l_2 = 83$ mm and $l_3 = 50$ mm. The obtained impedance bandwidth ($VSWR \leq 2$) and 3-dB AR bandwidth are 32.3% (1.3–1.8 GHz) and 42.6% (1.22–1.88 GHz), respectively. The maximum antenna gain is found to be 8.8 dBic at 1.55 GHz. In addition, a broadband dual L-probe fed CP antenna with a broadband balun is demonstrated in [13], as shown in Figure 1.10. The circular patch with a diameter of D is supported by an air substrate of thickness H above a grounded Rogers RO4003 dielectric substrate. The feed network is printed on the top layer of the substrate. Two L-shaped probes formed by its vertical and horizontal portions are orthogonally oriented and positioned at a distance of S away from the circumference of the patch. The L-probe feeds are soldered to the output lines of the feed network and excite the radiating patch by proximity coupling. The broadband feed network consists of a cascade of a 3-dB Wilkinson power divider for wideband impedance matching and balanced power splitting, and a novel broadband 90° Schiffman phase shifter for wideband consistent 90° phase shifting. The measured 10-dB return loss and 3-dB AR bandwidths of the dual L-probe fed CP antenna can reach 60.24% and 37.7%, respectively.

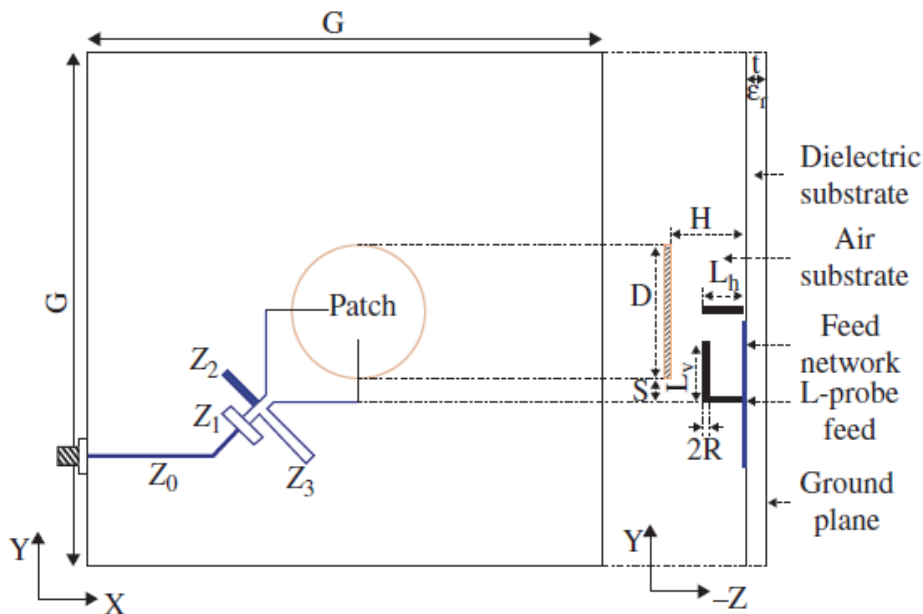


Figure 1.10: Geometry of the dual L-probe fed circular patch antenna [13].

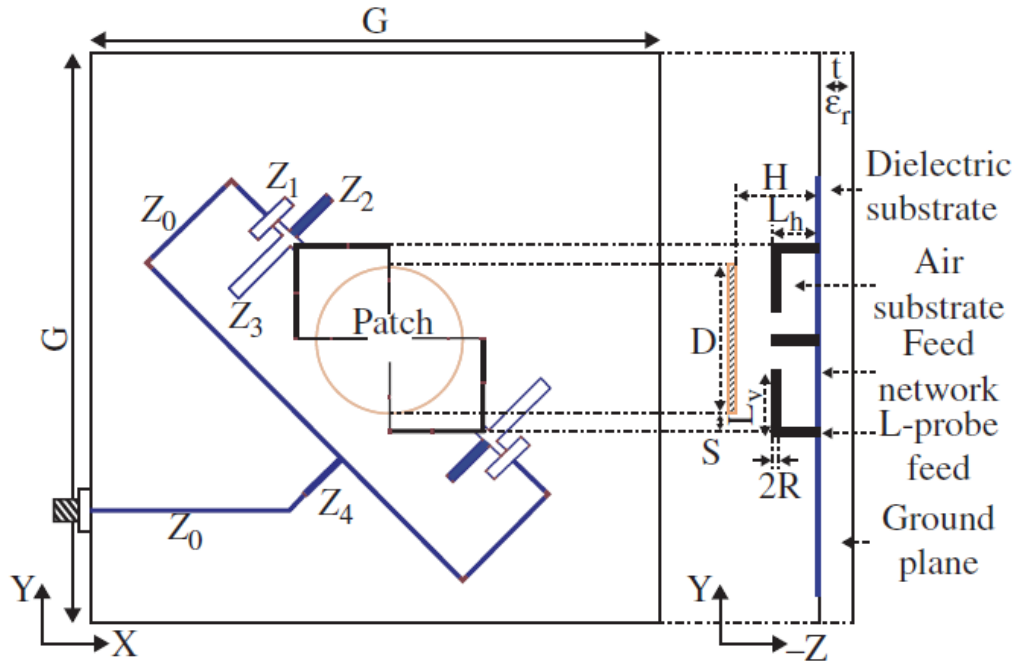


Figure 1.11: Geometry of the quadruple L-probe fed circular patch antenna [13].

It is reported in [13] that the antenna bandwidth can be further increased by using four feeds instead of two feeds, as shown in Figure 1.11. The quadruple L-probe antenna has the same antenna parameters with the dual L-probe antenna. The feed network consists of a pair of the aforementioned 90° broadband baluns connected by a 180° transformer. The length difference of the microstrip branches is selected to be $\lambda_g/2$ (λ_g is the guided wavelength at the center operating frequency) for providing a 180° phase shift. The input transmission line is connected to the two microstrip branches through a quarter-wavelength transformer. In the case of four feeds, the 10-dB return loss and 3-dB AR bandwidths can reach 71.28% and 81.6%, respectively. However, the multi-feed CP antenna requires a complicated feed network which also occupies more space. For example, the four-feed CP antenna requires a complicated feed network to provide 0° , 90° , 180° and 270° phase shift at four feeds, respectively.

1.2.3 Ring Slot with a Broadband Coupler

The hybrid coupler which is used in the broadband CP patch antenna can also help the CP ring slot antenna increase the bandwidth. Figure 1.12 presents the geometry of a ring slot antenna with a hybrid coupler. A square ring slot is embedded in the ground which is printed on the bottom layer of an FR4 substrate. Two adjacent sides of the

slot loop are excited by a three-stub hybrid coupler which is printed on the other side of the substrate. It is noted that two stubs are added to improve impedance matching. The characteristic impedances of the stubs are: $Z_1 = 50 \Omega$, $Z_2 = 35.4 \Omega$, $Z_3 = 120.8 \Omega$, $Z_4 = 67.6 \Omega$ and $Z_5 = 92.8 \Omega$. The antenna in [14] can achieve an impedance bandwidth (VSWR ≤ 2) of 55.6% (3.9–6.9 GHz). The measured 3-dB AR bandwidth reaches around 22.2% (4.8–6.0 GHz). The antenna gain ranges from -0.5 to 1.4 dBic across the operating frequency range.

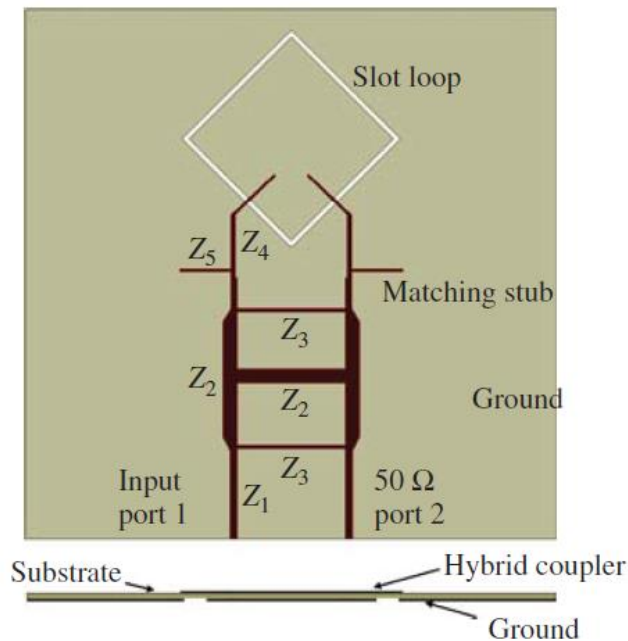


Figure 1.12: Geometry of a ring slot antenna with a hybrid coupler [14].

1.2.4 Circular/Square Slot with an L-Shaped Feed

Compared to microstrip antennas, the printed slot antennas, especially wide slot antennas, can have broader impedance bandwidths. Several approaches have been taken to achieve good CP performance over a wide frequency range. These include the L-shaped feedline [15, 16] or grounded strip [17–20]. In addition, circular polarization of the slot antenna can be obtained by applying modifications on the feedline with grounded strips [21–24].

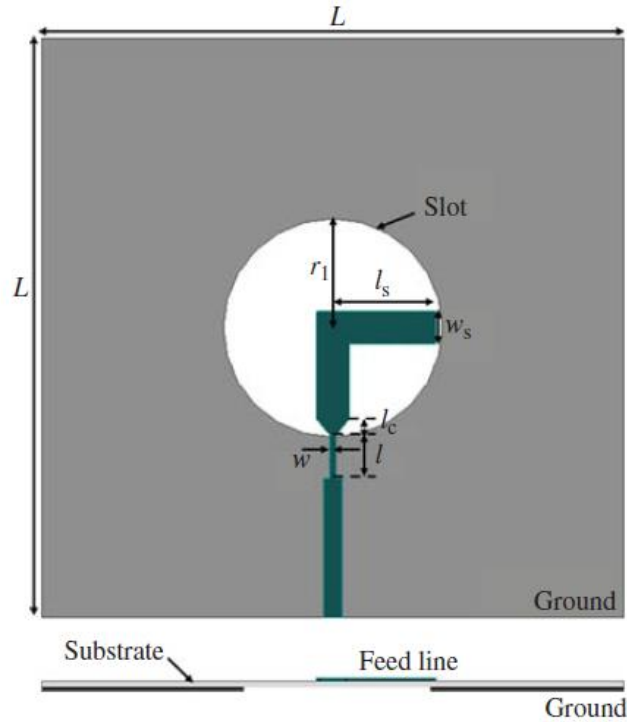


Figure 1.13: Geometry of a microstrip-fed CP slot antenna. Antenna dimensions:
 $r_1 = 18.8$ mm, $l_s = 17.7$ mm, $w_s = 5.5$ mm, $l_c = 11.7$ mm, $l = 7.2$ mm, $w = 0.5$ mm,
 $L = 100$ mm [1].

Figure 1.13 presents the geometry of a microstrip-fed CP slot antenna. A circular slot with a radius of 18.8mm is embedded in the ground plane which is printed on one layer of an FR4 substrate with a thickness of 1.6mm and a relative permittivity of 4.4. An L-shaped strip with a taper end is fabricated on the other side of the substrate to excite two orthogonal fields in phase quadrature. CP operation is obtained due to the L-shaped strip. A narrow line with a length of l and a width of w behaves as an impedance transformer between the taper end of the L-shaped strip and the 50Ω microstrip line. The length of the tapered portion is l_c . The simulated and measured results of return loss and AR are illustrated in Figures 1.14 and 1.15. The measured 10-dB return loss bandwidth is 1.42 GHz or 37.97% at 3.74 GHz. The measured result exhibits a 3-dB AR bandwidth of 1.65 GHz or 44.1% at 3.74 GHz. The slot antenna radiates towards both sides, and the patterns at both sides have different senses of circular polarization. The measured antenna gain varies from 4 to 5 dBi across the operating frequency band. In addition, a CPW-fed slot antenna with an embedded square slot and an L-shaped strip connected to the edge of the slot is studied in [16]. The width of the L-strip is larger than that of the signal line. The obtained 10-dB return loss and 3-dB AR bandwidths of the CPW-fed slot antenna are 43% and 17%, respectively.

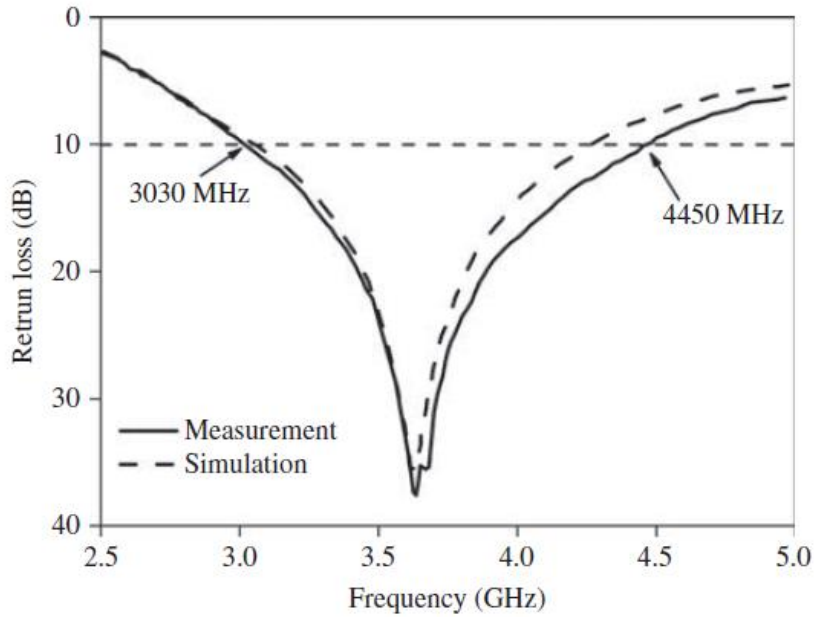


Figure 1.14: Simulated and measured return loss for the slot antenna [15].

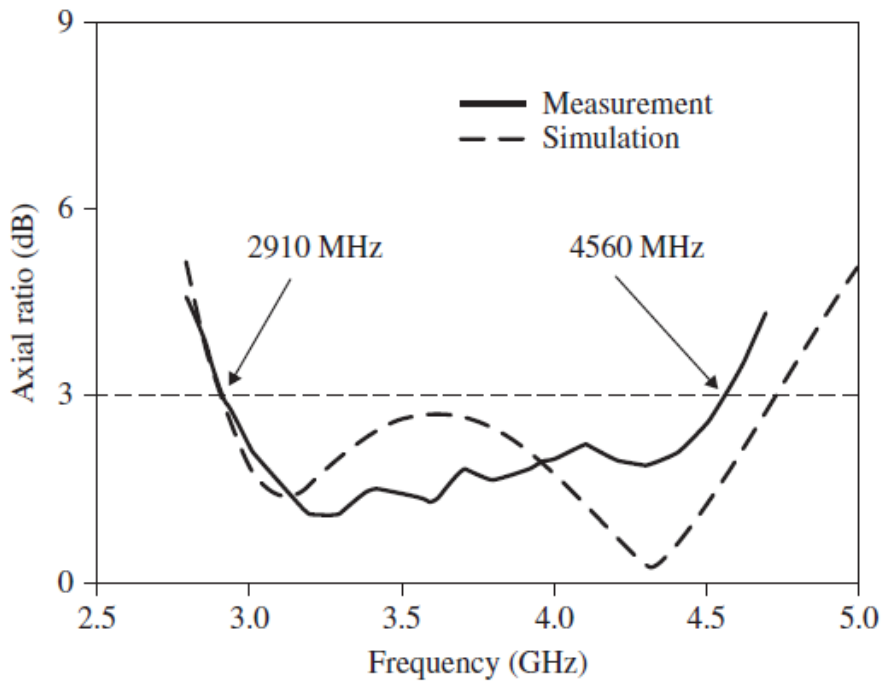


Figure 1.15: Simulated and measured AR for the slot antenna [15].

1.2.5 Grounded Strip

Figure 1.16 presents the geometry of a CPW-fed CP slot antenna which is printed on a single layer of an FR4 substrate with a thickness of 1.6mm and a relative permittivity of 4.4. A square slot with a side length of $L = 40\text{mm}$ is embedded in a square ground with a side length of 70 mm. A T-shaped strip with a width of $w_2 = w_3 = 1\text{mm}$ is protruded toward the slot center at the center of one slot edge. The horizontal and

vertical portions of the T-shaped strip have the lengths of l_4 and l_3 , respectively. A narrow strip with a width of w_1 and a length of l_1+l_2 is protruded from the end of the signal line with a width of $s=6.4$ mm. The gap between the signal strip and the ground plane has a length of $g = 0.5$ mm. Good CP performance over a wide frequency range can be achieved by tuning the dimensions of l_1 , l_2 , l_3 , l_4 and w_1 . It is also worthwhile to mention that the design in Figure 1.16 gives LHCP radiation. The obtained impedance bandwidth defined by $VSWR \leq 2$ is 874MHz or 44.5% at 1.965 GHz. The measured 3-dB and 1-dB AR bandwidths are 18.8% and 12.7%, respectively. The slot antenna without a reflector has bi-directional radiation patterns. The gain variation is less than 1 dB with a peak gain of around 3.7 dBi. Similarly, the circular CPW-fed slot antenna with a circular slot and having a broader CP bandwidth is proposed in [18]. Circular polarization is obtained by protruding a metallic mono-strip from the circular ground plane towards the slot center.

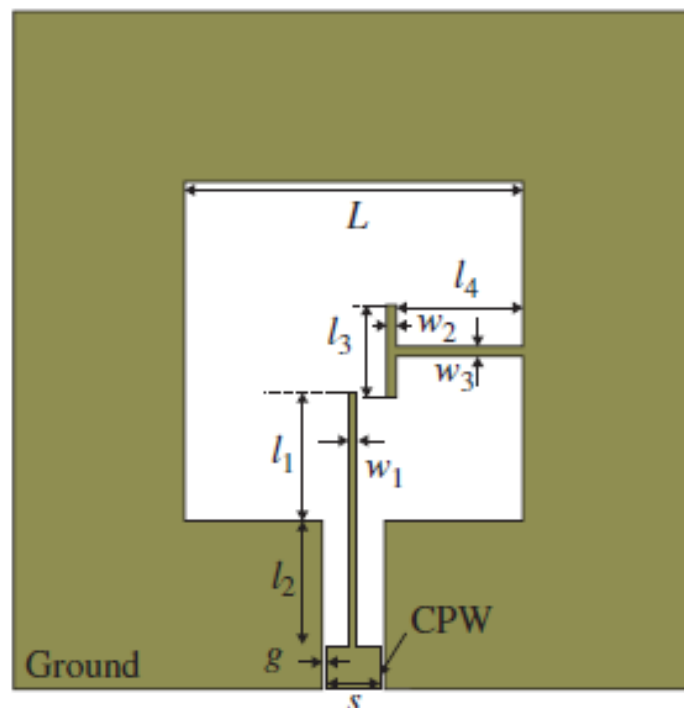


Figure 1.16: Geometry of a CPW-fed CP slot antenna with a T-shaped strip protruding the ground [19] ($l_1 = 15$ mm, $l_2 = 9.7$ mm, $l_3 = 9.2$ mm, $l_4 = 15$ mm and $w_1 = 1$ mm).

The circular slot antenna in [4] has an impedance bandwidth ($|S_{11}| \leq -10$ dB) and a 3-dB AR bandwidth of 50% and 36%, respectively. Instead of using CPW feed, the microstrip-fed slot antenna in [19] consists of a microstrip T-junction, a rectangular

wide-slot and a T-shaped stub protruded at the slot edge. A portion of microstrip line with a high characteristic impedance is arranged between the T junction and the 50- Ω feedline for improving the impedance matching. The microstrip-fed slot antenna in [19] can achieve a 10-dB return loss bandwidth of 58% and a 3-dB AR bandwidth of 22.2%. Furthermore, a CPW-fed square slot antenna with two grounded inverted-L metallic strips is studied in [20]. A square slot is embedded in the square ground plane and excited by a 50 Ω CPW. A strip with a larger width protrudes from the signal line of the CPW into the slot. The CP operation is mainly attributed to the two grounded inverted-L metallic strips located around two opposite corners of the square slot. The obtained impedance bandwidth ($VSWR \leq 2$) and 3-dB AR bandwidth are 52% and 25%, respectively. The impedance and AR bandwidths of the slot antennas can be further increased by using grounded strips and modifying the feedline, which has been investigated in [20-25]. Figure 1.17 presents the geometry of a CPW-fed square slot antenna [20]. The design has two main features: one for increasing the AR bandwidth and the other mainly for enhancing the impedance bandwidth. The AR bandwidth is enlarged due to the combination of the lightning-shaped feedline and two inverted-L grounded strips on the opposite corners of the square slot. The lightning-shaped feedline is realized by extending the signal line of the CPW to the lower left corner of the slot and then protruding into the slot at an inclined 45°. In order to increase the impedance bandwidth, two tuning stubs are embedded in the feedline. The vertical tuning stub is formed by shrinking a section of the CPW's signal line while the horizontal one is realized by extending the horizontal feed section. The second resonant mode will be shifted to a lower frequency band and combined with the first resonant mode to achieve a wider impedance band, when choosing proper dimensions for the tuning stubs. The antenna in [20] can achieve a 10-dB return loss and 3-dB AR bandwidths of 50.9% and 48.8%, respectively.

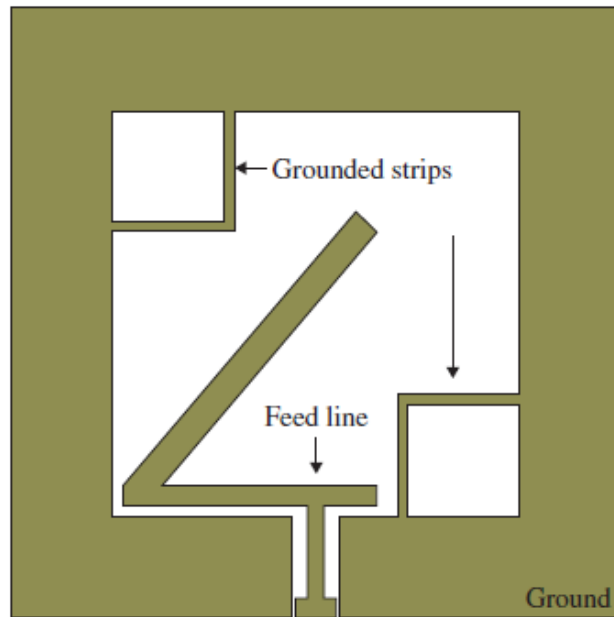


Figure 1.17: Geometry of a square slot antenna with a lightning-shaped feedline and inverted-L grounded strips [20].

More recently, a CPW-fed regular-hexagonal slot antenna is proposed in [21]. The ground plane is formed by a hexagonal ring and two L-shaped strips. An L-shaped monopole patch is connected to the signal line of the CPW. Wide impedance and AR bandwidths can be obtained by employing an L-shaped monopole patch protruding into the slot and two inverted-L grounded strips. Moreover, the impedance and AR bandwidths can be further enlarged by inserting a rectangular notch in the ground plane. The antenna in [21] can achieve a 10-dB return loss and 3-dB AR bandwidths of 86% and 50%, respectively.

Compared to adding two equal-size inverted-L strips, the square slot antenna in [22] has a square ground plane with a wide square slot and two unequal-sized inverted-L shaped strips at two opposite corners. Two orthogonal fields in quadrature can be generated by the grounded strips. A rectangular patch is connected to the signal line of the CPW. Also, a tuning slit is inserted in the feedline and a tuning vertical stub is attached to the signal line. The impedance bandwidth is significantly enlarged owing to these modifications. The slot antenna in [22] can operate over a wide frequency range with an impedance bandwidth ($VSWR \leq 2$) of 132% and a 3-dB AR bandwidth of 32.2%.

1.3 Array design

Previous section have already discussed the basics of CP antennas as well as various techniques for designing small CP antennas and broadband CP antennas. Array antennas are useful for applications where a high gain, low sidelobe beam reconfigurability are required, such as satellite communications, DBS, WLAN and space communications. CP arrays are important for applications that need a high gain to overcome the free-space loss due to the long distance between radio transmitter and receiver.

1.3.1 Sequential Rotation

Microstrip patch arrays are widely used in wireless communications due to their advantages of low profile, light weight, easy fabrication, low cost and conformability to curved structures [26]. CP arrays can be formed by using a number of CP or LP radiating elements. Each antenna element can be single-feed or dual-feed in phase quadrature. Better polarization purity can be achieved if four feeds are employed for each patch element as the undesired modes in the patch can be suppressed. However, the four-feed patch requires a more complicated feed network to provide four ports with 0° , 90° , 180° and 270° phase differences. For large CP arrays, these feed networks will occupy lots of space, leading to increased complexity and high cost. A technique that uses single-feed LP patches to design CP arrays is proposed in [27]. Figure 1.18 shows a CP array formed by using four linearly polarized elements. As shown, four elements are sequentially rotated and have a phase distribution of 0° , 90° , 180° and 270° . This technique enables a significant reduction in the size, complexity, weight and RF loss of the array feed networks, and is particularly attractive for applications in large arrays. Using this technique to design wide bandwidth CP microstrip patch arrays is also studied in [28], where the radiation performance of a CP microstrip patch array with an antenna element of either linear polarization or circular polarization is investigated. In [28], the radiation performance of the sequentially rotated array is analyzed by using its corresponding transmission line equivalent circuit model. In this analysis model, the equivalent circuit model of a LP patch antenna is described as a parallel circuit consisting of one inductor, one capacitor and one resistor. For the CP patch antenna, it is modelled as a series connection of two LP patches.

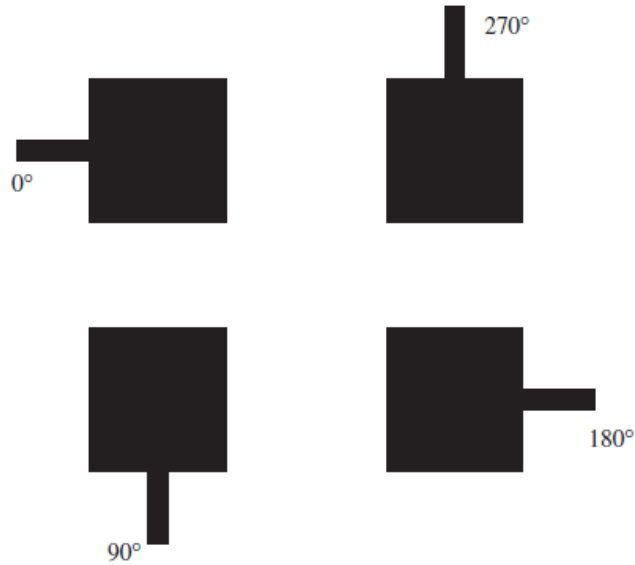


Figure 1.18: Configuration of the conventional CP patch antenna array using sequential rotated LP patch elements [27].

Details of CP arrays analysis using sequentially rotated LP elements and CP elements are presented in [28]. It is shown that clusters of three sequentially-rotated CP patch elements, in which case a triangular lattice configuration is employed, achieve broader bandwidth compared to that of clusters of two or four elements. Also the gain of sequentially-rotated arrays can benefit from using the CP elements. This implies that a wideband CP antenna array can be achieved by having a low-Q antenna as the radiating element and with a sequential rotation technique. One concern of using a LP antenna to design CP antenna arrays is the increased cross polarization level. After investigating a 2×2 sequential rotated CP microstrip antenna, the author in [29] points out that even using the LP antenna as the radiation element for a CP antenna array, low cross-polarization within the bandwidth can still be reached if there is a high-performing feed network that can provide accurate phase and amplitude for the array. Meanwhile, the mutual coupling between antenna elements also plays an important role in increasing the cross-polarization of the array. In the case where the antenna element is spaced with $0.6-0.7\lambda$, the contribution from the radiators to the cross-polarization is at least 10–12 dB [29].

1.3.2 Single-Feed Patch

The sequentially rotated technique is an effective method to improve the bandwidth of the CP antenna array. If there is a need to further increase both the impedance and AR

bandwidth of the CP antenna array, it can be realized by introducing the parasitic radiators to a sequentially rotated antenna array, like the one proposed in [30]. The layout of this array is presented in Figure 1.19. This CP array is designed to resonate at 10.2 GHz. Circular patches, which are printed on RT/Duroid 5880 ($\epsilon = 2.2$) with a thickness of 0.79 mm, are placed at a height of $0.11\lambda_{0.2}$ GHz above the quasi-elliptical patches as the parasitic radiator. The four sequentially rotated square patch antennas are printed on 0.63-mm thick RO3006 ($\epsilon = 6.15$) and are fed with 0° , 90° , 180° and 270° phase differences by employing a microstrip feed network, as shown in Figure 1.19. Two corners of each square patch are truncated to generate the required CP operation and the $50\text{-}\Omega$ microstrip line is located 45° clockwise relative to the major axis of the square patch, which results a RHCP radiation. To reach the LHCP, the feeding line can be changed to 45° counterclockwise relative to the major axis of the square patch. The measurement results of the single antenna element (square patch with the parasitic element) and a 2×2 subarray with sequential rotation is summarized in Table 1.1. As can be seen from this table, the single antenna element exhibits 10-dB return loss bandwidth of 18.5% and 3-dB axial ratio bandwidth of 7.5% with central frequency of 10.2 GHz. Compared to the conventional microstrip antennas, which normally only have a bandwidth of only a few percent [31], there is a significant improvement on the antenna operation bandwidth by using the parasitic radiator. After employing the sequential rotation techniques to the 2×2 subarray, the 10-dB return loss bandwidth further increases to 27.7% whereas the axial ratio bandwidth improves to 23.5%. The measurement results also show that the gain of the CP array is 12.5 dBi at 10.2 GHz.

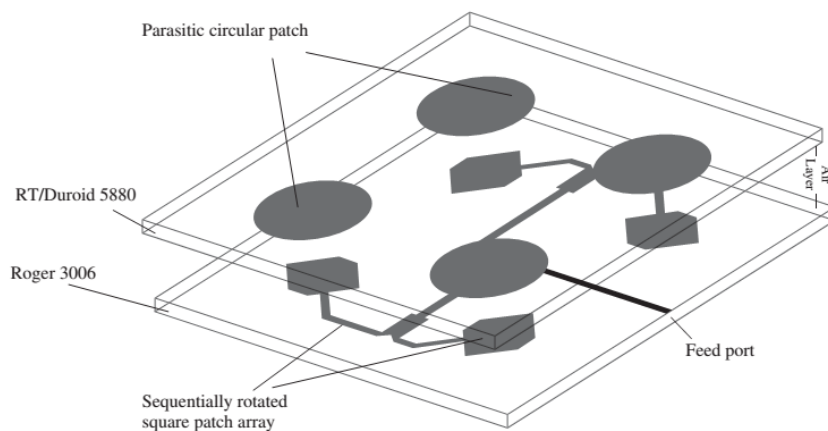


Figure. 1.19: Geometry of the wideband stacked CP antenna array [30].

Table 1.1: Comparison of the radiation performance between single antenna element

	Single antenna element (square patch with a parasitic element)	2×2 subarray (with sequential rotation and parasitic elements)
10-dB return loss bandwidth (with central frequency at 10.2 GHz)	18.5 %	27.7 %
AR bandwidth (with central frequency at 10.2 GHz)	7.5 %	23.5 %
Gain	7.5 dBi	12.5 dBi

From the measurement results given in Table 1.1, it can be concluded that after employing the sequential rotation technique and introducing parasitic radiators, the CP patch array can have both 10-dB return loss and 3-dB AR bandwidth larger than 20%, which is several times larger than a conventional microstrip patch array.

1.3.3 Dual-Feed Patch

As well known, CP patch antennas can be designed using a single-feed or multi-feed technique. Using a single-feed technique to design CP patch antenna leads to a simpler feed network; however, without using any bandwidth enhancement techniques, it has the inherent disadvantages of narrow impedance and AR bandwidth. The use of a dual-feed antenna can solve this issue at the expense of increased system complexity, especially when a large number of antenna elements are used. Investigations have been done in order to apply the dual-feed technique to the CP antenna array design with reduced system complexity. One such design is proposed in [32], where the dual-feed slot-coupling feeding technique is used in the design of a wideband CP patch array. Figure 1.20 shows the configuration of the antenna element proposed in [32]. This antenna array is designed for the operation at WiMAX frequency band (3.3–3.8 GHz). A square patch is printed on the bottom side of a 1.58-mm thick FR4 ($\epsilon = 4.4$) substrate. One slot ring and two orthogonal microstrip feed lines are printed on each side of a 1.53-mm thick Roger 4003 ($\epsilon = 3.55$) substrate.

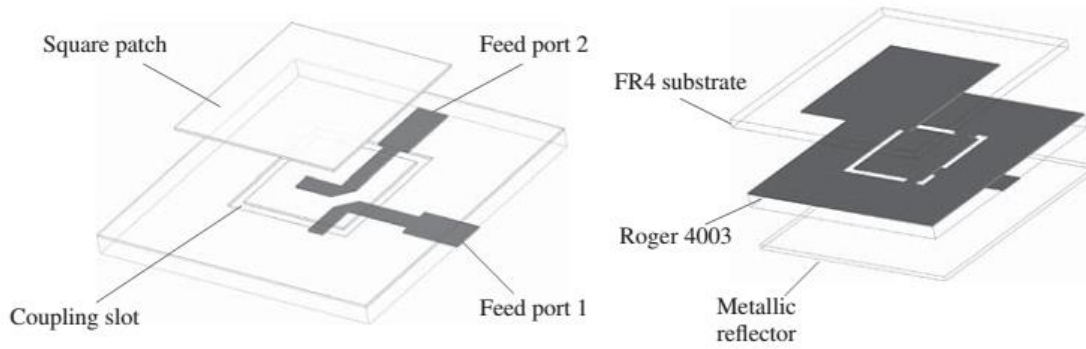


Figure 1.20: Configuration of the dual-feed slot-coupling CP patch. The Figure in the left shows the detailed view of the patch with two feed lines and the Figure on the right presents the overall structure of this CP patch [32].

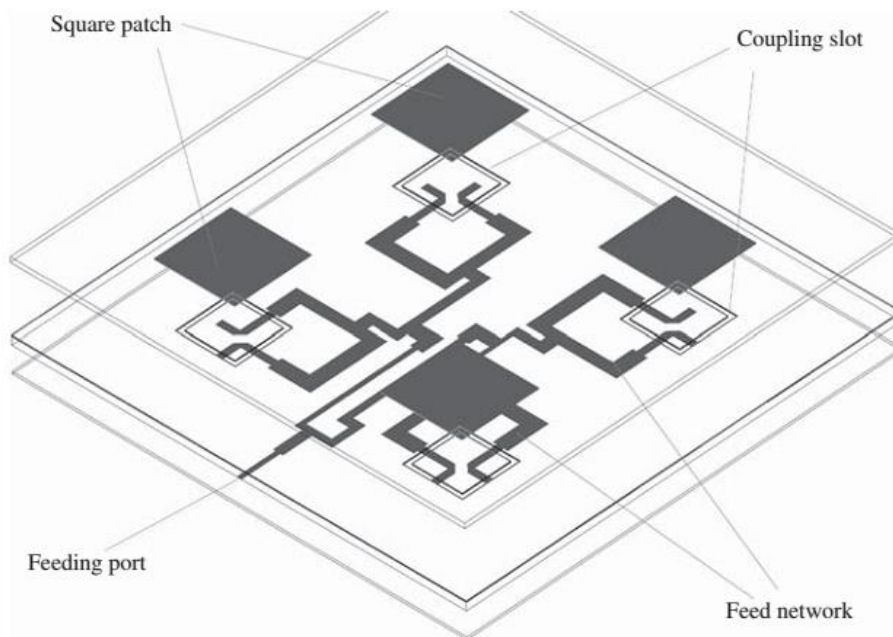


Figure 1.21 the layout of the 2×2 sequentially rotated CP array [32].

There is an 11 mm air gap between the FR4 and Roger 4003 substrate. One metallic ground plane is added below the feed line to reduce the back radiation. By using the slot coupled feeding technique, the feed line can be printed on different layers and in this way more space for the feed network can be allocated compared to the microstrip-fed antenna arrays that have antennas and the feed network printed on the same layer. To further increase the bandwidth of the array, a sequential rotation technique is used. The sequential rotation technique is a well-known method that can be used to improve

the CP purity, radiation pattern symmetry and impedance as well as AR bandwidth. Therefore, combining both techniques, dual-feed slot coupling and sequential rotation feeding, wideband operation of the CP antenna array can be achieved. Figure 1.21 shows the feed network of the resulting 2×2 array. This antenna is designed to have an RHCP radiation and the measurement results show that this antenna array has 3-dB AR bandwidth of 30% with central frequency of 3.55 GHz and a 10-dB return loss bandwidth of 50% (from 2.6–4.4 GHz), which is much larger compared to the conventional CP patch antenna arrays and even larger than the sequentially rotated antenna array with parasitic radiators. The measurement results also indicate that the cross polarization is 20 dB less than the co-polarization within the HPBW. The maximum measured gain is about 12.8 dBi. As can be seen from this design, the use of dual-feed or multi-feed radiating elements in sequentially rotated CP arrays can increase the bandwidth of CP arrays at the expense of increased system complexity, size and losses of the array feed networks. Such arrays are rather difficult to implement on a single layer due to the space problem. The space problem can become more serious if RF and microwave active circuits are required to be integrated with antenna elements and feed networks. It is possible to alleviate this space problem of CP arrays by using a slot-coupled multi-layer structure that is, the patch antenna and feed network are placed at different layers, such as the one shown in Figure 1.21.

1.3.4 Multi-Band CP Patch Antenna Arrays

The multi-band CP antenna array gains its application in the field of satellite communications, where the transmitting and receiving bands are allocated with different frequencies [8,9], and RFID applications, where one high gain RFID reader is required to operate at different RFID bands [33]. The difficulty in designing a multi-band CP patch array lies in the fact that at different resonant frequencies, the corresponding mode must have two orthogonal components with equal amplitude and phase quadrature, conditions which are not easy to meet simultaneously.

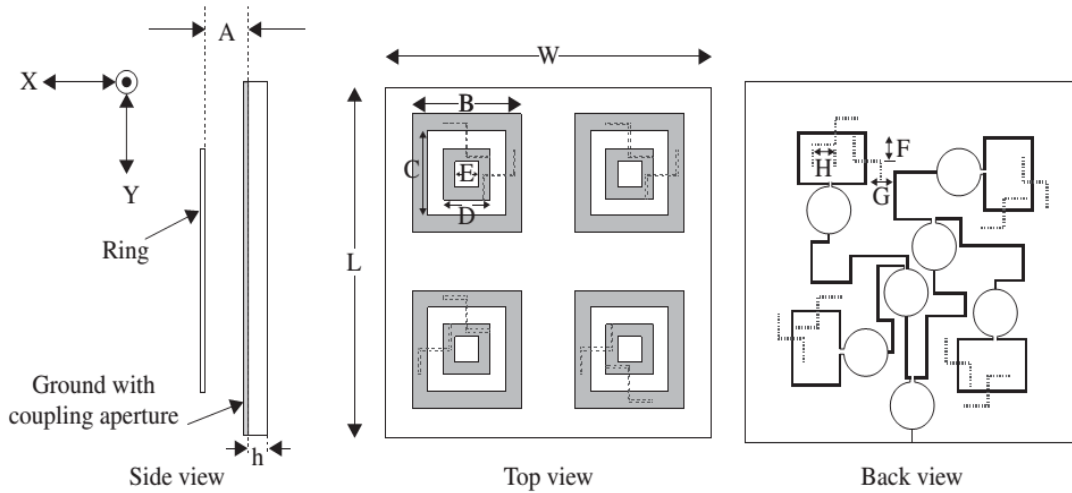


Figure 1.22: Side, top and back view of the dual band CP antenna array for RFID reader application [33].

A high-gain CP dual-band antenna array for RFID reader applications is recently proposed by [33]. Different from the two approaches presented previously, a single layer dual-band dual-ring radiator is employed as the array element. Figure 1.22 shows the side, top and back view of this dual band CP antenna array. The antenna element consists of two rings, each of which can resonate at different frequencies: 900 MHz and 2.4 GHz. The dual-band antenna is excited with 90° phase offset through apertures. Wilkinson power dividers are used to distribute the excitation from the input to the individual elements. Since the frequency ratio for the dual band antenna is close to 3:1, it is possible to maintain the phase offset at both band to the desired value.

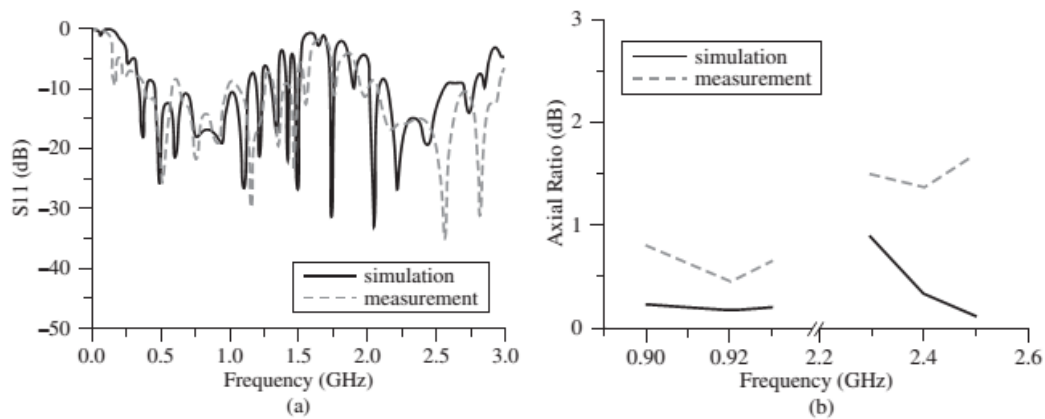


Figure 1.23 Measured and simulated S_{11} , axial ratio of the dual band CP antenna array for RFID reader application [33].

To improve the CP performance, the antenna elements are sequentially rotated. This antenna is fabricated on a 0.508-mm thick FR4 substrate. Figure 1.23 presents the measured and simulated S_{11} , axial ratio of this dual band CP antenna array. There is a good impedance matching at both bands and the axial ratio at the desired frequency bands is always below 2dB. At the lower band, 8 dBi peak gain is reached while at the higher band, the peak gain is about 10 dBi.

1.3.5 High-Efficiency CP Patch Arrays at the Ku Band and Above

When designing a microstrip antenna array consisting of a large number of elements with the microstrip feeding lines printed on the same layer, the loss and undesired radiation from the feed network are problematic, especially for the application at millimeter-wave frequencies. To reduce these unwanted effects from the feed lines, besides using the aperture coupled feeding like the one already presented, several other approaches have also been proposed. One effective method is the double use of sequential rotation technique in large arrays. A 64-element wideband CP microstrip antenna array that can operate in the frequency band of 27–31 GHz is presented in [34]. The antenna element is a square-shaped patch with two truncated corners and the four-element subarray is arranged with sequential rotation to achieve better CP bandwidth, as shown in Figure 1.24. Then, the subarray is used to form a full array containing a total number of 64 elements, which is shown in Figure 1.25. As can be seen from this Figure, different to the conventional array configuration where the subarrays are arranged symmetrically, the 4×4 subarray is arranged in a clockwise rotation sequence. According to [34], this double sequential rotation can cancel the undesired radiation from the feed network and thus contributes to the polarization purity and radiation pattern symmetry.

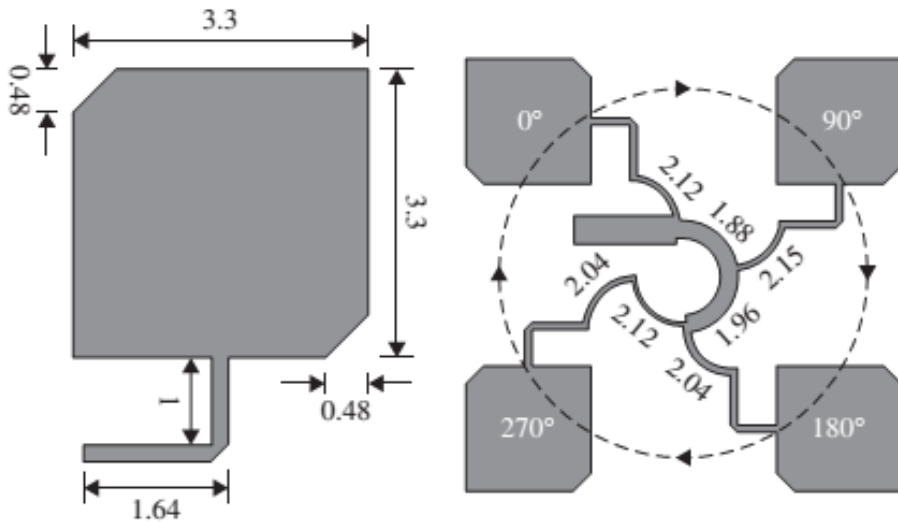


Figure 1.24: Geometry of the single radiation element and configuration of the subarray [34].

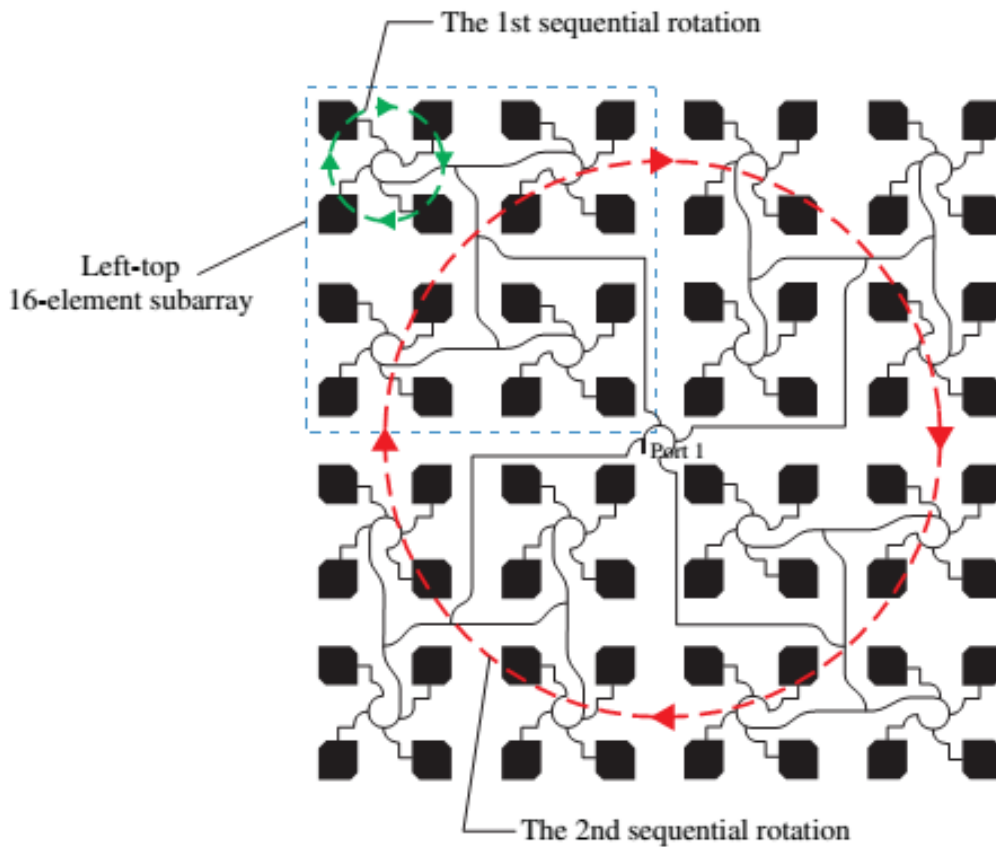


Figure 1.25: Configuration of the full array using the double sequential rotation technique [34].

This microstrip antenna array is printed on a 0.254-mm thick RT/Duroid 5880 ($\epsilon = 2.2$) and the distance between each antenna element is $0.77\lambda_{g-29\text{ GHz}}$. Low permittivity dielectric material is chosen to obtain good AR and impedance bandwidth. Figure 1.26 shows the measured S_{11} and axial ratio of this 64-element antenna array. The measurement results show that both the 10-dB return loss and 3-dB axial ratio bandwidth cover the frequency band of 27–31 GHz, which corresponds to a wide bandwidth of more than 13.8% with central frequency of 29 GHz. Moreover, the measured radiation patterns indicate that this antenna array exhibits a high polarization purity and good radiation performance, which means that the unwanted radiation from the feed lines has been largely reduced. The peak gain of this array is around 20 dBi and the efficiency is about 70%.

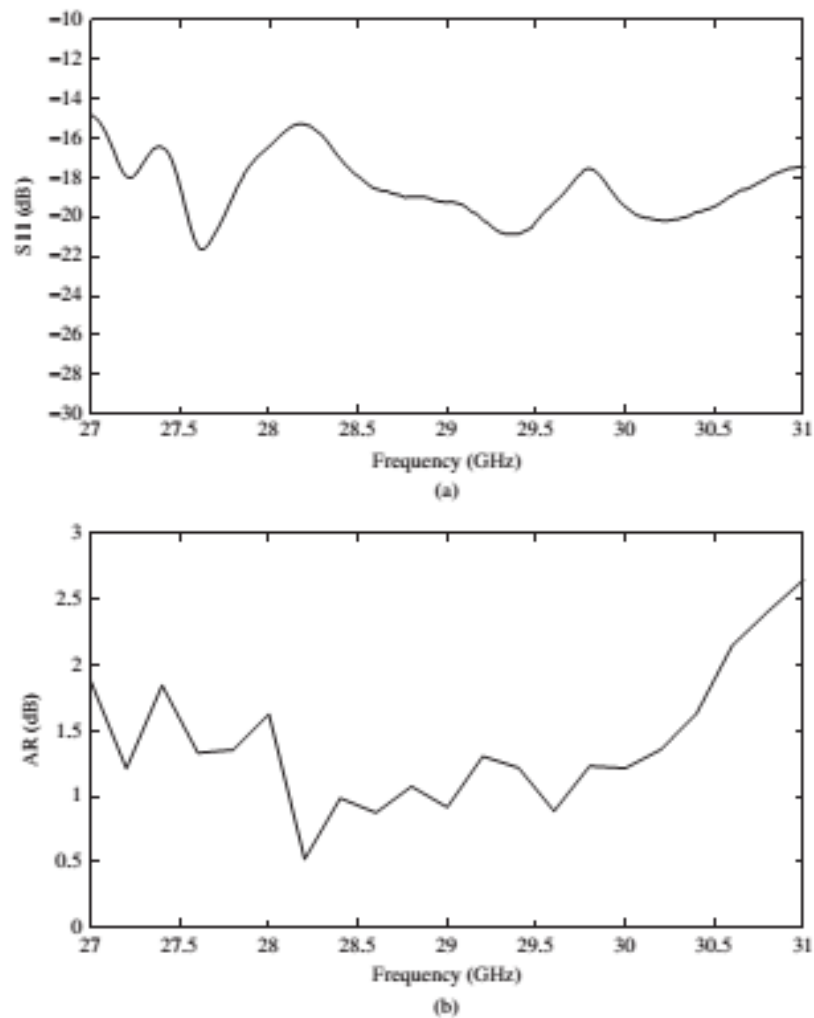
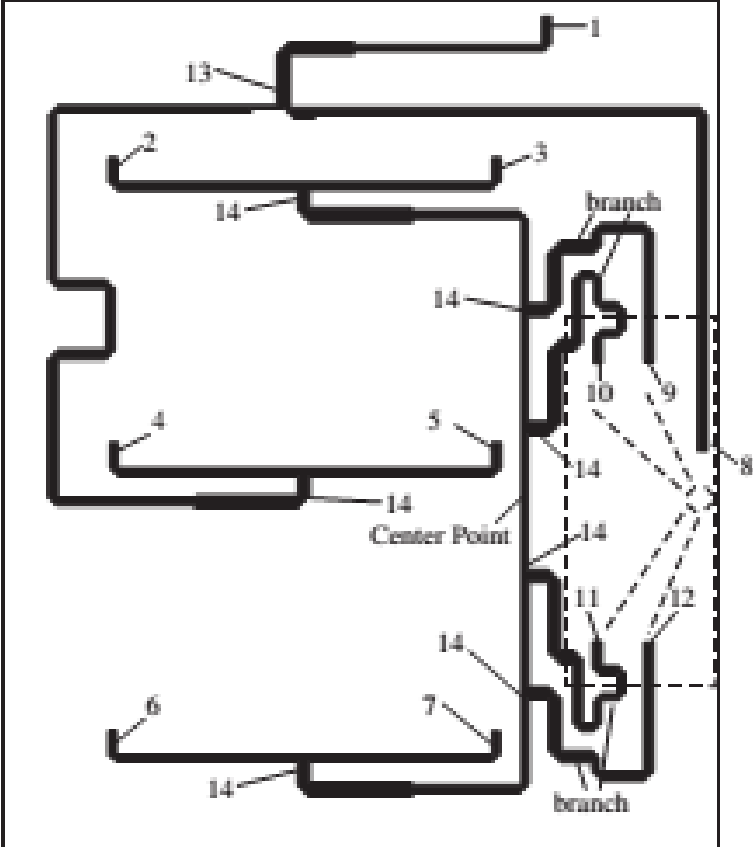
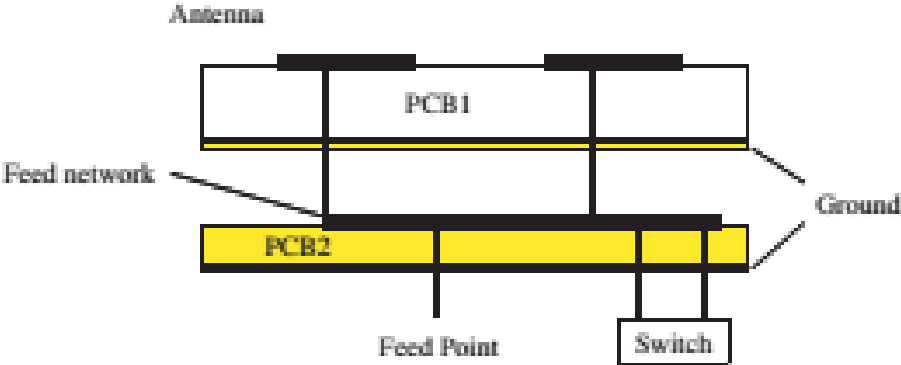


Figure 1.26: Measured S_{11} and AR bandwidth of the array using the double sequential rotation technique [34].

Purity and good radiation performance, which means that the unwanted radiation from the feed lines has been largely reduced. The peak gain of this array is around 20 dBi and the efficiency is about 70%.



(a)



(b)

Figure 1.27:The switch feed network for the switch-beam antenna array [35].

1.3.6 CP Array with Reconfigurable Beams

It is known that the total radiation field of the antenna array is determined by the vector addition of the far-fields radiated from the radiating elements. As the result, the radiation pattern of the antenna array can be controlled by adjusting the excitation amplitude and phase of the individual elements. The design of the CP antenna array has already been presented in the previous sections. In order to give the CP antenna array the ability to do the beam switching or beam-steering, it is critical to design a suitable feed network that is able to control the phase as well as the amplitude of the excitation signal for each antenna element. One method that can be employed to design a beam-switching CP antenna array is to use a reconfigurable switch feed network, such as the one presented in [35].

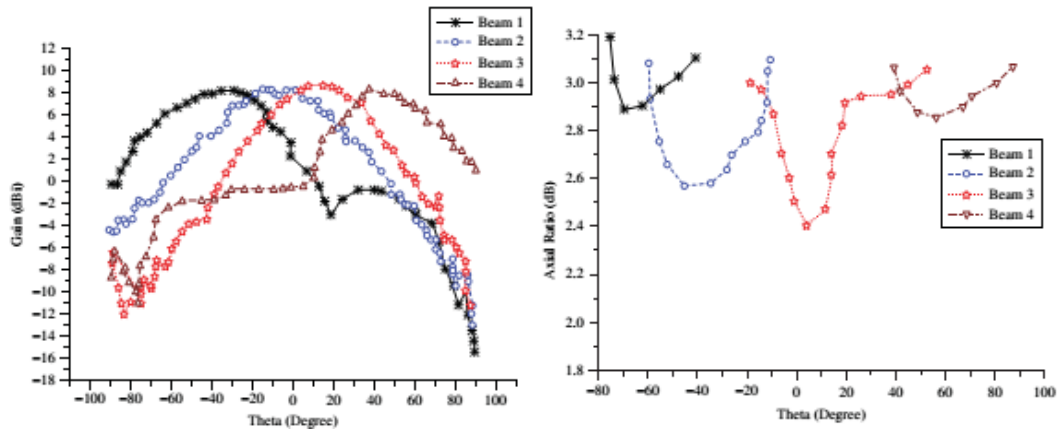


Figure 1.28 Measured radiation patterns and AR bandwidth of the antenna array with different sets of excitation phase [35].

The advantages of this technique are low cost and easy fabrication. Figure 1.27 shows the layout of the switch feed network proposed by [35] and the side view of the overall antenna array structure. To switch the main beam to different angles, a single-pole multi-throw (SPMT) microwave P-I-N switch is used, which can switch between different feed lines with varied length and can result a CP array with different excitation phase. The function of the ports labeled in the Figure 1.27 is explained in Table 1.2. The antenna element used in this design is a simple square patch with a feeding probe on the diagonal line of the patch. By connecting the Port 8 to a different input port of the feed line (Port 9 to Port 12), several sets of phase distribution for the radiating element can be created. For instance, by connecting Port 8 to Port 10, the excitation phase of the antenna array is $(0^\circ, 0^\circ, 140^\circ, 140^\circ, 275^\circ, 275^\circ)$.

Table 1.2: Meaning of the ports shown in Figure 1.24

	Function
Port 1	Input port
Port 2 to port 7	Output port for antenna feeding
Port 8	Input port connected to the SPMT
Port 9 to port 12	Input port for feeding lines with different phase

The antenna array is designed to operate at 1.8 GHz and is printed on a 3.8-mm thick substrate with a relative dielectric constant of 4.316. The feed network is printed on a 0.787-mm thick PCB board with relative dielectric constant of 2.55. Figure 1.28 shows the measured radiation patterns and AR bandwidth of this array. With different sets of excitation phase. It is found that this antenna array can have its main beam switched up to 40° with good CP radiation performance.

1.3.7 Beam-Switching CP Array using Butler Matrix Network

Another approach can be employed to design beam-switching CP antenna array is to use the Butler Matrix network. Butler matrix is a $2^n \times 2^n$ network with $2n$ input, 2^n output, $2^{n-1} \log_2 2^n$ hybrid junctions and some phase shifters. As the single layer microstrip printed circuit technique is used for the implementation of the matrix, there are several presences of cross lines in the planar layout, several crossovers are needed to isolate the signal. In this study, 4×4 Butler matrix has been designed because four beams are needed to produce by the system. The matrix has four inputs and four outputs, and it is implemented to excite an array of four patch radiating elements to produce four beams in desired directions.

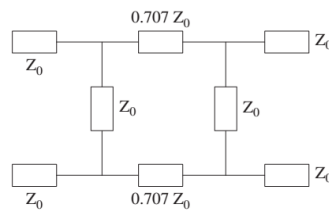


Figure 1.29: Circuit model of the branchline coupler.

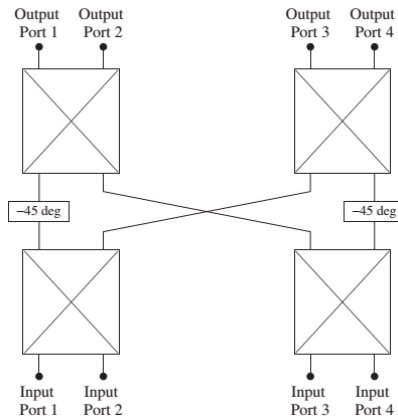


Figure 1.30: A generic version of a four-beam Butler Matrix.

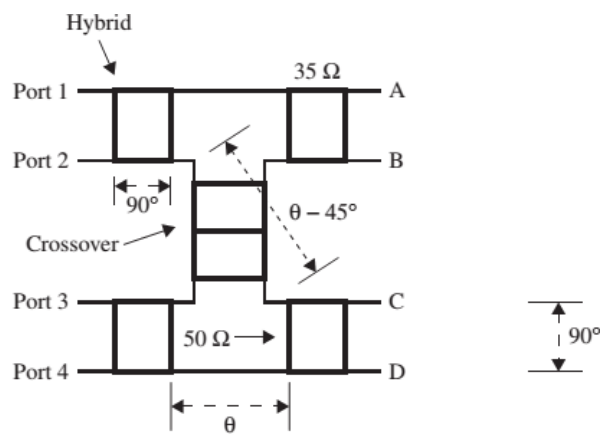


Figure 1.31: Layout of the feed network [36].

The Butler Matrix can be realized by a branchline quadrature coupler. The equivalent circuit model of the branchline coupler is depicted in Figure 1.29. In this model, each section of the transmission line has a length of quarter wavelength at the desired frequency. To produce more beams, several two-beam Butler Matrixes can be connected by introducing the crossover structure. Figure 1.30 shows a generic version of a four-beam Butler Matrix. Table 1.3 summarizes the phase of output signals when different ports are excited.

Table 1.3: the phase of output signal when different ports are excited

	Output port 1	Output port 2	Output port 3	Output port 4
Input port 1	-45	-90	-135	180
Input port 2	-135	0	135	-90
Input port 3	-90	135	0	-135
Input port 4	180	-135	-90	-45

Several beam-switching CP antenna arrays using the Butler Matrix as the feed network have been reported in the literature [36, 37, and 38]. In [36], a planar microstrip antenna array with a Butler Matrix is designed to operate at 2.4 GHz for indoor wireless dynamic environments. The microstrip antenna array consists of four sequentially rotated inset-fed rectangular patch antennas to achieve CP radiation. Figure 1.31 shows the layout of the feed network used in this design. The 4×4 Butler Matrix consists of four branchline couplers and a crossover to isolate the cross-lines. By selecting a different input port, different sets of the output phase can be produced and either RHCP or LHCP waves can be excited. Figure 1.32 shows the measured normalized radiation patterns of this microstrip antenna array at 2.4 GHz when different input port is excited. As can be seen from the measured results, RHCP can be obtained when port 1 or port 2 is selected while LHCP can be generated when port 3 or port 4 is excited. Moreover, beam-switching can also be reached when port 1/port 3 or port 2/port 4 is selected.

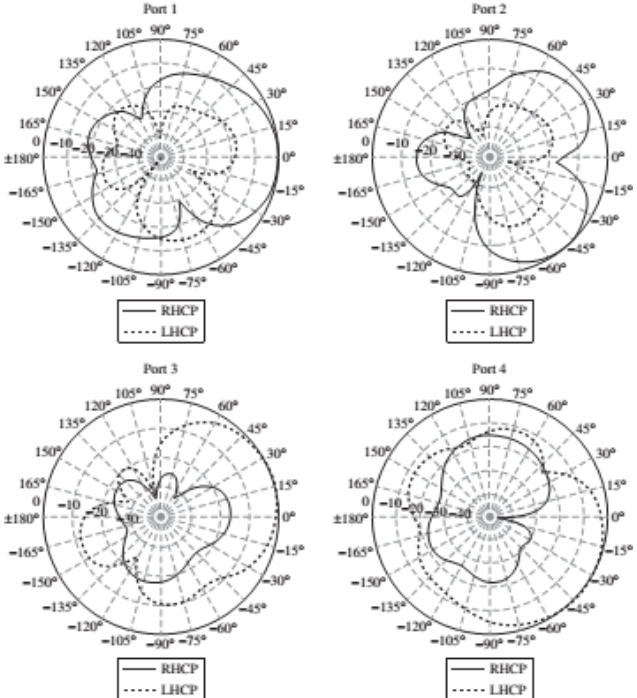


Figure 1.32: Measured normalized radiation patterns of the microstrip antenna array with different excitation port [36].

Similar design approaches are demonstrated in [37, 38], except that these CP arrays are designed to operate at different frequencies and different antenna elements are used.

Satellite technology is developing fast, and the applications for satellite technology are increasing all the time. Not only can satellites be used for radio communications, but they are also used for astronomy, weather forecasting, broadcasting, mapping and many more applications. With the variety of satellite frequency bands that can be used, designations have been developed so that they can be referred to easily. The higher frequency bands typically give access to wider bandwidths, but are also more susceptible to signal degradation due to 'rain fade' (the absorption of radio signals by atmospheric rain, snow or ice). Because of satellites' increased use, number and size, congestion has become a serious issue in the lower frequency bands. New technologies are being investigated so that higher bands can be used. C-Band Primarily used for satellite communications, for full-time satellite TV networks or raw satellite feeds. Commonly used in areas that are subject to tropical rainfall, since it is less susceptible to rainfade than Ku band (the original Telstar satellite had a transponder operating in this band, used to relay the first live transatlantic TV signal in 1962).

One of most important problem in satellite communication is employed of broadband and high gain CP antenna. In order to investigate its, in followe chapter step by step to design of CP antenna is mentioned. In two first section designing an antenna element with broadband impedance BW and CP BW is considered. Then, by utilizing and improving feed network is tried to enhance gain with save BW. Details and techniques of designing are mentioned in followe section.

2. PUBLISHED WORK

2.1 Circularly Polarized Square Slot Antenna Using Crooked T-Shape Technique

Source: *Applied Computational Electromagnetics Society Journal*. Mar2015, Vol. 30 Issue 3, p327-331. 5p.

2.1.1 Abstract

This paper presents the investigation results on a novel circularly polarized square slot antenna (CPSSA) designed to operate at a frequency of 5.5 GHz. In order to realize the proposed antenna, miniature circular polarized square slot antenna is used with L-shape and crooked T-shape grounded strips located at the slots opposite corners to reduce cross-polarization. The antenna is fed by coplanar waveguide. The 3 dB axial-ratio of the CPSSA extends to approximately 2 GHz. The CPSSA was designed to operate over the frequency range between 3 and 11.1 GHz corresponding to an impedance bandwidth of 115% for $VSWR < 2$. Acceptable agreement between the simulation and measured results validates the proposed design.

Index Terms — Circularly polarized, coplanar waveguide feed, planar antenna, slot antenna.

2.1.2 Introduction

Recently, circularly polarized planar patch antennas have gain more attention in the field of wireless communication. CPW-fed print slot antennas have many advantages, such as low profile, lightweight, ease of integration and wider impedance bandwidth; moreover, circularly polarized is much superior to linearly polarized duo to its agility of choosing polarization at the receiving locations and have good performance of anti-interference in bad weather [1-15]. For generating circular polarization (CP) radiation using a single feed, many microstrip antenna designs have been reported [1-9]. The

obtained CP bandwidth (3-dB axial-ratio bandwidth), however, is usually narrow and less than 2%. When the same microwave substrate is used, corresponding printed slot antennas usually have a much wider CP bandwidth than single-feed circularly polarized microstrip antennas [2]. To benefit from broadband and low profiles, various shapes and designs of broadband circularly polarized slot antennas have been developed to overcome both the narrow impedance and axial-ratio bandwidths (ARBWs) by applying different techniques on patch and ground structures [2-4]. In [9], by embedding two inverted-L-shaped grounded strips around two opposite corners of slot, circular polarization is obtained. The idea of embedding a T-shaped grounded metallic strip that is perpendicular to the axial direction of the CPW feed line is used in [4], and a corrugated slot antenna with a meander line is presented in [10]. In [11], a square slot antenna with a lightning-shaped feed line and inverted-L grounded strips is presented. To produce the circular polarization, the arc-shaped grounded metallic strip is utilized in [12-13]. In this letter, a novel design of a CPW-fed circularly polarized square slot antenna composed of a square ground plane, an inverted-L-shape strips, two crooked T-strips and a vertical stub is presented. In this design, 3-dB AR bandwidth can reach as large as 2000 MHz (5-7 GHz) which is about 33.3%, to cover the WLAN/WiMAX band. The proposed design also has the $VSWR \leq 2$ impedance bandwidth of 8100 MHz (3-11.1 GHz) which is about 115%. Details of the proposed antenna design and experimental results of the broadband operation are presented. The proposed of this article is designed an ultra-wide band antenna with utilizing of novel methodology which can be provided broadband circular polarization. The simultaneous use of the crooked T-shape and L-shape techniques has readied the above conditions.

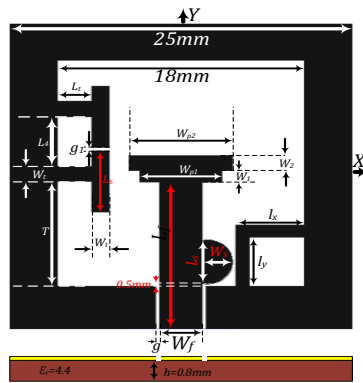


Figure 1: Configuration of the proposed CPSSA structure. Dimensions of the structure's parameters are: $W_f=3.1$, $L_t=8$, $g=0.3$, $h=0.8$, $W_t=1.25$, $W_{p1}=6$, $W_{p2}=7.6$, $L_s=3.5$, $W_s=3.5$, $g_1=0.4$, $L_4=4$, $W_1=1$, $W_2=1.2$, $L_t=2.5$, $l_x=5$, $l_y=4$, $L_6=4.5$ (units in mm).

2.1.3 Antenna Configuration

The geometrical layout and photograph of the proposed CPW-fed broadband CPSS antenna is shown in Figure 1. The proposed antenna is printed on a square microwave substrate FR4, with a side length of 25 mm, a thickness of 0.8 mm and a dielectric constant of relative permittivity $\epsilon_r=4.4$. The antenna is fed by a 50 Ω CPW feeding line, where the signal strip and gaps have widths of 3.1 and 0.3 mm, respectively.

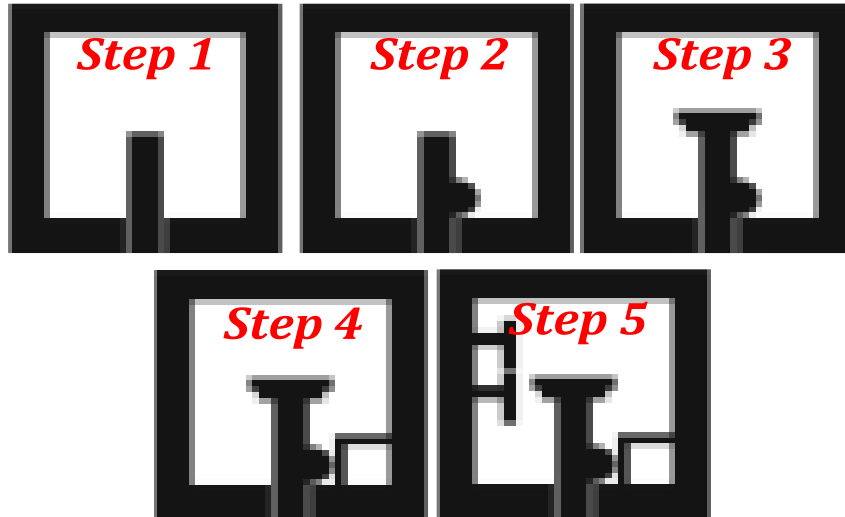


Figure 2: Five improved prototypes of the antenna

2.1.4 Experimental Results and Discussion

The simulated CPSSA structures have been fabricated using conventional printed circuit board (PCB) techniques. In each step of the design procedure, the full-wave analyses of the proposed antenna were performed using Ansoft HFSS (ver.11) based on the finite element method (FEM) to find optimized parameters of the antenna structure [13].

As indicated in Figure 2, five improved designs of the proposed CPSS antenna are presented. The antenna design is started by applying a simple strip feed line (step 1) and then improved through adding the vertical tuning stub formed by extending the feed section to the right (+y-direction) by a width of $W_s=3.5\text{mm}$ and a length of $L_s=3.5\text{mm}$ (step 2). Our simulations show that width (W_s) of the tuning stub has great effect on improving the impedance matching in the 3 dB AR band. A further improvement is achieved by adding two embedded rectangular strip patches with W_{p1} , W_{p2} , W_1 and W_2 dimensions (step 3). -10 dB impedance matching curves of the antenna are presented in Figure 3. As it is observed from Figure 3, by employing a

simple strip as the feed line, a great impedance mismatch is experienced (step 1) and consequently, any bandwidth of the antenna under -10 dB is available.

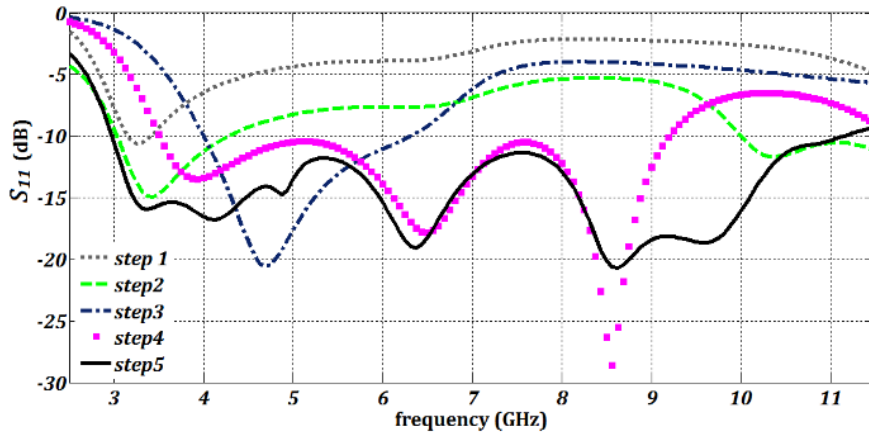


Figure 3: Improved S_{11} of the antenna (step 1~5)

By adding the vertical tuning stub and two embedded rectangular strip patches on the feed line, antenna operates between 4~6.3 GHz. The simulation results show that embedding rectangular strip patches on the feed line (step 1 - step 5) and adjusting the parameters, an improvement on the impedance bandwidth as well as CP characteristic can be accomplished for the proposed antenna. To obtain CP operation by exciting two orthogonal polarizations, the design is improved by adding an inverted-L strip to the right bottom corner of the structure. This structure is presented as step 4 in Figure 2. According to simulation results for step 4, we have found that choosing l_y and l_x of the inverted-L strips equal to 5 mm (0.275L), not only increases the ARBW but also improves impedance bandwidth. S_{11} variations of step 4 is presented in Figure 3. Considering the CP characteristic of the antenna, the changing regulation of the right hand side feed is similar to that of left hand side one. Through Figure 4, it can be observed that by adding an inverted-L strip to the antenna structure, a small improvement in the axial ratio of the antenna is created and antenna operates CP about 2.6% (7.4~7.6 GHz). To further improve the CP characteristic of the antenna, two crooked T-shape strips are sequentially added to the structure (step 5). As it is seen from Figure 3, adding two crooked T-shape strips to step 5 make the antenna operate UWB; and it can be seen in Figure 4, that the ARBW of the antenna is increased to 5~7 GHz for step 5.

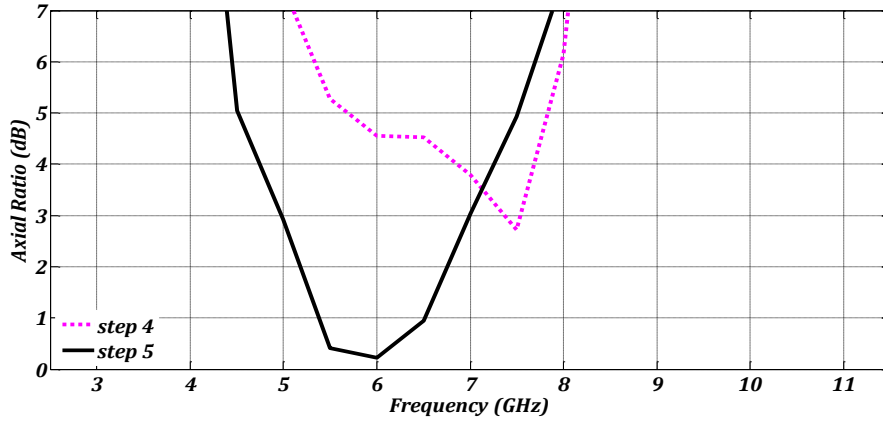


Figure 4: Improved axial ratio of the antenna (step 4~5)

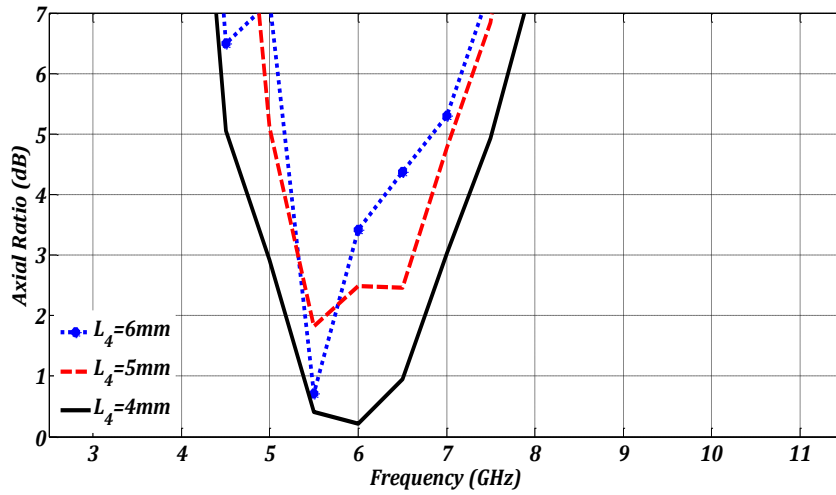


Figure 5: Axial ratio for different value of L_4

Through extensive simulations, it was found that length of the crooked T-shape strips (L_6) should be selected as $0.25L$, and the distance between them (L_4) should be $0.22L$, to attain the 33.3% ARBW. Changing the length or distance between these strips will degrade the axial ratio and subsequently CP characteristic of the antenna seriously. Considering Figure 5, it is understood that increasing the distance of L_4 will decrease axial ratio bandwidth. The simulation results of surface current distribution for antenna in step 5 are shown in Figure 6. As indicated in Figure 6, the current distribution of proposed antenna at counterclockwise. It is observed that the surface current distribution in 180° and 270° are equaling magnitude and opposite in phase of 0° and 90° . If the current rotates in the clockwise (CW) direction, the antenna can radiate the right-hand circular polarization (RHCP).

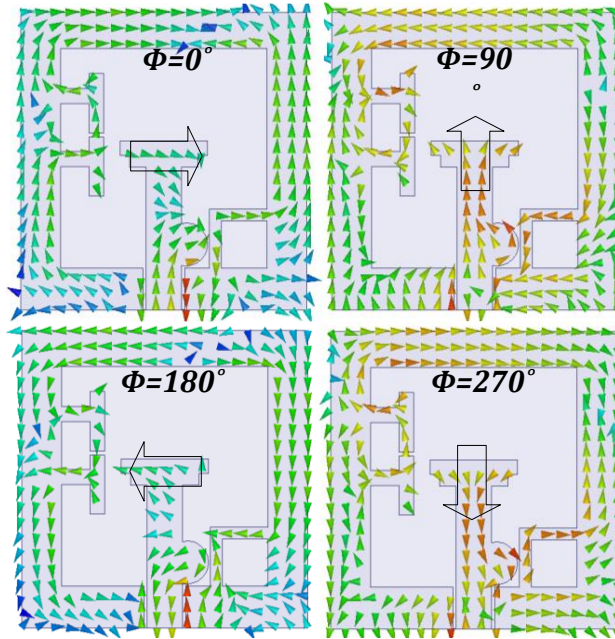


Figure 6: Distribution of the surface current on the feed and ground of the CPSS antenna at 5.5 GHz in 0° , 90° , 180° and 270° phase

An Agilent 8722ES vector network analyzer was used to measure S_{11} and impedance bandwidth for simplification in the antenna design. The simulated and measured S_{11} of the proposed antenna is shown in Figure 7. As seen in Figure 7, the simulated and measured impedance bandwidth of antenna are 115% (from 3 GHz to 11.1 GHz) and 119% (from 2.9 GHz to 11.5 GHz), respectively. The difference between measured and simulated impedance bandwidth are originating from different substrate specifications and fabricated problems.

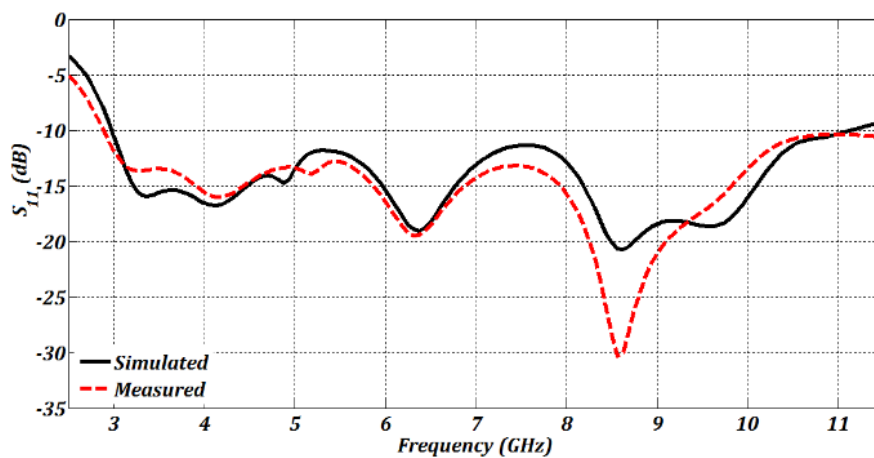


Figure 7: Measured and simulated S_{11}

Figure 8 indicated the close correspondence between the measured and simulated curves of gain and AR for the proposed antenna with optimized values presented in Figure 1. As plotted in Figure 8, the simulated ARBW of the suggested antenna is from 5000 MHz to 7000 MHz (33.3%), and the measured ARBW of antenna is from 5050 to 7100 (33.7%). Also, the measured peak gain of antenna is 4.25 dBic at 10 GHz. The average measured gain of the antenna is about 3.5 dBic. The measured results of the normalized radiation patterns of the CPSS antenna are presented in Figure 9. The radiation pattern is left-hand circular polarization (LHCP) for $z > 0$ and RHCP for $z < 0$, as can be deduced from surface current distributions in Figure 6. The proposed antenna has a compact size of 25 mm \times 25 mm. When compared with the previous CPSSA structures presented in Table 1, our proposed antenna shows significantly increased impedance bandwidth and axial-ratio bandwidth; i.e., the impedance and AR bandwidths are, respectively, more than three and two fold wider than the previous designs. Dielectric substrate used is FR4 with $\epsilon_r = 4.4$, $\tan \delta = 0.024$. The impedance bandwidth is for a frequency range where the $VSWR \leq 2$; and ARBW is the 3-dB axial-ratio bandwidth.

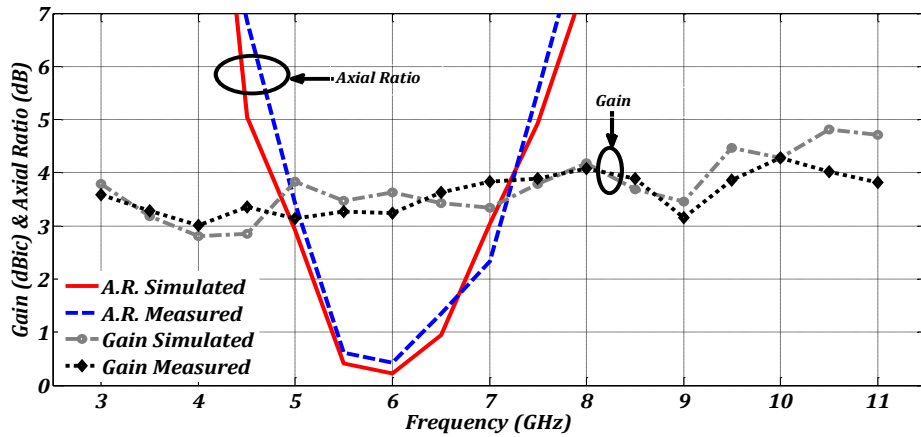


Figure 8: Measured and simulated gain and axial ratio of the CPSSA

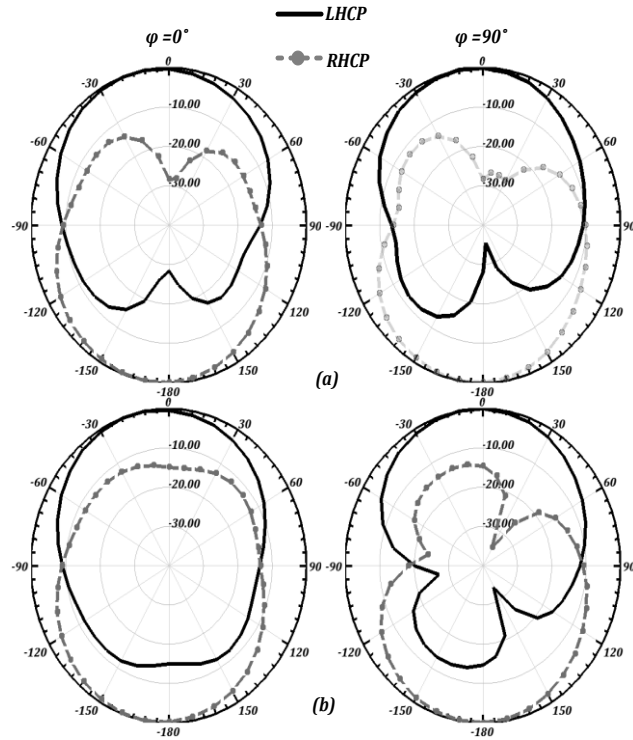


Figure 9: Measured normalized radiation patterns of the CPSS proposed antenna at: (a) 5.5 GHz, and (b) 6 GHz

Table 1: Comparison of the proposed CPSS antenna size and measured characteristics with other references

Ref.	Size (mm ³)	BW (GHz)	ARBW (freq. range) (GHz)	Peak Gain (dBic)
[3]	70×70×1.60	0.85 (1.75-2.6)	0.4 (1.7-2.1)	3.7
[4]	70×70×1.60	0.20(1.5-1.7)	0.3(1.5-1.8)	3.5
[5]	70×70×1.60	0.80(1.6-2.4)	0.2(1.8-2.0)	3.5
[14]	25×25×0.80	1.90(4.6-6.5)	0.8(4.9-5.7)	3.6
[15]	25×25×0.8	7.8(3.1-10.9)	2(4.5-6.5)	3.2
This work	25×25×0.80	8.6(2.9-11.5)	2(5-7)	4.25

The suggested antenna with optimal structure, as shown in Figure 10, was fabricated and tested in the Antenna Measurement Laboratory at Iran Telecommunication Research Center (ITRC).

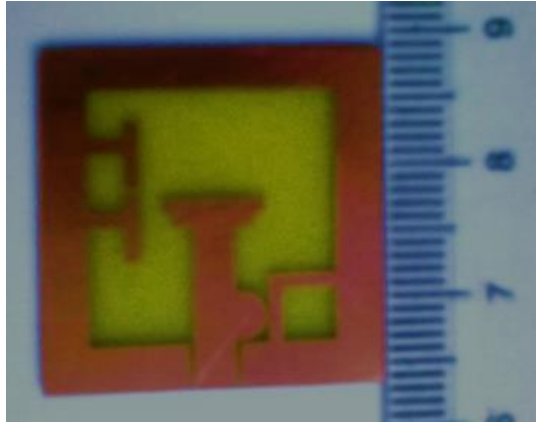


Figure 10: Photograph of fabricated Antenna.

2.1.5 Conclusion

This paper presents circularly polarized square slot antenna (CPSSA) fed by coplanar waveguide (CPW) with a crescent shaped patch. All of the important parameters that are determinant in antenna characteristics were depicted one by one while keeping the others fixed. The attributes of the proposed CPSSA include a relatively simple structure, low fabrication cost, and UWB operation across 3-11.1 GHz. The measured results show the impedance bandwidth is 115% for $VSWR < 2$, and axial-ratio < 3 dB is 33.3%. An antenna gain of around 3.5 dBic has been obtained.

References

- [1] J. Pourahmadazar and S. Mohammadi, "Compact circularly-polarised slot antenna for UWB applications," *Electron. Lett.*, vol. 45, no. 15, pp. 837-838, August 12, 2011.
- [2] J. Pourahmadazar, C. Ghobadi, J. Nourinia, N. Felegari, and H. Shirzad, "Broadband CPW-fed circularly polarized square slot antenna with inverted-L strips for UWB applications," *IEEE AWPL*, vol. 10, April 2011.
- [3] J. Y. Sze, K. L. Wong, and C. C. Huang, "Coplanar waveguide-fed square slot antenna for broadband circularly polarised radiation," *IEEE Trans. Antennas Propag.*, vol. 51, pp. 2141-2144, August 2003.
- [4] J. Y. Sze and Y. H. Ou, "Compact CPW-fed square aperture CP antenna for GPS and INMARSAT applications," *Microw. Opt. Technol. Lett.*, vol. 49, no. 2, pp. 427-430, February 2007.
- [5] C. C. Chou, K. H. Lin, and H. L. Su, "Broadband circularly polarized cross-patch-loaded square slot antenna," *Electron. Lett.*, vol. 43, no. 9, pp. 485-486, April 2007.
- [6] J. Y. Sze, J. C. Wang, and C. C. Chang, "Axial-ratio bandwidth enhancement of asymmetric-CPW-fed circularly-polarised square slot antenna," *Electron. Lett.*, vol. 44, no. 18, pp. 1048-1049, August 28, 2008.

- [7] J. Y. Sze and C. C. Chang, "Circularly polarized square slot antenna with a pair of inverted-L grounded strips," *IEEE Antennas Wireless Propag. Lett.*, vol. 7, pp. 149-151, 2008.
- [8] P. S. Hall, J. S. Dahele, and J. R. James, "Design principles of sequentially fed, wide bandwidth, circularly polarised microstrip antennas," *Proc. Microw. Antennas Propag.*, vol. 136, pp. 381-389, August 1989.
- [9] S. Fu, S. Fang, Z. Wang, and X. Li, "Broadband circularly polarized slot antenna array fed by asymmetric CPW for L-band applications," *IEEE AWPL Lett.*, vol. 8, pp. 1014-1015, September 2009.
- [10] J. Pourahmadazar and V. Rafii, "Broadband circularly polarized slot antenna array for L and S-band applications," *Electron. Lett.*, vol. 48, no. 10, pp. 542-543, 2012.
- [11] J. Huang, "A technique for an array to generate circular polarization with linearly polarized elements," *IEEE Trans. Antennas Propag.*, vol. AP-34, no. 9, pp. 1113-1119, September 1986.
- [12] S. Gao, Q. Yi, and A. Sambell, "Low-cost broadband circularly polarized printed antennas and array," *IEEE Antennas and Propagation Magazine*, vol. 49, no. 4, pp. 57-64, August 2007.
- A. Mousazadeh, M. Naser-Moghaddasi, F. Geran, S. Mohammadi, and P. Zibadoost, "Broadband CPW-fed circularly polarized square slot antenna with arc-shaped and inverted-L grounded strips," *Applied Computational Electromagnetics Society (ACES) Journal*, vol. 28, no. 4, pp. 314-320, April 2013.
- [13] V. Rafii, J. Nourinia, C. Ghobadi, J. Pourahmadazar, and B. S. Virdee, "Broadband circularly polarized slot antenna array using sequentially rotated technique for C-band applications," *IEEE Antennas and Wireless Propagation Letters*, vol. 12, pp. 128,131, 2013.
- [14] S. Karamzadeh, V. Rafii, M. Kartal, O. N. Ucan, and B. S. Virdee, "Circularly polarised array antenna with cascade feed network for broadband application in C-band," *Electronics Letters*, vol. 50, no. 17, pp. 1184,1186, August 14, 2014.

2.2 Compact UWB CP Square Slot Antenna with Two Corner Connected by a Strip Line

Source: *Electronics letters*, August 2015 doi: 10.1049/el.2015.2817.

2.2.1 Abstract

This paper proposes a novel method to design a compact, broadband circularly polarized square slot antenna with a considerably wide AR bandwidth. A coplanar waveguide fed square slot antenna with an impedance matching stub and a cross-shape radiating patch together with a strip line that connects the two opposite corners of the ground section is designed to provide the desired characteristics. The obtained results for the proposed antenna give us a good agreement with the expected performance with a compact size of 20×20mm. The measured impedance bandwidth is as large as 11050 MHz (2950–14000 MHz) or about 130.38% with respect to the center frequency. The measured 3-dB AR is 3373 MHz (35.7%) from 3729 to 7102 MHz and the average measured gain of CPSSA is almost 3.5 dBi in the operating band.

2.2.2 Introduction

Due to the capability of preventing multipath interference and flexibility in orientation angle between transmitting and receiving antennas, circularly polarized (CP) antennas are required for many applications, such as satellite and mobile communications [1]. CP square slot antenna (CPSSA) with broadband impedance and 3-dB axial ratio (AR) bandwidth have considerably role in CP antenna. Hitherto, many studies have been reported about design methods of broadband CPSSA [1-9]. In [2], a broad CP operation is achieved by protruding the T-shaped metallic strip from the ground plane toward the slot center and a coplanar waveguide (CPW) feeding with a protruded signal strip that is perpendicular to the T-shaped strip. A broadband CPW-Fed CPSSA operation can be attained by using lightning-shaped feedline and a pair of inverted-L strips grounded into the slot and adjusting the dimensions of the lightning-shaped feedline [3]. It is reported that some single-layer antenna composed of a square ground plane embedded with two [4-6] and three [7] inverted-L strips around corners of the slot. In [8], it is presented a new design of a CPW-fed CPSSA loaded with cross-patch embedded in the square slot. A printed wide-slot antenna with an inverted-L tuning stub extended from the signal line of the feeding CPW and a pair of grounded strips

fixed in the slot is proposed in [9]. In [10], a CPW-fed CPSSA including a pair of rectangular-shaped notches located at two opposite corners of the slot and a pair of reverse L-shaped ground arms in the slot for realizing circularly polarized radiation is proposed for enhancing impedance bandwidth.

The aim of this paper is to present a compact size CPSSA by using novel methods. Implementation of novel methods in CPSSA can cover an impedance bandwidth (BW) of 130.38% and axial ratio bandwidth of 35.7%. Table 1 shows the comparison of the performance of the proposed antenna with the other works using CPSSA technique. It is clearly seen that proposed antenna is superior to others in every aspects with the exception impedance BW of reference [10]. The reason of this exception is that lower frequencies are better covered at larger scales, since a lower frequency requires antennas with larger physical size.

Table 1. Comparison of the proposed CPSSA with recent similar works

reference	Size (mm ³)	Impedance BW(MHz) S11<-10dB ($f_h \sim f_l$) (f_h-f_l)	3dB Axial Ratio BW ($f_h \sim f_l$) (f_h-f_l)
[2]	70×70×1.6	(1750~2624) (874)	(1850-2070) (220)
[3]	60×60×0.8	(2023~3421) (1398)	(2075-3415) (1340)
[4]	25×25×0.8	(2985~11232) (8247)	(5012~7382) (2370)
[5]	60×60×0.7	(1600~3055) (1455)	(2300-3030) (730)
[6]	60×60×0.8	(2674~13124) (10450)	(4995-6945) (1950)
[7]	60×60×0.8	(2000~7071) (5071)	(2030-5120) (3090)
[8]	70×70×1.6	(1604~2450) (846)	(1840~2080) (240)
[9]	60×60×0.76	(1772~2591) (819)	(1880~2560) (680)
[10]	25×25×0.8	(2760~14820) (12060)	(4270-6130) (1860)
This work	20×20×0.8	(2950~14000) (11050)	(3729-7102) (3373)

2.2.3 Antenna design

The proposed CPSSA is printed on 0.8mm thickness of FR4 substrate (20×20 mm²) with relative permittivity $\epsilon_r=4.4$ and loss tang of 0.02. As seen in Figure 1, the antenna consists of a single radiating cross shaped patch and is excited by a CPW feed-line. The dimensions of the CPW feed-line dimensions of 2.48 and 5.8 mm correspond to a characteristic impedance of 50 Ω . The CPW gap size is 0.24mm. In order to prevent

the current accumulation at two opposite corners of the ground loop of CPSSA, a strip line connecting the two opposite corners is used. This connection leads to increase CP bandwidth and, because of the effective length of the radiation element is increased, the impedance BW is also improved in a compact size. The optimized dimensions of the antenna structure are given in Figure 1a. All parameters have been optimized using finite element methods by commercial HFSS software. The stages describing the evolution of the antenna structure are shown in Figure 1b. A feed line is constructed within the rectangular slot in the first stage; in the second stage, in order to increase radiation resistant a cross-shape patch is embedded following the feed line; the third stage involves the feedline modification by adding a circular stub to ensure impedance matching; finally a strip line which connected at two opposite corners of the grounded loop is added.

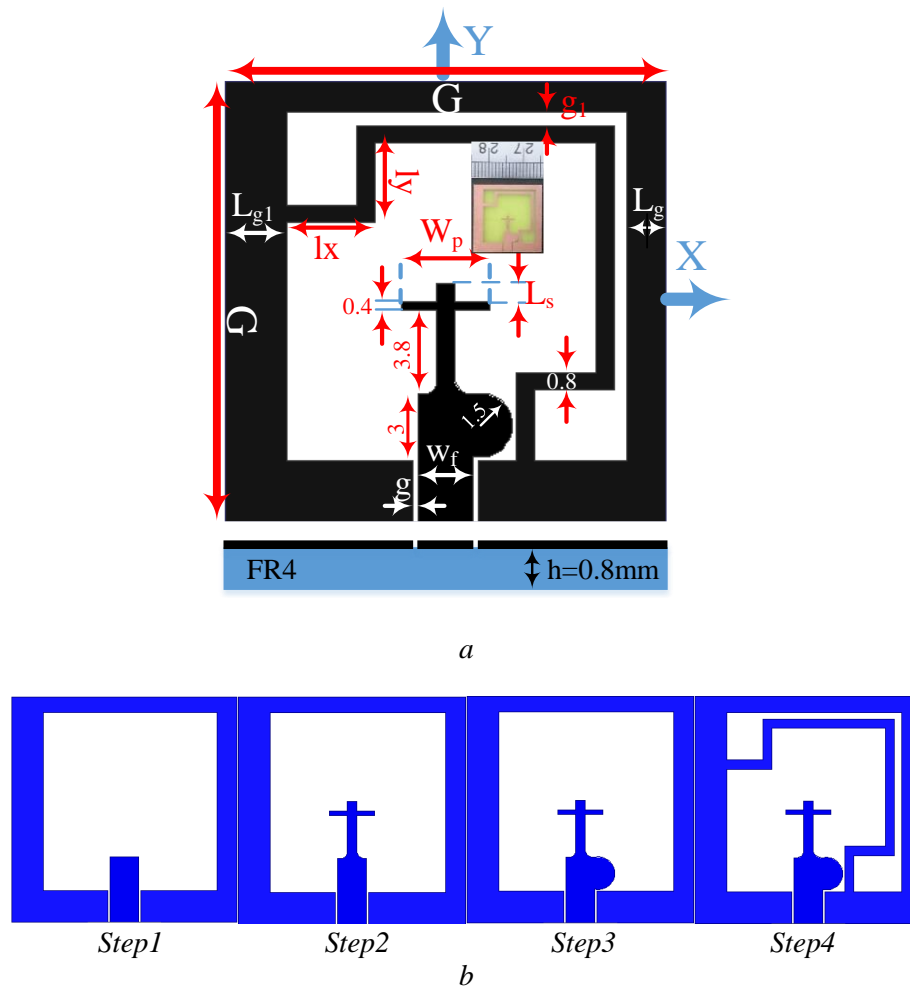
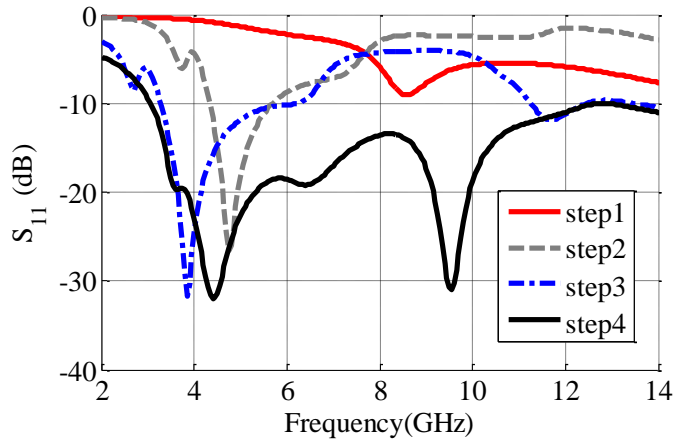
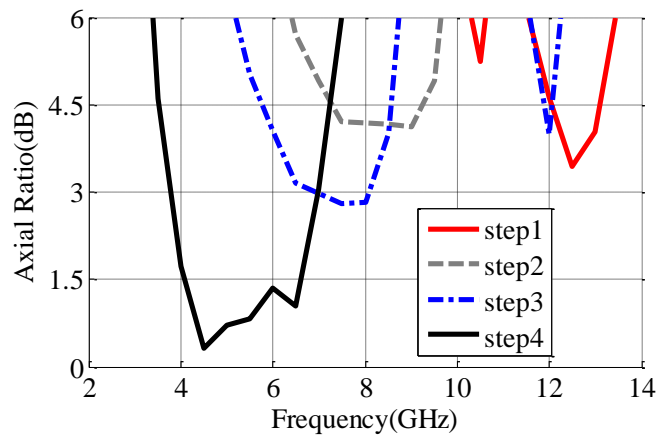


Figure 1: Configuration and design steps of the CPSSA ($G=20$; $L_{g1}=2.8$; $L_{g2}=1.8$; $L_x=4$; $L_y=3.6$, $L_s=0.8$; $W_p=4$; $g_1=0.6$; $g=0.24$; $W_f=2.48$)(all value in mm); a)Basic structure of proposed antenna; and b) Design steps.



a



b

Figure 2: Simulation result of S_{11} and AR of antenna in four implementation steps; a) S_{11} response of antenna; and b) AR curves of antenna.

The return loss response (S_{11}) and the 3-dB axial ratio (AR) bandwidth of the CPSSA in the four stages are displayed in Figure 2. Results show that sequential steps improve the impedance and 3dB AR bandwidths of the antenna. Application of strip line connector in the fourth step creates additional surface current paths and prevents of aggregation of current in opposite corner which significantly increase impedance band width (IBW) to 11050 MHz (2950~14000MHz) for $S_{11} \leq -10$ dB. The addition of ground-plane strip line in the fourth step significantly enhances ARBW between 3729 and 7102 GHz for an $AR \leq 3$ dB.

2.2.4 Results and discussions:

The simulated CPSSA structure was fabricated by the printed circuit board (PCB) technique. The S_{11} response of the CPSSA was measured by utilizing the Agilent 8722ES network analyzer. Figure 3 displays measured and simulated S_{11} comparison

of the proposed antenna. Worthy impedance matching of measured and simulated S_{11} is obtained. It is seen that the measured impedance BW ($S_{11} < -10\text{dB}$) is as large as 11050MHz (2950–14000 MHz) or about 130.38% with respect to the center frequency at 8475 MHz.

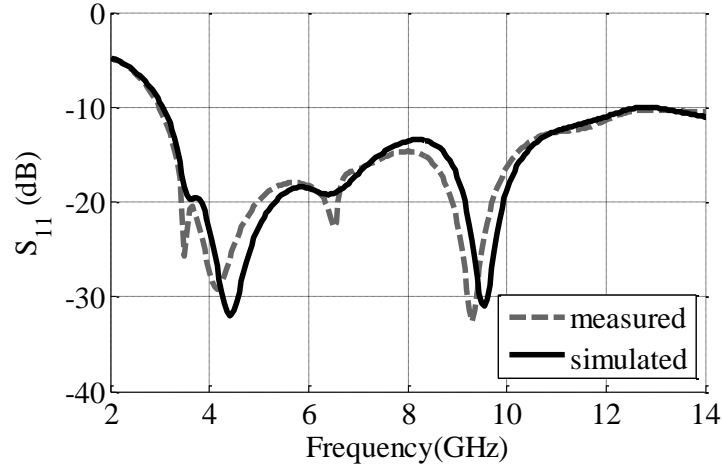


Figure 3: Comparison between measured and simulated S_{11} of proposed CPSSA.

For measuring the axial ratio and gain of the fabricated antenna, a standard dipole antenna and a log periodic antenna were used in two orientations, respectively. In order to measure the gain of CPSSA, vertical (G_{TV}) and horizontal (G_{TH}) of gain in linear state are combined to yield the total CP gain as [7]:

$$G_T = 10 \text{ Log } (G_{TV} + G_{TH}) \text{ [dBic].}$$

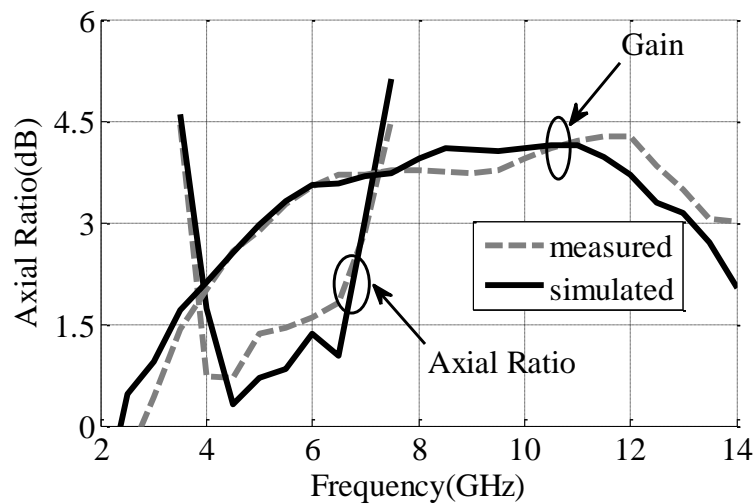


Figure 4: Measured and simulated AR and gain of CPSSA.

The simulated and measured gains and AR curves are demonstrated in Figure 4. The measured 3-dB AR is 3373 MHz (35.7%) from 3729 to 7102 MHz and the average

measured gain of CPSSA is almost 3.5 dBi in the operating band (2950–14000 MHz), and the peak gain is about 4.2 dBi at 12GHz. As seen in Fig 4, a close correspondence between the measured and simulated results is obtained and whatever difference is assigned to dielectric loss, measurement errors and fabrication tolerance. Figure 5 depicted the measured normalized RHCP and LHCP radiation characteristics of the antenna at 5.1 (Figure 5a) and 6.5 GHz (Figure 5b). As seen in Figure 5, the CPSSA is generated RHCP in the +z direction and LHCP in the -z-direction.

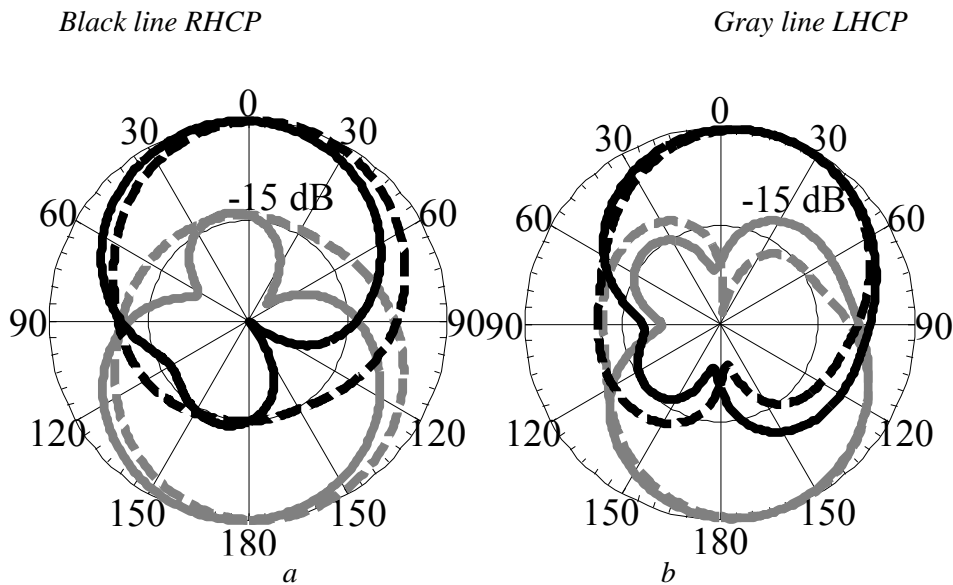


Figure 5: Measured RHCP and LHCP patterns of proposed CPSSA (Solid line is $\phi=0^\circ$ and dash line is $\phi=90^\circ$); a) 5.1GHz; and b) 6.5GHz.

2.2.5 Conclusion:

A new compact broadband circularly polarized square slot antenna is design and fabricated in this work. To improve the impedance and AR bandwidth of the antenna in a compact sized structure, impedance matching section and antenna radiation patch elements are designed and optimized. The most important improvement for the proposed antenna is performed by applying an additional current path that connects the two opposite corners of the ground layer. This technique, by preventing the current accumulation at the corners, gives us a significant enhancement for the impedance and AR bandwidths and thus allows this design to come to a challenging position among the other similar works.

References

- [1] Ding, K., Gao, C., Yu, T.-b. and Qu, D.-x. (2015), CPW-fed C-shaped slot antenna for broadband circularly polarized radiation. *Int J RF and Microwave Comp Aid Eng.* doi: 10.1002/mmce.20909
- [2] Jia-Yi Sze; Kin-Lu Wong; Chieh-Chin Huang, "Coplanar waveguide-fed square slot antenna for broadband circularly polarized radiation," *Antennas and Propagation, IEEE Transactions on* , vol.51, no.8, pp.2141,2144, Aug. 2003 doi: 10.1109/TAP.2003.815421
- [3] Jia-Yi Sze; Hsu, C.-I.G.; Zhi-Wei Chen; Chi-Chaan Chang, "Broadband CPW-Fed Circularly Polarized Square Slot Antenna With Lightning-Shaped Feedline and Inverted-L Grounded Strips," *Antennas and Propagation, IEEE Transactions on* , vol.58, no.3, pp.973,977, March 2010 doi: 10.1109/TAP.2009.2039335.
- [4] Pourahmadazar, J.; Mohammadi, S., "Compact circularly-polarised slot antenna for UWB applications," *Electronics Letters* , vol.47, no.15, pp.837,838, July 21 2011 doi: 10.1049/el.2011.1430
- [5] Jia-Yi Sze; Chi-Chaan Chang, "Circularly Polarized Square Slot Antenna With a Pair of Inverted-L Grounded Strips," *Antennas and Wireless Propagation Letters, IEEE* , vol.7, no., pp.149,151, 2008 doi: 10.1109/LAWP.2008.921341
- [6] Pourahmadazar, J.; Ghobadi, C.; Nourinia, J.; Felegari, N.; Shirzad, H., "Broadband CPW-Fed Circularly Polarized Square Slot Antenna With Inverted-L Strips for UWB Applications," *Antennas and Wireless Propagation Letters, IEEE* , vol.10, no., pp.369,372, 2011 doi: 10.1109/LAWP.2011.2147271
- [7] Felegari, N.; Nourinia, J.; Ghobadi, C.; Pourahmadazar, J., "Broadband CPW-Fed Circularly Polarized Square Slot Antenna With Three Inverted-L-Shape Grounded Strips," *Antennas and Wireless Propagation Letters, IEEE* , vol.10, no., pp.274,277, 2011 doi: 10.1109/LAWP.2011.2135832
- [8] Chou, C.C.; Lin, K.-H.; Su, H.L., "Broadband circularly polarised crosspatch-loaded square slot antenna," *Electronics Letters* , vol.43, no.9, pp.485,486, April 26 2007 doi: 10.1049/el:2007018
- [9] Sze, J.-Y.; Wang, J.-C.; Chang, C.-C., "Axial-ratio bandwidth enhancement of asymmetric-CPW-fed circularly-polarised square slot antenna," *Electronics Letters* , vol.44, no.18, pp.1048,1049, August 28 2008 doi: 10.1049/el:20081858
- [10] Shokri, M.; Rafii, V.; Karamzadeh, S.; Amiri, Z.; Virdee, B., "Miniaturised ultra-wideband circularly polarised antenna with modified ground plane," *Electronics Letters* , vol.50, no.24, pp.1786,1788, 11 20 2014 doi: 10.1049/el.2014.3278.

2.3 Circularly Polarized Slot Antenna Array with Sequentially Rotated Feed Network for Broadband Application

Source: *International Journal of RF and Microwave Computer-Aided Engineering*, Volume 25, Issue 4, May 2015, p. 358-363.

2.3.1 Abstract

This paper presents a novel Circularly Polarized Sequentially rotated Slot Antenna Array (CPSSAA) designed to operate at a frequency of 5.5GHz. This antenna is suitable for communication applications such as WLAN/WiMAX. Method of feeding is based on sequential rotation with seven quarter-wavelength transformers. In this case, the elements with 200 ohm impedance could be replaced by other elements with different input impedance. Reducing the elements input impedance, maximum power can be transferred to the elements. Because the lower losses in transmission line occur in presence of lower impedance, the 3 dB axial-ratio bandwidth of the CPSSAA extends to approximately 1.3 GHz. The CPSSAA was designed to operate over the frequency range between 4.5 and 6.4 GHz corresponding to an impedance bandwidth of 34.86% for VSWR<2. Acceptable agreement between the simulation and measured results validates the proposed design. © 2009 Wiley Periodicals, Inc. *Int. J RF and Microwave*

Keywords: Planar Antenna, Slot antenna, Array Antenna, Circularly Polarized, Feed Network

2.3.2 Introduction

The use of circularly polarized (CP) antennas have advantages such as: very effective in combating multi-path interferences or fading, able to reduce the ‘Faraday rotation’ effect due to the ionosphere and no strict orientation between transmitting and receiving antennas are required[1-23]. The inherent narrow axial-ratio (AR) bandwidth of the conventional patch antenna leads to limit their applications. The printed CP slot antennas attract much attention due to their capabilities of providing wide impedance and AR bandwidths while maintaining the low profile. Coplanar Waveguide (CPW) and microstrip line feeds are the most preferred feeding structures for the slot antenna design. Hitherto, several feed techniques are introduced for

achieving CP property in microstrip arrays, for instance: (I) series feed [3] (II) parallel feed [4] and (III) sequentially rotation feed [5]. Methods I & II are traditional and have some drawbacks in realization of this types of arrays, which can be noted: increment effective length of array and hard to realize in method I, unbalanced pattern and mutual coupling effect between elements and feed network in method II. Many researches have been suggested the coplanar corporate-fed arrays that consist of sequentially rotated circularly polarized elements [1], [5], [19], [22] and [23] and a significant improvement has been achieved in the axial-ratio bandwidth. However, such feeding structures for microstrip patch arrays leads to performance deteriorations due to feed radiation [10]. Then, to overcome this problem, coplanar serial-fed antenna arrays have been reported in [13]–[21]. The serial feed sequentially rotated element technique improves the bandwidth, radiation pattern, and polarization purity over a wider frequency band compared to the classical coplanar corporate feed network, but thin substrate is recommended at the cost of narrow bandwidth [17]. Besides additionally, 3-dB axial-ratio bandwidth of the antenna arrays is no more than 20%. One of the ways that leads to greater gain and CP bandwidth in antenna array will be used the circularly polarized element. The antennas composed of linearly polarized elements leads to a gain reduction exceeding 4 dB compared to that for circularly polarized elements when the element spacing exceeds 0.75 of free-space wavelength [1-2].

The most important characteristic of this antenna is to use an element with input impedance of 50 Ohm. Generally, an element with 200 Ohm input impedance element was used and to match with 50 Ohm input impedance, two 200 Ohm impedances were placed. On the other hand, low input impedance value of radiated element causes an increase in power into the element and increase in gain too. The other important characteristic of this antenna is the usage of gapped ground at the bottom of the element which causes yields an increase in the bandwidth of the whole array. The general opposite relationship between gain and bandwidth stands here too [16]. But in this paper the proposed method which has used an element with low impedance, results in adjustment in gain of the Antenna. A broadband circularly polarized array antenna composed of the circularly polarized elements fed by the microstrip lines is presented. A detail of the antenna configuration, simulation, and practical results for the proposed array antenna are discussed. This paper is organized as follows. Section 2 describes the design and configuration of the broadband circularly polarized antenna element.

Section 3 explains the design of the broadband circularly polarized 2×2 antenna array. Both measured and simulated results are presented and discussed. Section 4 gives the conclusions.

2.3.3 Single Element Design

The geometry and dimensions of the proposed CP slot antenna element is shown in Figure 1. The antenna array element has been designed on FR4 dielectric substrate with relative permittivity $\epsilon_r = 4.4$, and loss tangent ($\tan\delta$) = 0.02. The dimensions of element are $30 \times 30 \times 0.8 \text{ mm}^3$, where the parameters defining the structure (units in millimeter) is given in Table I.

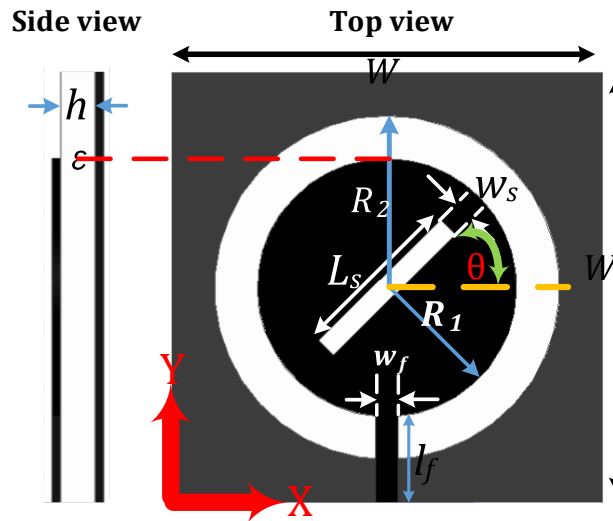


Figure1: Geometry of the proposed circularly polarized slot antenna.

Table 1: The optimized geometrical parameters of the antenna element

Parameter	Value(mm)	Parameter	Value(mm)
W	30	W_s, W_f	1.5
R_1	9	L_f	6
R_2, L_s	12	h	0.8

The antenna array element is consist of a circular slot with a radius R_2 is etched on the ground plane with an area of $W \times W$ and a rectangular slot is notched on the circular disk with a radius R_1 . All parameters of the proposed single element antenna has designed and optimized by High Frequency Structure Simulator (Ansoft HFSS v.13). To achieve the 50Ω microstrip fed line is utilized of $W_f = 1.5\text{mm}$. To attain a deeper insight of how the antenna's parameters influence its performance a parametric study was necessary. Figure 2 shows the effect of the length parameter R_2 on the antenna's

S_{11} response. As shown in Figure 2, R_2 mainly affects the impedance frequency bandwidth. This is the key parameter that enables the desired WLAN Band (5-6 GHz) for which $R_2 = 12\text{mm}$. Furthermore Figure 3 shows the simulated 3dB axial ratio characteristics of the antenna as a function of angle θ . When θ is changed from 15 degree to 30 degree, the 3dB axial ratio bandwidth at maximum direct of gain increasing from 0% to at around 9%. Therefore through this analysis θ was fixed at 30 degree.

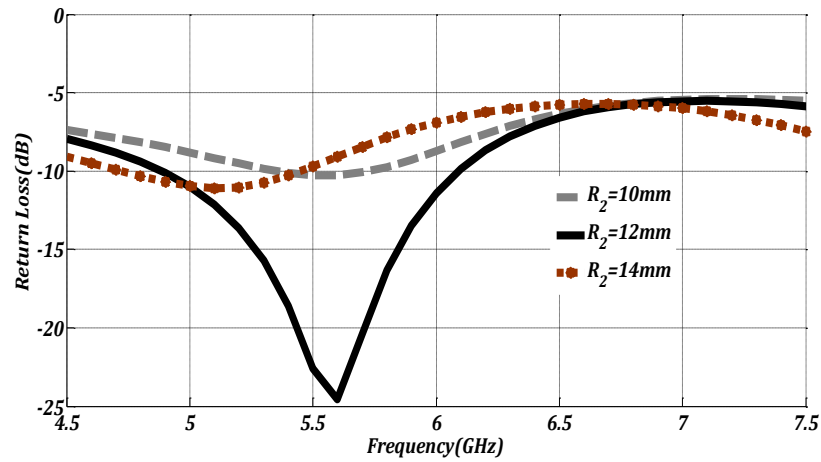


Figure 2: the S_{11} curve for various patch slot length R_2 as a function of frequency.

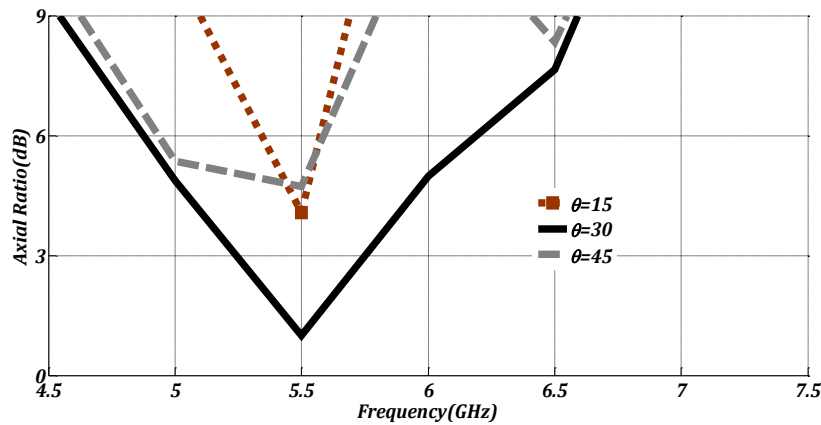


Figure 3: Simulated axial ratio for changing angle θ .

The current distribution on the disk is changed by the rectangular slot. The rectangular slot alters the current distribution on the disk to excite the circular slot to generate LHCP radiation in +z direction. The AR bandwidth of the antenna can be improved by tuning the size (L_s and w_s) and angle (θ) of the rectangular slot. The resonant frequency is mainly determined by the size of the circular disk and circular slot. A parametric study is undertaken to evaluate the effects of the antenna dimensions on the return loss and AR. The proposed CP Antenna has an area of 900 mm^2 ($30\text{ mm} \times 30$

mm), which is considerably less than the previously published slot antennas as summarized in Table II along with other salient parameters. Compared to other similar types of CP slot antennas fabricated on the same substrate the proposed antenna exhibits an impedance bandwidth which is significantly larger and with no reduction in the gain performance, as well as having a larger circular polarization bandwidth. The gain is comparable to previous designs.

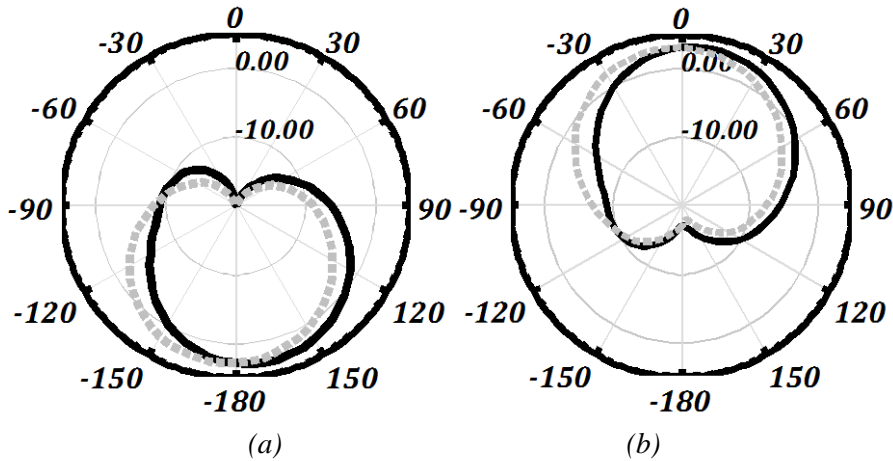


Figure 4: the simulated pattern of single element antenna (a) RHCP (b) LHCP at 5.5GHz.

Table 2: Comparison of the proposed cpssa antenna size and measured characteristics with other references. Dielectric substrate used is FR4 with $\epsilon_r=4.4$, $\tan\sigma=0.024$. the impedance bandwidth is for a frequency range where the VSWR ≤ 2 ; and ARBW is the 3-dB axial-ratio bandwidth.

Ref.	Size (mm ³)	BW (GHz)	3dB ARBW (GHz)	Peak Gain (dBic)
[17]	70×70×1.60	0.85 (1.75-2.6)	0.4 (1.7-2.1)	3.7
[18]	70×70×1.60	0.20 (1.5-1.7)	0.3 (1.5-1.8)	3.5
[19]	70×70×1.60	0.80 (1.6-2.4)	0.2 (1.8-2.0)	3.5
[20]	60×60×0.76	0.80 (1.7-2.5)	0.7 (1.8-2.5)	3.5
[21]	60×60×0.74	1.40 (1.6-3.0)	0.7 (2.3-3.0)	4.0
This work	30×30×0.80	1.2 (4.9-6.1)	0.5 (5.25-5.75)	3.7

2.3.4 Feed Network Design

Effects of the sequentially rotated technique in constructing antenna array have been reported in many papers [1], [5], [22] and [23]. A 2×2 sequentially rotated array is designed by using the proposed broadband circularly polarized slot antenna. The proposed CP feed network consists of seven quarter-wavelength transformers that are

linked together in a sequential rotation manner with alternative parallel and series connections to form a four port network. Ports 1–4 are output ports, which are connected to respective microstrip patch elements with their impedance $Z=50\Omega$ (as shown in Figure 1). Consequently, all four patch elements are positioned symmetrically and can generate a circular polarization with good axial ratios. Seven quarter-wave transformers were designed in a circular shape, in order to reduce the discontinuity.

All the line sections are a quarter-wavelength in length, but with different characteristic impedances. The network then produces a phase shift of 90° and equal power split between adjacent output ports. In other words, the signal amplitudes at the four ports that are fed to each patch element are theoretically identical, but with a 90° phase difference among two adjacent ports. The required input impedance to the overall feed network or the main input feed line is $Z_0=50\Omega$. The configuration of the array network was designed and simulated by using Agilent™ Advance Design System (ADS) commercial software. The simulated S, as a function of frequency is presented in Figure 6a.

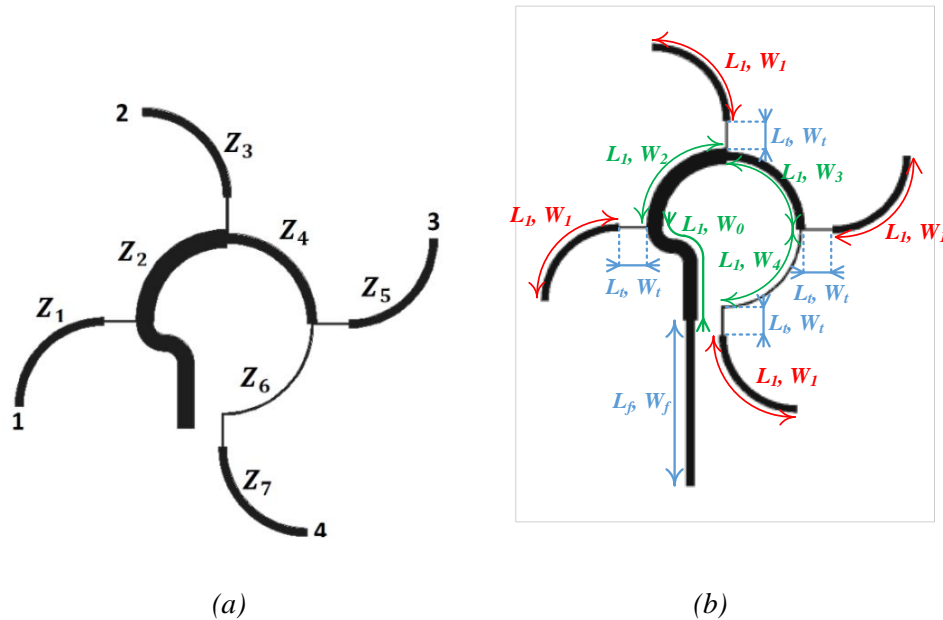
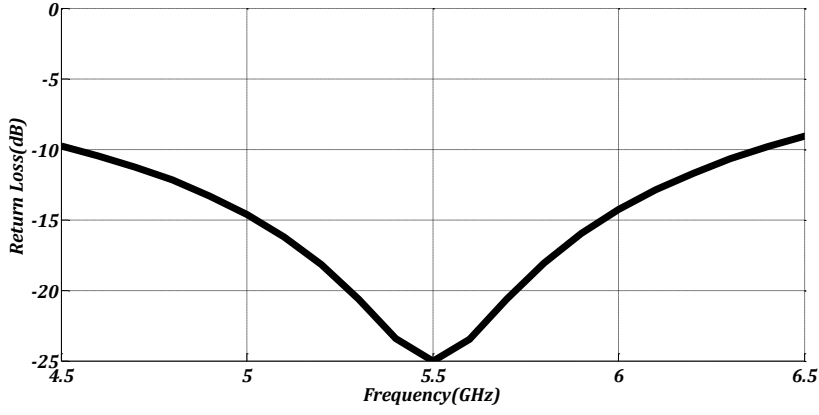
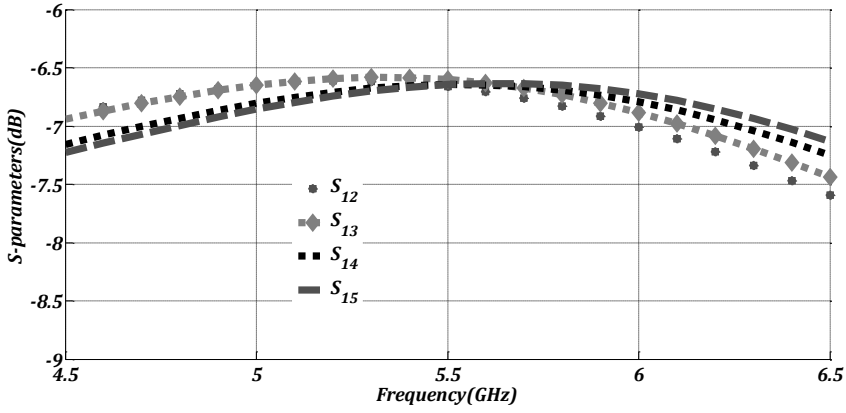


Figure 5: (a) Feed network of the CPSSAA. (b) Configuration of the feed network of the proposed CPSSAA.



(a)



(b)

Figure 6: (a) The simulated S_{11} values of the feed network and (b) The simulated S_{12} , S_{13} , S_{14} , and S_{15} values of the feed network.

The impedance bandwidth of this feeding network, defined as the frequency with an S_{11} above 10 dB, covered the frequency band from 4.56 GHz to 6.41 GHz. Figure 6b plots the S parameters of the five port feed network. According to this Figure, all ports were matched, and the transmission coefficient was 6.6 dB from the input port to each output port. Length (L) and width (W) of each intersection transmission line lettered in Figure 2(b) are as follows: $L_1=20$ mm, $L_f=30$ mm, $L_t=5$ mm, $W_0=2.6$ mm, $W_1=1.3$ mm, $W_2=2.8$ mm, $W_3=1.5$ mm, $W_4=0.3$ mm, $W_f=1.5$ mm and $W_t=0.3$ mm.

2.3.5 Experimental Results and Discussion

The proposed configuration of CPSSAA is shown in Figure 3. The array antenna consists of four elements (2 x 2) with 0.75 free space wavelength distances. The S_{11}

and axial-ratio of the proposed antenna array were measured, and the S_{11} was measured using the Agilent™ 8722ES network analyzer. The measurements of the fabricated array were made and compared to the simulations. Figure 7 shows the input reflection coefficient of the array versus frequency. The measured results corroborate well with the simulated results. As can be seen, the simulated bandwidth is 1.9 GHz, or 34.86%, from 4.5 to 6.4 GHz, while the measured 10-dB impedance bandwidth is 1.7 GHz, or 31.77%, from 4.5 to 6.2 GHz.

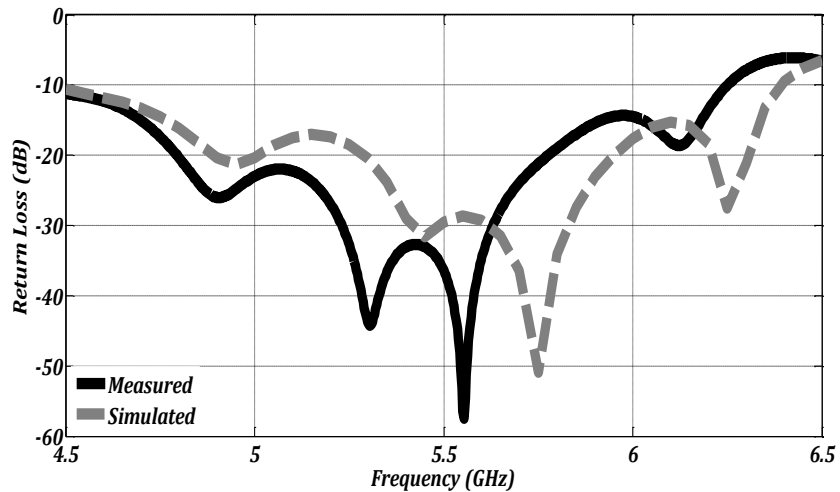


Figure 7: The differences between the simulation and measurement results of return loss.

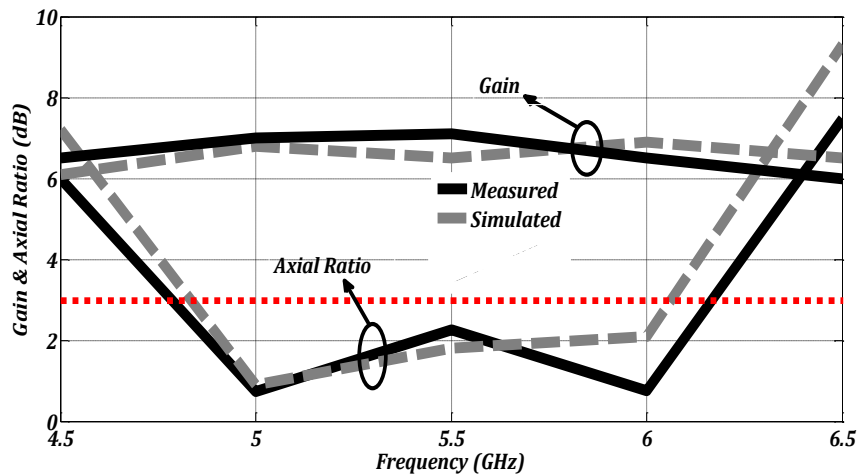


Figure 8: The differences between the simulation and measurement results of axial ratio and gain of proposed CPSSAA.

The differences between the simulation and measurement results could be attributed to practical factors such as fabrication imperfectness, material parameters errors, and measurement errors. However, both simulated and measured bandwidths are much larger than that of the single patch element that is 0.77 GHz (from 4.95 to 5.72 GHz).

Figure 8 shows the measured and simulated results of axial ratio of polarization and gain of the array. It can be seen that the simulation shows a 3dB axial-ratio bandwidth of 1.29 GHz from 4.8 to 6.09 GHz. The measurement shows a much wider 3-dB bandwidth from 4.75 to over 6.22 GHz. Besides, the axial-ratio bandwidth is much larger than that of the single patch antenna, which is 0.52 GHz (from 5.2 GHz to 5.72 GHz).

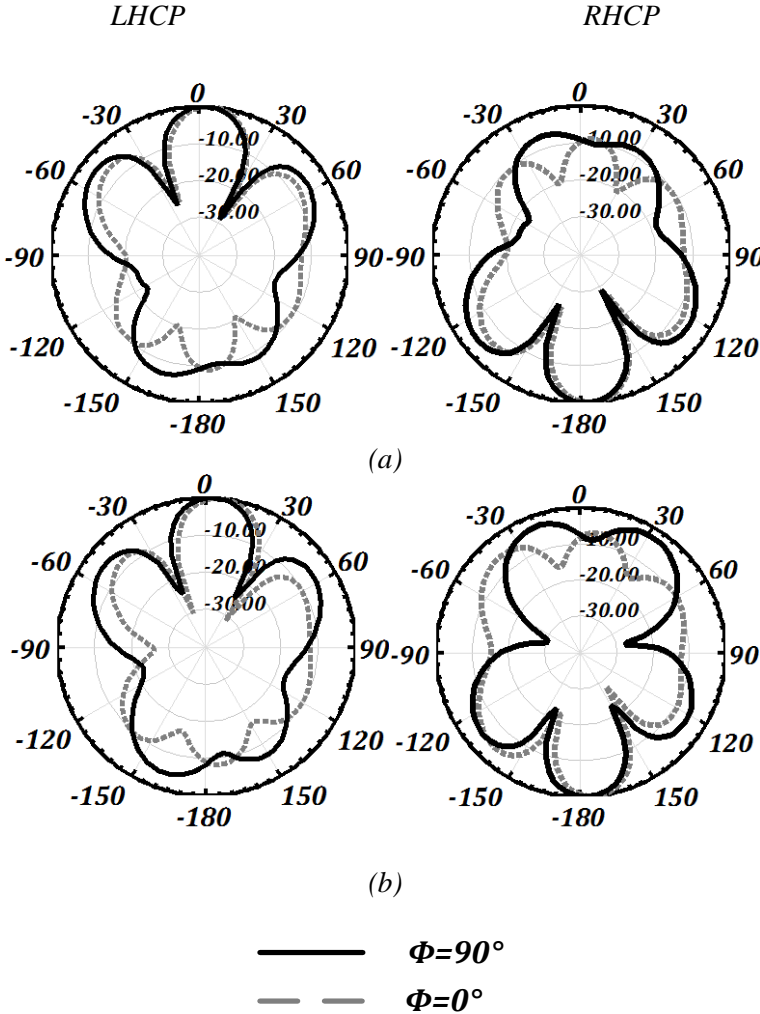


Figure9: The normalized (a) measured and (b) simulated radiation patterns, at $\varphi=0^\circ$ and $\varphi=90^\circ$ at 5.5 GHz.

A standard linearly polarized waveguide BJ320 was used to measure the total gain characteristics. The measured peak gain at 5.5 GHz is 7.2 dBic. The measured and simulated of normalized SSAA radiation patterns (LHCP at +z direction and RHCP at -z direction) at $\varphi=0^\circ$ and $\varphi=90^\circ$ is shown in Figure 9(a, b). The first reason of side lobe in this antenna is the elements distance from each other (free-space wavelength of

0.75) that increase the zeros of array factor. The second reason is related to substrate. It is well known that when using FR4, high tangent losses would be inevitable. Photograph of the fabricated antenna is indicated in Figure 10. However, an appropriate gain was achieved in this study for the proposed structure. The design when compared with the previous CP array structures with sequential feed network and arc feed-line presented in Table II show significantly increased impedance bandwidth and axial-ratio bandwidth, i.e. the impedance and AR bandwidth are, respectively, more than three and two fold wider than the previous designs.

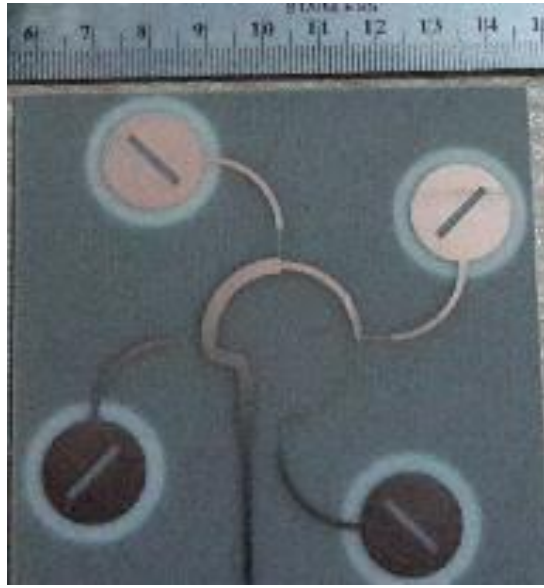


Figure10: Photograph of the fabricated antenna.

TABLE II: comparison of the proposed feed network structure and measured characteristics with other array antennas. the impedance bandwidth (bw) is the frequency range where the $vswr \leq 2$; and arbw is the 3-db axial-ratio bandwidth.

Ref.	Feed Network	BW (freq. range) (GHz)	ARBW (freq. range) (GHz)	PG (dBic)	Substrate
[22]	Asymmetric CPW	0.80 (1.1-1.9)	0.80 (1.1-1.9)	~7.5	FR4
[23]	Aperture Coupled	0.80 (1.6-2.4)	0.60 (1.7-2.3)	~15	RT/Duroid 5880
This work	Symmetric Microstrip Slot	1.7 (4.5-6.2)	1.47 (4.75-6.22)	7.2	FR4

2.3.6 Conclusion

This paper presents circularly polarized sequentially rotated slot antenna array with seven quarter-wavelength transformers. Four quarter wavelength usage for matching impedance between 50Ω in element input impedance and array feed network. In this study by decreasing input impedance, an increase in current transmission, an increase in power, occurred. Antenna array consist of 4 elements (2×2) which each element have circular polarization. The measured results show the impedance bandwidth as 1.7 GHz, or 31.77%, from 4.5 to 6.2 GHz. For $VSWR < 2$, and axial-ratio < 3 dB is 4.75 to over 6.22 GHz.

References

- [1] Rafii V., Nourinia J, Ghobadi C., Pourahmadazar J., Virdee B.S., Broadband Circularly Polarized Slot Antenna Array Using Sequentially Rotated Technique for C-Band Applications, *Antennas and Wireless Propagation Letters, IEEE* , vol.12, no., pp.128,131, 2013
- [2] Karamzadeh S., Rafii, V.; Kartal, M.; Ucan, O.N.; Virdee, B.S., "Circularly polarised array antenna with cascade feed network for broadband application in C-band," *Electronics Letters*, vol.50, no.17, pp.1184,1186, Aug. 14 2014
- [3] K. sood, R. Jyoti, S. B. Sharma, Linear array modules with prescribed using waveguide shunt slot-fed Microstrip patch elements, *International Journal of Microw. And Wireless Technol.*, vol. 5, no. 5, pp. 637–644, Oct. 2013.
- [4] J. Huang, A parallel-series-fed microstrip array with high efficiency and low cross polarization. *Microw. Opt. Technol. Lett.*, vol. 5, no. 5, pp. 230–233, Jan. 2007
- [5] Pourahmadazar J., Rafii V., Broadband circularly polarised slot antenna array for L- and S-band applications, *Electronics Letters*, vol.48, no.10, pp.542, 543, May 10 2012
- [6] K.L. Wong, and T.W. Chiou, Broad-band single-patch circularly polarized microstrip antenna with dual capacitively coupled feeds, *IEEE Trans. Antennas Propag.* vol. 49, no. 1, pp.41-44, Jan. 2001.
- [7] Nasimuddin, K.P. Esselle, and A.K. Verma, Wideband circularly polarized stacked microstrip antennas, *IEEE Antennas Wireless Propag. Lett.* vol. 6, pp. 21-24, 2007.
- [8] Y.X. Guo, L. Bian, and X.Q. Shi, Broadband circularly polarized annular-ring microstrip antenna, *IEEE Trans. Antennas Propag.* vol. 57, no. 8, pp.2474-2477, Aug. 2009.
- [9] C.H. Chen, and E.K.N. Yung, Dual-band dual-sense circularly-polarized CPW-fed slot antenna with two spiral slots loaded, *IEEE Trans. Antennas Propag.* vol. 57, no. 6, pp.1829-1833, Jun. 2009.
- [10] C.J. Wang, and C.H. Chen, CPW-fed stair-shaped slot antennas with circular polarization, *IEEE Trans. Antennas Propag.* vol. 57, no. 8, pp.2483-2486, Aug. 2009.
- [11] J. Pourahmadazar, C. Ghobadi, J. Nourinia, N. Felegari, and H. Shirzad, Broadband CPW-fed circularly polarized square slot antenna with inverted-L strips for UWB applications, *IEEE Antennas Wireless Propag. Lett.*, vol. 10, pp. 369-372, 2011.

- [12] Y.Y. Chen, Y.C. Jiao, G. Zhao, F. Zhang, Z.L. Liao, and Y. Tian, "Dual-band dual-sense circularly polarized slot antenna with a C-shaped grounded strip," *IEEE Antennas Wireless Propag. Lett.*, vol. 10, pp. 915-918, 2011.
- [13] N. Felegari, J. Nourinia, C. Ghobadi, and J. Pourahmadazar, Broadband CPW-fed circularly polarized square slot antenna with three inverted-L-shape grounded strips, *IEEE Antennas Wireless Propag. Lett.*, vol. 10, pp. 274-277, 2011.
- [14] J.Y. Sze, C.I.G. Hsu, M. H. Ho, Y.H. Ou, and M.W. Wu, Design of circularly polarized annular-ring slot antennas fed by a double-bent microstrip line, *IEEE Trans. Antennas Propag.* vol. 55, no. 11, pp.3134-3139, Nov. 2007.
- [15] A. Rezaeieh and M. Kartal, A new triple band circularly polarized square slot antenna design with crooked and f-shape for wireless applications, *Progress In Electromagnetics Research*, Vol. 121, 1-18, 2011.
- [16] Davide M. Pozar, *Microwave Engineering*, 4th ed, Copyright 2012, by John Wiley & Sons, Inc.
- [17] J. Y. Sze, K. L. Wong, and C. C. Huang, Coplanar waveguide-fed square slot antenna for broadband circularly polarised radiation, *IEEE Trans. Antennas Propag.*, vol. 51, pp. 2141–2144, Aug. 2003.
- [18] J.-Y. Sze and Y.-H. Ou, Compact CPW-fed square aperture CP antenna for GPS and INMARSAT applications, *Microw. Opt. Technol. Lett.*, vol. 49, no. 2, pp. 427–430, Feb. 2007.
- [19] C. C. Chou, K. H. Lin, and H. L. Su, Broadband circularly polarized cross-patch-loaded square slot antenna, *Electron. Lett.*, vol. 43, no. 9, pp. 485–486, Apr. 2007.
- [20] J.-Y. Sze, J.-C. Wang, and C.-C. Chang, Axial-ratio bandwidth enhancement of asymmetric-CPW-fed circularly-polarised square slot antenna," *Electron. Lett.*, vol. 44, no. 18, pp. 1048–1049, Aug. 28, 2008.
- [21] J.-Y. Sze and C.-C. Chang, Circularly polarized square slot antenna with a pair of Inverted-L grounded strips, *IEEE Antennas Wireless Propag. Lett.*, vol. 7, pp. 149–151, 2008.
- [22] S. Fu, S. Fang, Z. Wang, X. Li, Broadband circularly polarized slot antenna array fed by asymmetric CPW for L-band applications, *IEEE AWPL. Lett.*, vol. 8, pp. 1014–1015, Sep 2009.
- [23] S. Gao, Q. Yi, A. Sambell, Low-Cost Broadband Circularly Polarized Printed Antennas and Array, *IEEE Antennas and Propagation Magazine*, vol.49, no.4, pp.57-64, Aug. 2007.

2.4 Circularly Polarized Array Antenna with Cascade Feed Network for Broadband Application in C-Band

Source: *Electronics letters Volume 50, Issue 17, August 2014, p. 1184 - 1186.*

2.4.1 Abstract

A new configuration of a circularly polarized square slot antenna (CPSSA) array operating in C-Band is presented in this paper. The array consists of 2×2 CPSSA elements and is fed by a novel feeding network consisting of the circuit strip-line couplers and delay lines. The proposed feeding technique is applied to the 2×2 antenna array to increasing the axial ratio (AR) bandwidth. The measured impedance bandwidth for VSWR < 2 is around 78.5% (3.4 – 7.8 GHz) and 3dB axial-ratio bandwidth is about 35.7% (4.6–6.6 GHz) and average 14.2 dBic gain over the 3 dB ARBW. The measured results corroborate well with the simulated results.

2.4.2 Introduction:

In recent years, Antenna arrays are widely used in radar and microwave communications because of their high gain, decent directivity and extensive coverage area. For the patch antennas, the CP waves are generated by exciting two or more orthogonal linearly polarized modes in equal amplitude but in phase quadrature. There are different techniques that can excite two orthogonal modes for square slot antennas. Loading the square slot antenna by appropriate perturbation structures such as two inverted-L grounded strips around two opposite corners of the slot [1], a T-shaped grounded metallic strip that is perpendicular to the axial direction of the coplanar waveguide (CPW) feed line [2] and extending across the square slot a slot line-loaded inductively coupled conducting strip [3] are some of these techniques. Moreover, various techniques have been investigated to improve the axial ratio and impedance performance of circularly polarized microstrip antennas [4-9]. In this letter, the design of a circularly polarized square slot antenna array (CPSSAA) which has a feed network comprises a 180 degree ring hybrid coupler linked to two branch-line hybrid couplers for generating broadband circular polarization performance is proposed. The presented array employs a pair of branch-line couplers to feed CPSSA elements, which improves the performance of the array considerably. Details of the proposed 2×2 sequentially

rotated planar CPSSA array configuration are given, and simulation and experimental results are discussed in the following sections.

2.4.3 Antenna elements:

The configuration of proposed antenna element is shown in Figure 1. The antenna element is printed on an inexpensive FR4-epoxy laminate which has a thickness h of 0.8 mm with manufacturer specified dielectric constant ϵ_r of 4.4 and loss tangent $\tan\delta$ of 0.024. To generate CP radiation, two inverted-L metallic strips are inserted around two opposite diagonal corners of the square slot. Each of the 1mm-width metallic strips has a length of L_x and L_y , respectively, in the directions perpendicular and parallel to CPW. The simulation results show that the impedance bandwidth and axial ratio (AR) of the proposed CPSSA element is 111% (3.1~10.9GHz) for $VSWR < 2$, and 40.7% (4.5~6.8GHz) - 21.9% (7.3~9.1GHz) for $AR < 3dB$, respectively. The proposed CPSSA element has a compact size of $25 \times 25 \text{ mm}^2$ operating at the frequency of 6.4 GHz. The design principles of proposed CPSS antenna are summarized in detail in reference [4].

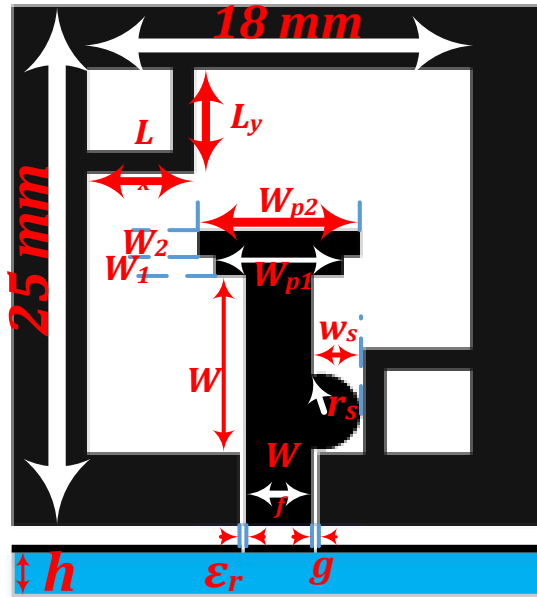


Figure 1: Geometry of proposed CPW-fed CPSSA: $W_f=3$, $W=8.5$, $W_{p1}=6$, $W_{p2}=7.6$, $g=0.3$, $W_1=1$, $W_2=1.2$, $L_x=L_y=5$, $W_s=2.5$, $r_s=2$ (All Parameters in mm.)

2.4.4 Feed Network and CPSSAA Configuration

A 2×2 planar array antenna has been established by using the proposed CPSSA element. In Figure 3, the configuration of the proposed feed network is shown. The basic principle of operation can be explained as follow. The feed network utilizes a

180-degree ring hybrid coupler to achieve a 3dB power split, equal in magnitude, but 180-degrees out of phase. Two supplementary branch-line hybrid couplers then divide the signal energy into two paths and give the signal to each of the output branches with the same amplitude but phase-shifted by 90°, wherein the relative phases at four feed points are 0°, 90°, 180° and 270°, respectively. The feeding network is fed with an SMA panel connector located at the backside of the board. The total size 2×2 elements array is 112×97×0.8 mm³. The proposed antenna is simulated by commercial Ansoft™ HFSS software. The spacing between two elements is 35mm (0.7λ₀) in two dimensions.

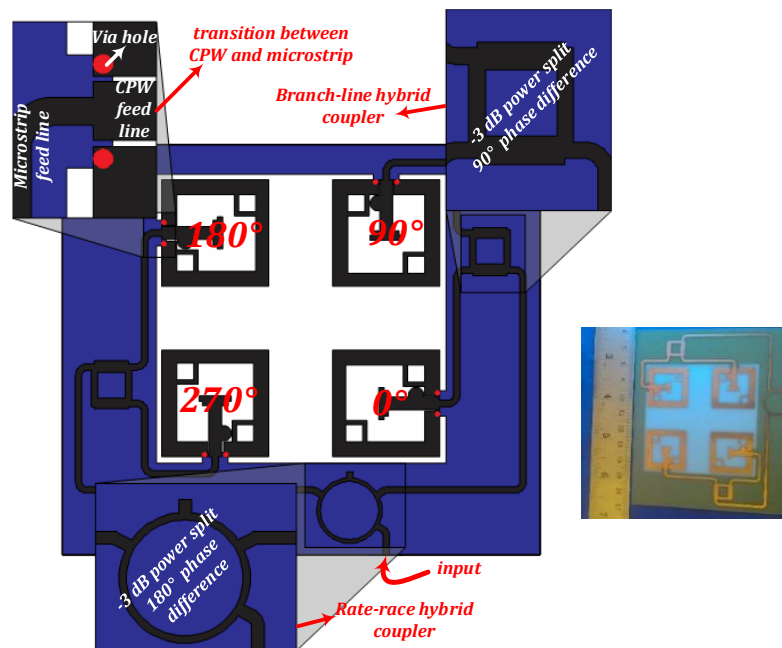


Figure 2: Configuration of feed network and CPSSAA

2.4.5 Results and Discussion:

The measurements of the fabricated array were done and compared with the simulations. Since the antenna was manufactured by handwork, there were slightly differences between the measured and simulated results. In Figure 3(a) Compare between measured and simulated Return loss of the proposed CPSSAA is presented. The antenna array delivers a measured impedance bandwidth of 78.5% from 3.4GHz to 7.8GHz for VSWR < 2 and simulated impedance bandwidth of CPSSAA is from 3.4GHz to 8GHz. a measured 3-dB axial-ratio bandwidth of 35.7% from 4.6GHz to 6.6GHz. As shown in Figure 3(b), the minimum value of axial ratio is achieved 0.57dB at 5.5GHz. Minimum value of measured Gain is 8.3dBic and maximum value of gain is 14.8dBic at 6.5GHz and average gain of antenna array in whole of bandwidth

frequency is 11.8 dBic. The measured radiation pattern of the antenna array at three frequency in the principal plane are shown in Figure 4, the measured patterns at three frequency (4.6, 5.5 and 6.6 GHz at beginning, minimum and end of 3dB axial ratio bandwidth, respectively.) are shown. As shown the side lobe level of antenna array in Figure 4(a), 4(b) and 4(c) are lower than -10 dB, -14dB and -9dB and angular width is 39 degree, 30 degree and 34 degree, respectively.

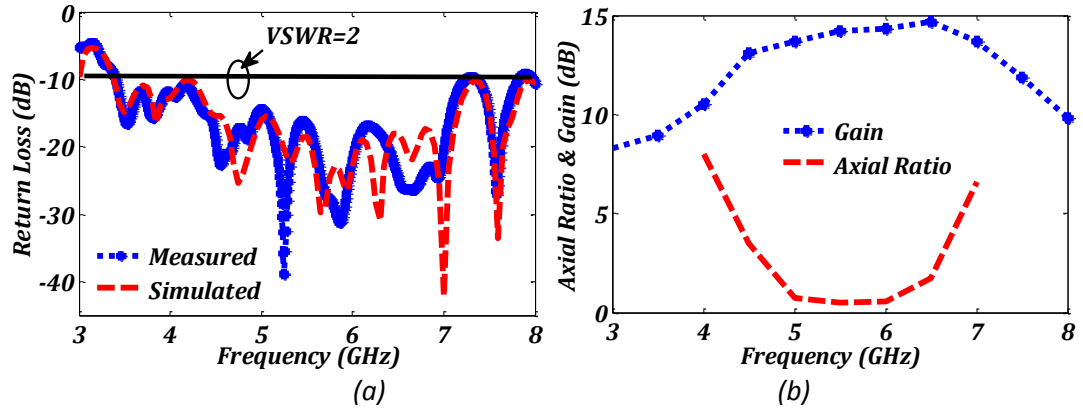
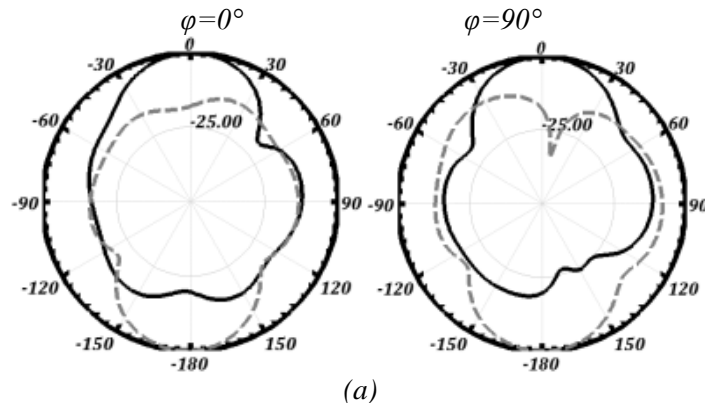


Figure 3: (a) Compare between measured and simulated Return loss of the proposed CPSSAA (b) Measured gain and axial ratio.

2.4.6 Conclusion:

In this letter, a design of a CPSSA array using a two-section cascaded coupler feeding system for generating broadband circular polarization performance has been presented. The feeding network of the array is comprised of a 180-degree ring hybrid coupler connected to two branch-line couplers generating circular polarization. The proposed antenna array architecture presents a number of well-behaved attributes including the flexibility of mixed type of feeding, low parasitic radiation from the feeding network, high polarization purity (35.7% (4.6–6.6 GHz) 3dB axial-ratio bandwidth) and a very high gain (14.8dBic).



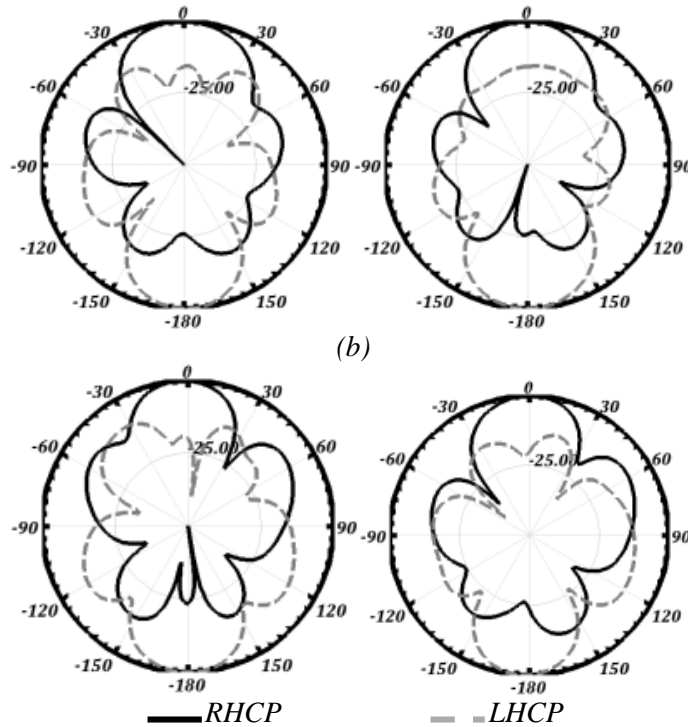


Figure 5: The array measured normalized RHCP and LHCP at (a) 4.6GHz, (b) 5.5GHz and (c) 6.6GHz.

References

- [1] Jia-Yi Sze and Chi-Chaan Chang, "Circularly Polarized Square Slot Antenna with a Pair of Inverted-L Grounded Strips," *IEEE Antennas and Wireless Propag. Lett.*, vol. 7, july 2008, pp. 149 – 151.
- [2] J. Y. Sze, K. L. Wong, and C. C. Huang, "Coplanar waveguide-fed square slot antenna for broadband circularly polarized radiation," *IEEE Trans. Antennas Propag.*, vol. 51, no. 8, Aug. 2003, pp. 2141–2144.
- [3] C. Deng, R. J. Lin, K. M. Chang, and J. B. Chen, "Study of a circularly polarized CPW-fed inductive square slot antenna," *Microw. Opt. Technol. Lett.*, vol. 48, no. 8, Aug. 2006, pp. 1665–1667.
- [4] J. Pourahmadazar and S. Mohammadi, "Compact circularly-polarised slot antenna for UWB applications", *Electron. Lett.*, Vol. 47 No. 15, July 2011.
- [5] J. Y. Sze, J. C. Wang, and C. C. Chang, "Axial-ratio bandwidth enhancement of asymmetric-CPW-fed circularly-polarised square slot antenna," *Electron. Lett.* vol. 44, no. 18, Aug. 2008, pp. 1048–1049.
- [6] J.S.Row and S.W.Wu, "Circularly-polarized wide slot antenna loaded with a parasitic patch," *IEEE Trans. Antennas Propag.*, vol. 56, no. 9, Sep. 2008, pp. 2826–2832.
- [7] L. Y. Tseng and T. Y. Han, "Microstrip-fed circular slot antenna for circular polarization," *Microw. Opt. Technol. Lett.*, vol. 50, no. 4, Apr. 2008, pp. 1056–1058.
- [8] Vahid Rafii, J. Nourinia, Ch. Ghobadi, Javad Pourahmadazar and Bal S. Virdee, "Broadband Circularly Polarized Slot Antenna Array Using Sequentially Rotated Technique for C-Band Applications", *IEEE AWPL. Lett.*, vol. 12, Sep 2013, pp. 128–13.
- [9] J. Pourahmadazar, and V. Rafii, "Broadband circularly polarized slot antenna array for L and S-band applications," *Electron. Lett*, vol. 48, no. 10, 2012, pp. 542-543.

2.5 Circularly Polarized MIMO Tapered Slot Antenna Array for C-Band Application

Source: *Electronics letters Volume 51, Issue 18, September 2015, p. 1394 - 1396.*

2.5.1 Abstract

A novel configuration of a Multiple-Input-Multiple-output (MIMO) circularly polarized (CP) antenna array operating in C-band is presented. The array consists of 2×2 antipodal tapered slot antenna (TSA) elements created in the sides of rectangular as the rectangular grid that supply a broadband Impedance bandwidth and high gain array. In order to provide broadband MIMO with polarization diversity antenna uses a dual ports fed network consisting of the couplers, crossover and delay lines which the diversity of polarization changed by input ports.

2.5.2 Introduction:

In recent years, antenna arrays have been widely used in radar and microwave communications because of their high gain, good directivity and extensive coverage area [1]. The main problem facing the performance of array technology is the limited space available at each end of the communication link. Multiple-Input-Multiple-Output (MIMO) antenna with polarization diversity has the ability to solve this problem. In MIMO antenna, a physical antenna with different polarization diversity have same transmit and receive role. Hitherto, in most papers [2-4], with the change in the orthogonal polarization have been proposed to overcome this problem. But to resolve the other problems such as: combating multi-path interferences or fading; Faraday rotation' effect due to the ionosphere; and strict orientation between transmitting and receiving antennas, the usage of a circularly polarized antenna is inevitably. In [5, 6], by utilizing reconfigurable structures, polarization diversity CP antennas could be achieved. But the employment of active components such as PIN diodes causes a decrease in bandwidth; an increase in insertion loss and cost; and the addition of phase shift in array feed networks. In this letter, a broadband MIMO antenna array with Innovations such as i) broadband feed network that consisting the 90 and 180 degree couplers, crossover and delay lines that provide CP antenna with ability to changing RHCP and LHCP (polarization diversity) by input choice and ii) 2×2 TSA array elements are arranged in a square or rectangular grid configuration that

supply high gain antenna in wide frequency bandwidth with low mutual coupling is presented.

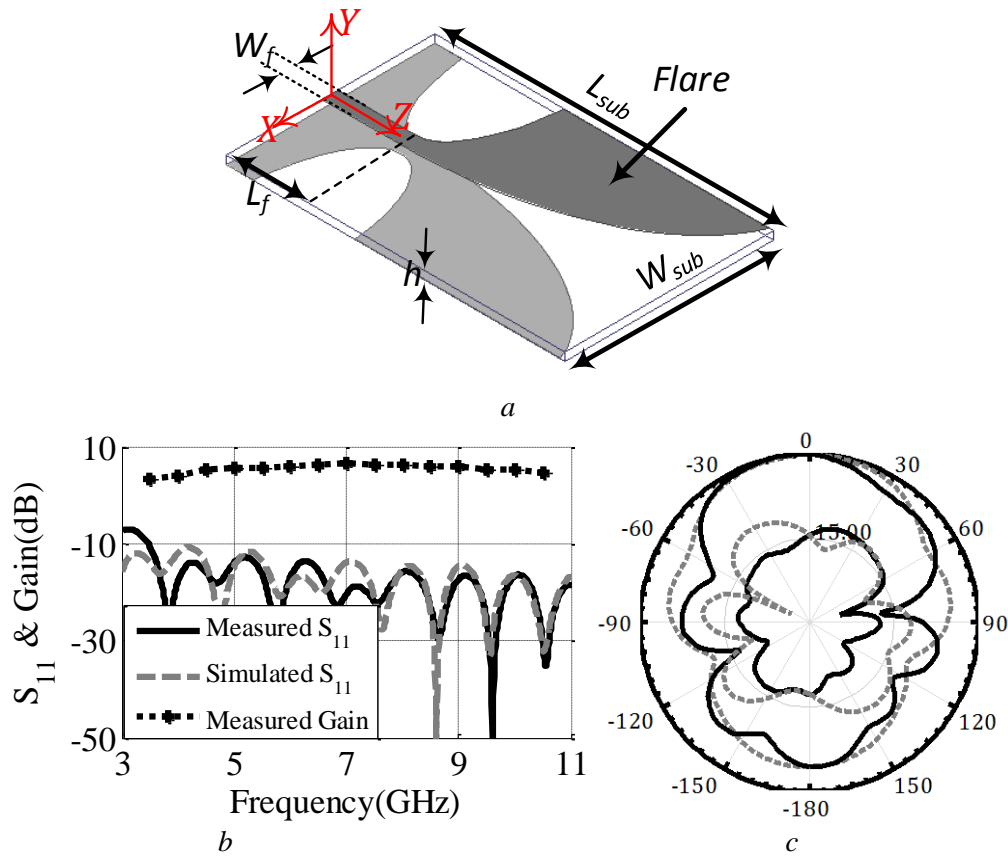


Figure 1: TSA configuration and results; *a*) the configuration of TSA; *b*) Comparison between simulated and measured S_{11} (dB); and measured gain, (dBi); and *c*) The normalized measured pattern of antenna at 5.5GHz (dash line Co and Cross of E-plane and solid line Co and Cross of H-plane).

2.5.3 Single element

The configuration of the proposed antenna element is shown in Figure 1a. The antenna element is printed on an inexpensive FR4-epoxy laminate which has a thickness h of 0.8 mm with a manufacturer specified dielectric constant ϵ_r of 4.4 and loss tangent $\tan\delta$ of 0.024. The radiating element configuration consists of elliptical taper profile in upper and bottom layer. W_{sub} is the width of the antenna and $(L_{sub}-L_f)$ is the length of the taper profile (Flare). The taper curves are obtained by [7].

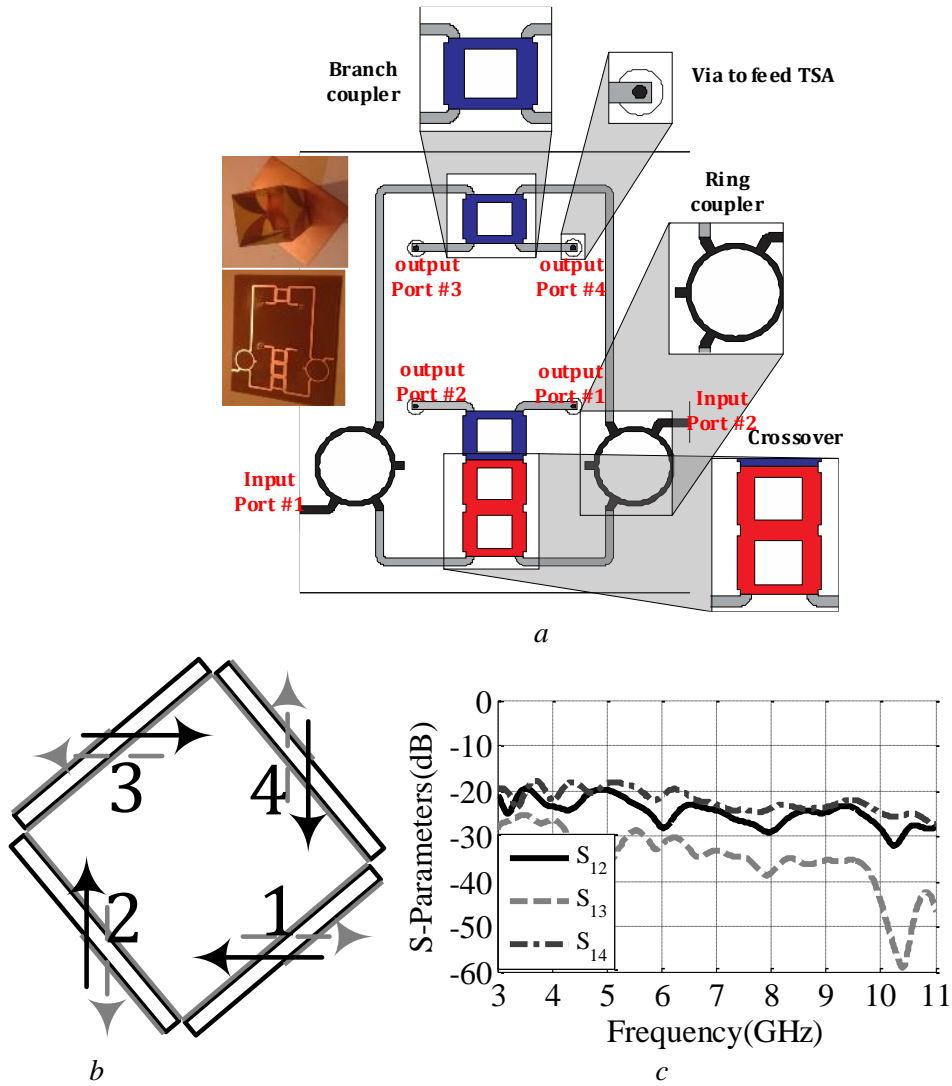


Figure 2: The overall structure of the antenna array and feed network with mutual coupling results; *a*) the feed network of polarization diversity MIMO array; *b*) methods of arrangement TSA array (phase variation: solid line =RHCP of Port1 and dash line =LHCP of Port2); and *c*) simulated mutual coupling between TSA elements.

In order to improve the impedance matching between microstrip feed line of width W_f and TSA and avoid the balanced to unbalanced transformer, two half elliptic slots in top and bottom flares are employed. The optimized antenna dimensions are: $R=0.52\text{mm}$, $W_f=1.5\text{mm}$, $W_{sub}=40\text{mm}$, $L_f=15\text{mm}$, $L_{sub}=65\text{mm}$ and $h=0.8\text{mm}$.

The simulated and measured S_{11} of TSA are presented in Figure 1b. The measured BW is 103.4% (3.5-11GHz). The measured gain of the antenna is also shown in Fig 1b with maximum value of 8.6dBi at 7GHz frequency. The normalized measured pattern of the antenna at 5.5GHz is shown in Figure 1c. The antenna pattern is End-Fire with HPBW of 76° and cross polarization less than -12dB of Co polarization.

Table 1: Distribution of phase difference between TSA elements by each input port and type of generated diversity

P=port	Output P1	Output P2	Output P3	Output P4	Diversity
Input P1	0+ θ	90+ θ	180+ θ	270+ θ	RHCP
Input P2	270+ θ	180+ θ	90+ θ	0+ θ	LHCP

2.5.4 Feed Network and MIMO array configuration

In order to attain a MIMO array with pattern diversity, a novel two input and four output ports feed network is designed. As seen in Figure 2a, the MIMO array feed network consists of two rate-race Ring coupler, two branch line coupler and a crossover. The MIMO feed network employs two 180° ring hybrid coupler to achieve a -3 dB equal magnitude power split with 180° phase shifting. Two supplementary branch-line hybrid couplers then divide the signal energy into two paths and give the signal to each of the output branches with the same amplitude and 90° phase-shifting [1]. In order to attain phase sequential rotation, between the ends of one side of the ring couplers and branch line coupler, a crossover is embedded. The created phase shift by crossover is compensated by a line length placed at the other side. The results of this arrangement of the components for each input ports, based on the designed structure mentioned above, are reported in Table 1. As well known, the CP waves are generated by exciting two or more orthogonal linearly polarized modes in equal amplitude, but in phase quadrature [1](seen Figure 2b). As reported, in the proposed MIMO array antenna structure, the exponential tapered slot antennas are arranged in 2×2 rectangular grid configuration and are fed by metalized via that isolated TSA input impedance from feed network impedance. The feed to feed spacing between the elements is 28.3 mm ($0.51 \lambda_{5.5GHz}$ - wavelength in free space). As shown in Figure 2c, though the space between TSA is decreased, the mutual coupling is reduced. The main reasons for this decline: 1) surface current of between TSAs at this methods of arrangement, reduces and 2) the TSA radiation pattern is End Fire.

2.5.5 Result and discussion

The proposed TSA array was fabricated and measured by 8722ES Agilent vector network analyser. In Figure 3a the measured value of S_{11} , S_{12} and S_{22} is demonstrated. The measured BWs ($S_{11} < -10\text{dB}$) for ports 1 and 2 are 60.8% (4.27-8GHz) and 59.17%

(4.26-7.84GHz), respectively, and mutual coupling between two ports in whole of BW is less than -17dB. The measured 3dB axial ratio bandwidth and gain of the proposed antenna for each input port is illustrated in Figure 3b.

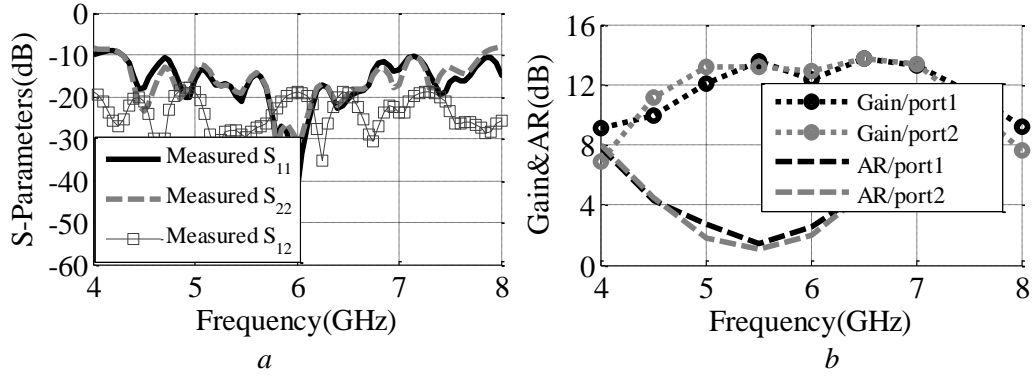


Figure 3: Comparison between simulated and measured results of MIMO array; *a)* the measured S_{11} , S_{22} and S_{12} *b)* the measured axial ratio and gain

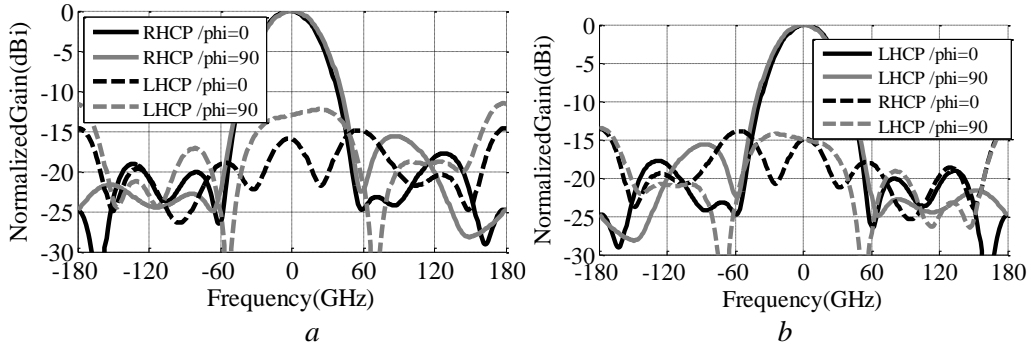


Figure 4: The normalized measured radiation patterns; *a)* for port 1; and *b)* for port 2.

The measured 3dB axial ratio bandwidth for ports 1 and 2 are 19.9% (4.98-6.08GHz) and 24.8% (4.81-6.17GHz), respectively. As illustrated in Figure 3b, the maximum gain for ports 1 is 13.87dBic and for ports 2 is 13.82dBic. In the array design, ground plane of feed network in other side of substrate acts as a reflector for TSA elements and as a result increases the gain of the antenna. That is why the gain of proposed antenna is higher than the basis one which is TSA gain \times array factor. The normalized measured radiation pattern of proposed array in 5.5GHz is shown in Figure 4. As it is seen from Figure4, by exciting ports 1 and 2, the array antenna is radiated in RHCP and LHCP, respectively, and polarization diversity changes are succeeded. The design when compared with the previous polarization diversity array structures presented in Table 2 show significantly increased impedance bandwidth and axial-ratio bandwidth, i.e. the impedance and AR bandwidth are, respectively, more than three and two fold wider than the previous designs.

Table 2: Comparison of the proposed feed network structure and measured characteristics with other array antennas. (BW) is the frequency range where the $S_{11} \leq -10$; ARBW is the 3-dB axial-ratio bandwidth and MePD is method of changing polarization diversity (PG=peak gain).

Ref.	MePD	BW [GHz]	ARBW [GHz]	PG[dBic]
[5]	PIN diode	0.82 (1.55-2.37)	0.31 (1.76-2.07)	~8
[6]	PIN diode	0.11 (2.03-2.14)	0.01 (2.07-2.08)	~7
This work	Input port	3.58 (4.26-7.84)	1.36 (4.81-6.17)	~13.9

2.5.6 Conclusion

A novel design in circularly polarized MIMO array antenna has been reported. The antenna element is designed and optimized to satisfy the expectations for bandwidth, pattern and the gain. Then the antenna array is configured with a novel feed network design. The array antenna with the feeding network give us an improved gain and the desired CP diversity property which is very important in some applications mentioned above. Another novelty for the designed array structure is the additional gain improvement obtained by the substrates acting as a reflector for the other array elements.

References

- [1] Karamzadeh, S.; Rafii, V.; Kartal, M.; Ucan, O.N.; Virdee, B.S., "Circularly polarised array antenna with cascade feed network for broadband application in C-band," *Electronics Letters*, vol.50, no.17, pp.1184, 1186, Aug. 14 2014; doi: 10.1049/el.2014.1147.
- [2] Lihong Wang; Lina Xu; Xinwei Chen; Rongcao Yang; Liping Han; Wenmei Zhang, "A Compact Ultrawideband Diversity Antenna With High Isolation," *Antennas and Wireless Propagation Letters*, IEEE , vol.13, no., pp.35,38, 2014 doi: 10.1109/LAWP.2013.2295414.
- [3] He Huang; Ying Liu; Shuxi Gong, "Uniplanar differentially driven UWB polarisation diversity antenna with band-notched characteristics," *Electronics Letters*, vol.51, no.3, pp.206, 207, 2 5 2015; doi: 10.1049/el.2014.3626.
- [4] Chacko, B.P.; Augustin, G.; Denidni, T.A., "Electronically Reconfigurable Uniplanar Antenna With Polarization Diversity for Cognitive Radio Applications," *Antennas and Wireless Propagation Letters*, IEEE, vol.14, no., pp.213, 216, 2015 doi: 10.1109/LAWP.2014.2360353
- [5] Wenquan Cao; Bangning Zhang; Aijun Liu; Tongbin Yu; Daosheng Guo; Kegang Pan, "A Reconfigurable Microstrip Antenna With Radiation Pattern Selectivity and Polarization Diversity," *Antennas and Wireless Propagation Letters*, IEEE , vol.11, no., pp.453,456, 2012 doi: 10.1109/LAWP.2012.2193549
- [6] Jia-Fu Tsai; Jeen-Sheen Row, "Reconfigurable Square-Ring Microstrip Antenna," *Antennas and Propagation, IEEE Transactions on*, vol.61, no.5, pp.2857, 2860, May 2013 doi: 10.1109/TAP.2013.2244554
- [7] J. D. S Langley, P. S. Hall and P. Newham, "Balanced Antipodal Vivaldi Antenna for Wide Bandwidth Phased Arrays", *IEEE Proc. Antennas and Propagation*, Vol. 143, No. 2, Apr 1996, pp. 97-102.

2.6 Modified circularly polarized beam steering array antenna by utilized broadband coupler and 4×4 butler matrix

Source: *IET Microwaves, Antennas & Propagation, Volume 9, Issue 9, June 2015, p. 975 – 981.*

2.6.1 Abstract

Among the other features, multiple beam antennas have the advantageous of reduced multi-path fading and co-channel interference. Because of the outstanding features of the Butler matrices, they have been proposed extensively in recent years as feed networks of the antenna array applications such as broadband and circular polarization. In this work, a beam steering array antenna composed of a broadband circularly polarized square slot antenna and a novel Butler matrix feed network designed with a proposed broadband branch line coupler is introduced. The Results show that a compact and its improvements are discussed. In this work a broadband double box coupler with impedance bandwidth over 5 - 7.4 GHz frequency and the phase error less than 3 degree is employed. Also the measured impedance bandwidth of the proposed beam steering array antenna is 39% (from 4.7GHz to 7 GHz). The minimum 3dB axial ratio (AR) bandwidth between ports, support 4.55 - 6.7 GHz frequency range. The measured peak gain of proposed array antenna is 10.1 dBic that could scan solid angle approximately 25 steradian.

Keyword: Butler matrix, slot antenna, antenna array, broadband coupler, beam steering.

2.6.2 Introduction

Multiple beam antenna technology, one of the most important techniques that can solve problems such as multi-path fading and co-channel interference, is an attractive candidate for mobile and satellite communication systems [1]. The main beam of the multiple beam antenna can be well controlled and directed to the directions subject to less interference. There are many different techniques to achieve multiple beam antenna including Blass, Nolen and Butler matrices. Butler matrix feed networks cited by all of the previous works are due to their advantages such as theoretically lossless and employs the minimum number of components, has received particular attention in

the literature. The Butler matrix has been utilized widespread in radar, electronic warfare and satellite systems for decades [1 - 8]. More recently, with an increasing solicitation for broadband wireless access technologies, techniques for exploiting the capacity and improving the transmission quality and coverage of a base station or an access point are currently under vigorous research. Significant attention is being disbursed to the performance of smart antenna systems with the Butler matrices. Another preponderance of Butler matrix is ability to produce circular polarization (CP). In other word, the use of the Butler matrix feed network with circular polarization is because of the following properties: I) Reducing the ‘Faraday rotation’ effect and II) Decreasing multi-path interferences or fading. A 4×4 Butler matrix with using linearly polarized element was presented in [2]. The impedance bandwidth and 3dB axial ratio (AR) of this antenna were 18.8% and 4.9% respectively. In [3], A CP switched-beam patch antenna array with butler matrix was reported. This array had an impedance and AR bandwidth over a frequency range of 5.75–6.2 GHz when the main beam of array was scanned to different directions. A proximity-coupled L-probe feeding wideband CP antenna was exploited for wideband CP beam-steering [4]. A modified Butler matrix [5]–[8], which is composed of four branch line couplers and two 45 degree phase shifters without any crossovers, was used in beam switching system. In this work, an ultra-wide band square slot antenna that provides the broadband CP operation is introduced in the first step. Then by utilizing a broadband branch line coupler, a novel Butler matrix is offered. Finally, with combining antenna element and Butler matrix feed network a beam steering array antenna is suggested and its significant improvements are discussed.

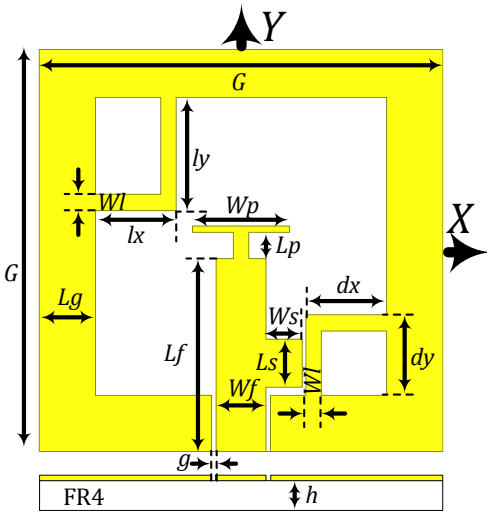


Figure 1: Geometry of the proposed CPSS antenna for UWB applications.

Table I. Characteristics of the Proposed CPSS Antennas (All value in mm)

l_x	l_y	dx	dy	W_s	L_s	W_p	l_p	W_l	W_f	g	G	L_f	L_g	h
5	7	5	5	1.5	3	5	1.5	0.5	3	0.3	25	12	3.5	0.8

2.6.3 Single element

Figure 1 depicts the physical structure and configuration of the proposed single layer co-planar waveguide (CPW)-fed circularly polarized square slot antenna (CPSSA). The configuration of this antenna is a combination of the square slot CP antenna [9] and the techniques introduced in [10], and [11]. The proposed CPSS antenna consists of a T-shape main patch embedded to the feed line (L_f). The presented antenna uses two inverted-L shaped strips around two opposite corners of the grounded slot and a tuning stub in feeding structure.

The main feature considered in this design is widening the 3-dB AR bandwidth across the whole impedance bandwidth. Through extensive simulations it was found that by embedding a T-shaped patch to the feeding mechanism and adjusting its parameters to the optimized values make the impedance bandwidth wider. The circular polarization excitation of the proposed circularly polarized square slot antenna is mainly performed through investment of two inverted-L shape strips located around two opposite corners of the square slot with $l_x \times l_y$ and $dx \times dy$ dimensions [10], [11]. By embedding inverted-L shape metallic strips, it is expected that a wideband circular polarization will be generated. Using the feed line in conjunction with grounded inverted-L shaped and T-shaped strips leads to a large ARBW. For the proposed CPSS antenna with the optimized values given in Table I, right and left handed circularly polarized (RHCP and LHCP) radiations will generate in the $+Z$ and $-Z$ directions, respectively. The proposed CPSS antenna is printed on a commercially cheap FR4-epoxy substrate with $\epsilon_r=4.4$, $\tan(\delta) = 0.024$ and compact dimension of $25 \times 25 \times 0.8 (= h)$ mm³. The width W_f of the CPW feed-line is fixed at 3 mm to achieve 50 Ω characteristic impedance. The horizontal feed section ($\pm X$ direction) is separated from the ground plane by a gap of $g=0.3$ mm. In Figure 2(a), simulated return loss and in Figure 2(b), simulated frequency response of the single element for axial ratio and gain are presented. Simulated LHCP and RHCP radiation pattern of the proposed single element CPSS antenna for $\phi=0^\circ$ and $\phi=90^\circ$ is demonstrated in Figure 2(c). In Figure 2(c), $+z$ and $-z$ direction are RHCP and LHCP, respectively. The proposed CPSSA has an area of 625 mm² (25 mm \times 25

mm), which is considerably less than the previously published slot antennas as summarized in Table II along with other salient parameters. Compared to other similar types of CP slot antennas fabricated on the same substrate, the proposed antenna exhibits an impedance bandwidth which is significantly larger and with no reduction in the gain performance, as well as having a larger circular polarization bandwidth. The gain is comparable to previous designs.

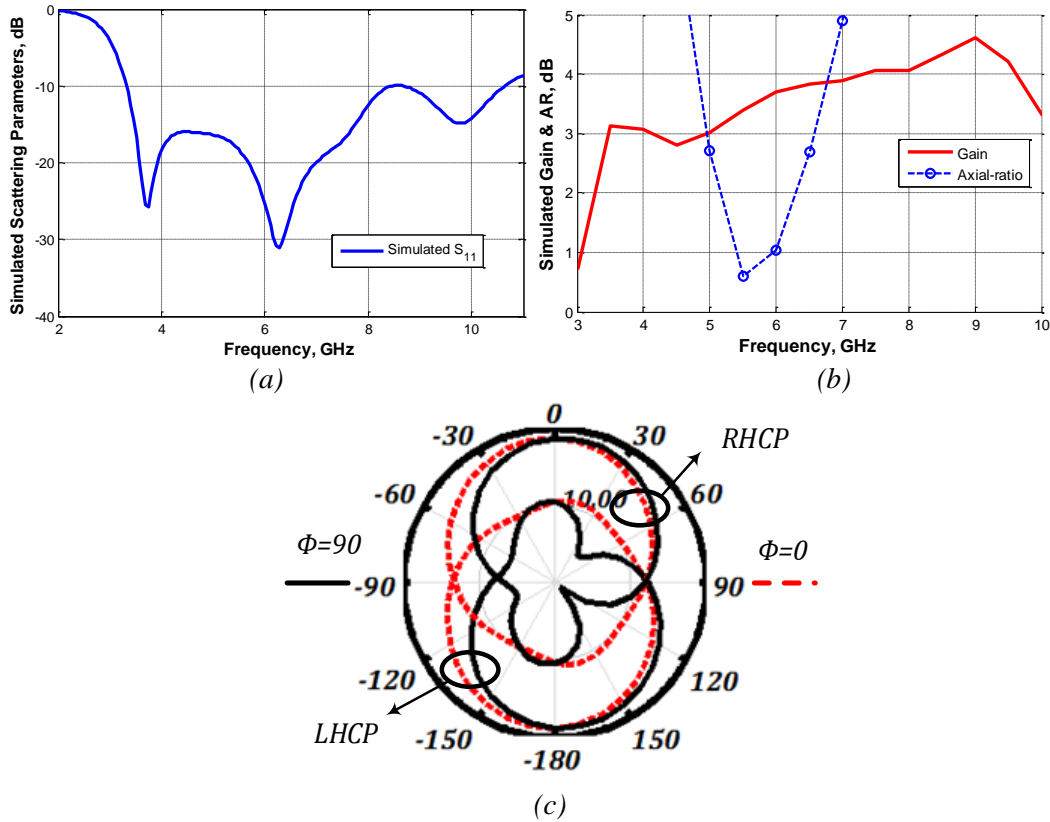


Figure 2: Simulated results of proposed single element antenna (a) return loss (b) Gain and Axial ratio (c) pattern at 5.5 GHz.

Table II: Comparison of the proposed CPSSA size and measured characteristics with other references. Dielectric substrate Used is FR4 with $\epsilon_r=4.4$, $\tan\delta=0.024$. The impedance bandwidth is for a frequency range where $VSWR \leq 2$; and ARBW is 3-dB axial-ratio bandwidth.

Ref.	Size (mm ³)	BW (GHz)	3dB ARBW (GHz)	Peak Gain (dBic)
[9]	70×70×1.60	0.85(1.75-2.6)	0.4 (1.7-2.1)	3.7
[12]	70×70×1.60	0.20 (1.5-1.7)	0.3 (1.5-1.8)	3.5
[13]	70×70×1.60	0.80 (1.6-2.4)	0.2 (1.8-2.0)	3.5
[14]	25×25×0.80	1.9 (4-6.6.5)	0.8 (4.9-5.7)	3.6
[15]	25×25×0.80	1.40 (3.1-10.9)	0.7 (4.5-6.8)	3.3
This work	25×25×0.80	7.4 (3.1-10.5)	1.7 (4.9-6.6)	4.5

2.6.4 Branch line coupler

As shown in Figure 3(a (i)), the branch-line coupler which is known to have a narrow-band characteristic is presented. To enhance the bandwidth, a double-box branch line coupler as a quadrature hybrid circuit is used (Figure 3a (ii)). However, it requires a large circuit area. The stub line is a favorite method to reduce the size of transmission-line circuits. A transmission line and its L-shaped equivalent circuit are shown in Figure 3 (b, c), and the design equations can be defined as follows [14]:

$$\frac{\tan\theta_p}{Z_p} = \frac{\cos\theta_s - \cos\theta_0}{Z_0 \sin\theta_s} \quad (1), \quad Z_s = \frac{Z_0 \sin\theta_0}{\sin\theta_s} \quad (2)$$

Where $0 \leq \theta_s \leq \theta_0 \leq 90^\circ$. A transmission line with the characteristic impedance Z_0 and electrical length θ_0 as a unit line section is demonstrated in Figure 3(b, c (i)), and its π -equivalent circuit model is presented in Figure 3(b, c (ii)). Each open stub is then subbed by a plicate open stub with equal characteristic impedance Z_P and total electrical length θ_P (i.e. $\theta_P = \theta_{P'} + \theta_{P''}$) to reduce the size of the circuit as shown in Figure 3(b, c (iii)). In order to achieve more size reduction, one of the folded stubs can be flipped vertically as shown in Figure 3(b, c (iii)). Finally, a compact structure of the transmission line is obtained by using its balanced π -equivalent with quasi L-shaped equivalent stubs and is called L-shaped equivalent as shown in Figure 3(b, c (iv)). The simulation results shows that this structure has acceptable frequency response within the operating bandwidth with attention to size reduction.

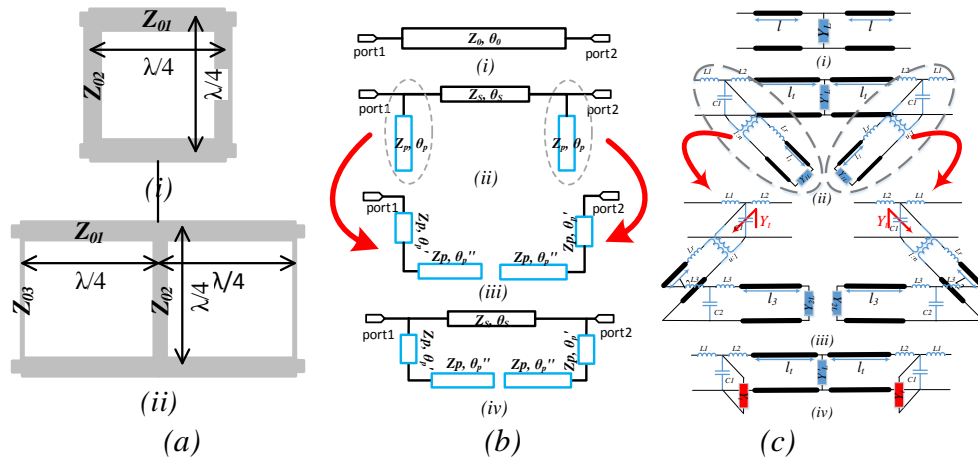


Figure 3: (a (i)) Formal 90° branch-line coupler, (a (ii)) formal double box broadband 90° branch-line coupler. (b, c (i)) A conventional transmission line, (b, c (ii)) π -equivalent transmission line of the conventional type, (b, c (iii)) flipped vertically and folded equivalent structure of the open stub, and (b, c (iv)) L-shaped equivalent structure of the conventional transmission line.

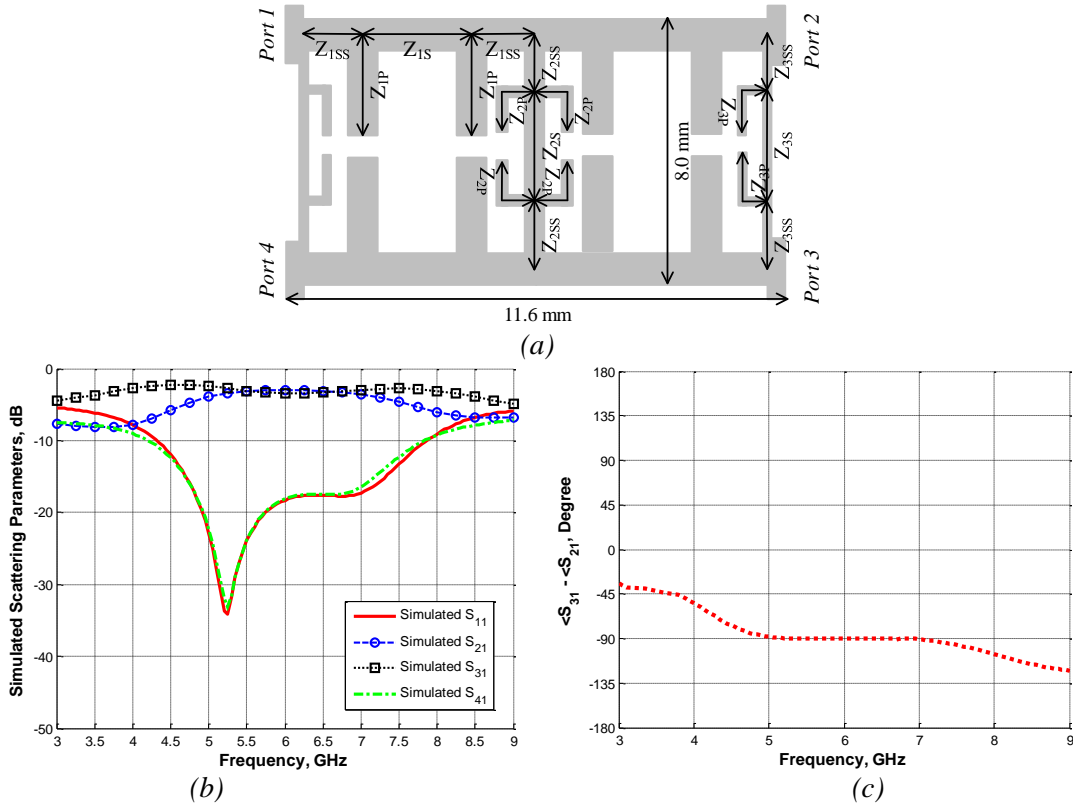


Figure 4: (a) The proposed broadband branch-line coupler with L-shaped equivalent structure of the conventional transmission line. (b) Magnitude of Simulated scattering parameters (c) Phase difference of proposed branch line coupler.

The proposed circuit is represented in Figure 4 and each formal transmission line has been replaced by an L-shaped equivalent structure. Impedance and electrical length of each transmission line lettered in Figure 4(a) are as follows:

$$Z_{1S}=74\Omega, \theta_{1S}=36^\circ, Z_{1P}=70\Omega, \theta_{1P}=57^\circ, Z_{1S}'=74\Omega, \theta_{1S}'=9^\circ, Z_{2S}=102.5\Omega, \theta_{2S}=33^\circ, Z_{2P}=115.5\Omega, \theta_{2P}=32.5^\circ, Z_{2S}'=102.5\Omega, \theta_{2S}'=14.5^\circ, Z_{3S}=137\Omega, \theta_{3S}=32^\circ, Z_{3P}=137\Omega, \theta_{3P}=21^\circ, Z_{3S}'=137\Omega, \theta_{3S}'=14^\circ.$$

The simulation results of the scattering parameters for the proposed branch-line coupler are indicated in Figure 4(b) and phase difference are shown in Figure 4(c). At the designed frequency of 5.5 GHz, the insertion loss is -3.25 ± 0.1 dB, the isolation is about -20 dB, and the phase difference is 89° . In addition, these Figures show that the performance of the proposed coupler has approximately coupling and phase errors within -3.25 ± 0.1 dB and 3° . Return loss and isolation are better than -15 dB over a 44.6% bandwidth (from 4.7 GHz to 7.4 GHz). Table III summarizes the recently published branch-line hybrid couplers with reduced wavelength in transmission line and the results obtained in this work. In addition, it shows significant improvement in

size reduction with wide bandwidth performance. Table III. Comparison of Published Compact Branch-Line Couplers and This Works.

Table III: Comparison of Published Compact Branch-Line Couplers and This Works.

Ref.	Phase Error	Substrate	f_0	BW (GHz)	Size Reduction
[16]	~5	RO4003	0.9	0.3	0.12
[17]	~2	FR4	0.825	0.15	0.26
[18]	~4	FR4	2.3	0.6 (2~2.6)	0.54
[19]	>5	RO4003	2.4	0.4	0.76
[20]	>5	FR4	2.4	0.8 (2~2.8)	0.29
[21]	~5	RO4003	5	2 (4~6)	0.5
This Work	~3	FR4	5.5	2.4 (5~7.4)	~0.3

2.6.7 Butler matrix feed network

In Figure 5 the diagram of the proposed Butler matrix feed network composed of the branch line couplers and delay lines is illustrated. Distance between elements is $0.7\lambda_0$ (fed by fed) and each port of the feeding network is excited through a 50Ω microstrip-feed network. The 4×4 Butler matrix has four input ports and four output ports. By selecting each input (of four ports) as a driving input, the Butler matrix provides four output signals with equal amplitude and phase differences of 45° , 90° , 135° and 180° respectively. As a consequence, four beams with different directions are obtained, one for each input.

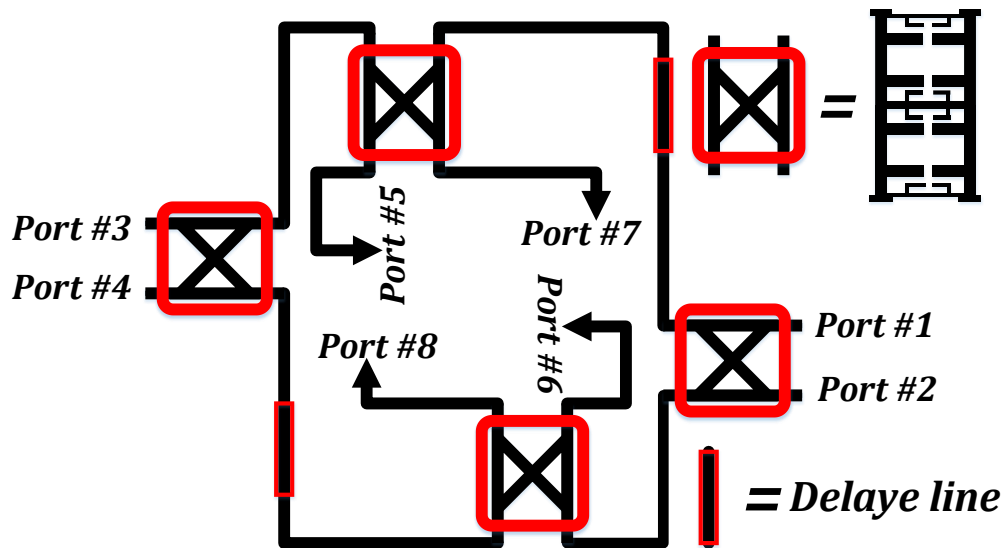


Figure 5: The diagram of the proposed feed network.

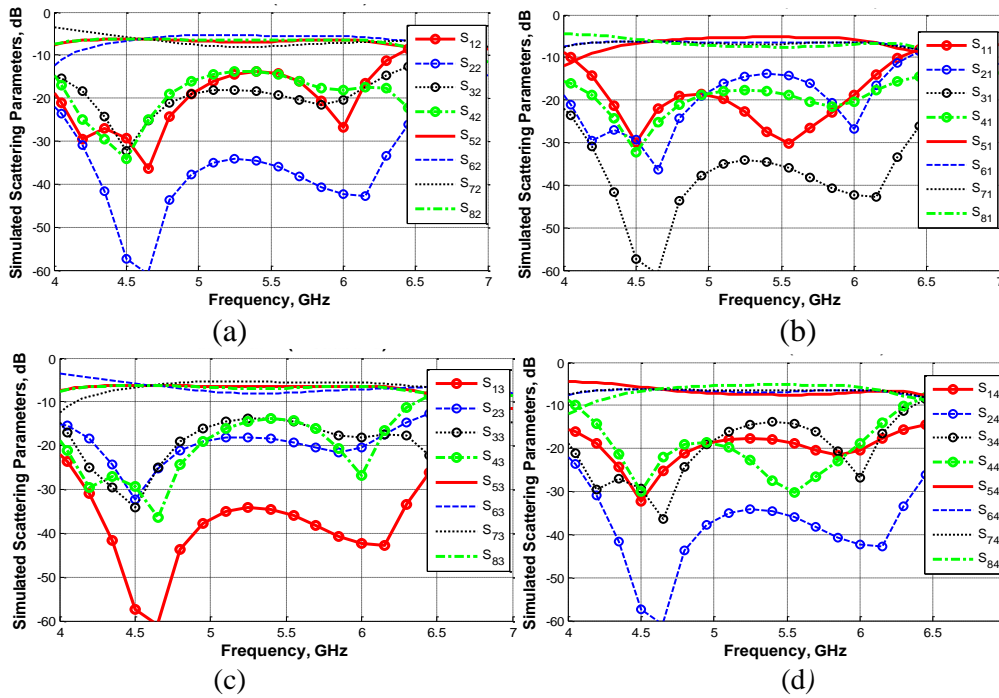


Figure 6: Magnitude results of the simulated scattering parameters of the proposed feed network for four ports. (a) port 1, (b) port 2, (c) port 3 and (d) port 4.

The suggested Butler matrix consists of four wideband branch line coupler so as to procure a wideband beam steering feed network and the tow 45° phase delay line. The 45° phase shifter in the matrix is designed by using a transmission line section, which produces a phase shift of $(2\pi l/\lambda_g)$, where l is the length of the transmission line section, with the use of any crossover on one layer of FR4 substrate. In addition, by rotating the microstrip line (with equal length), the 3dB axial ratio bandwidth of the array, as mentioned in the following section, is improved. The simulated scattering parameter results of the proposed feed network for four ports are demonstrated in Fig 6. These results indicated that the matrix has a good coupling efficiency which is around -7dB. The return loss is better than -14dB and the coupling to the output ports are well equalized. As displayed in Figure 7, the maximum dispersion in the simulated phase difference is less than 6° in the bandwidth.

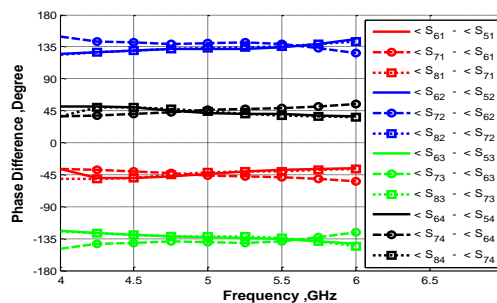


Figure 7: Simulated phase difference for all port.

2.6.8 Result and Discussion

The proposed beam-forming array antenna was fabricated and measured. A photograph of the fabricated beam steering antenna is shown in Fig 8. Return loss was performed by the Agilent8722ES vector network analyzer (VNA). As indicated in Figure9, the measured results for the return loss (Figure 9(b)) are in reasonable agreement with the simulated ones (Figure 9(a)) except for a little frequency shift [3] for most range of the impedance bandwidth. According to the reported results from Figure 9 and the array configuration, it can be concluded that the antenna acts nearly symmetrical. From measured results, a good impedance bandwidth over the frequency range of 4.7–7 GHz can be attained (as shown in Fig 9(b)).

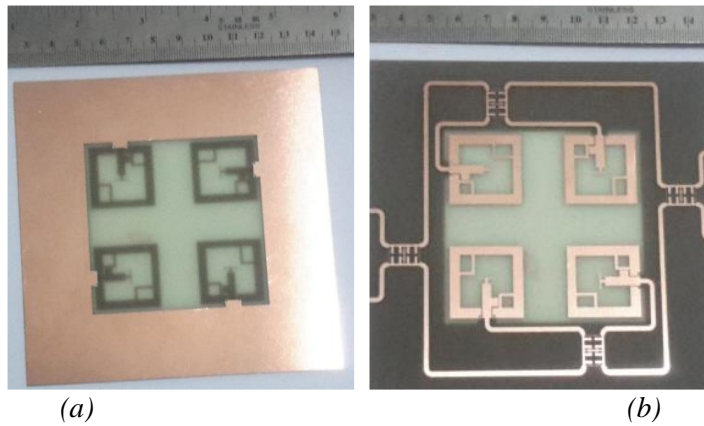


Figure 8: photograph of fabricated antenna, (a) back view, (b) front view

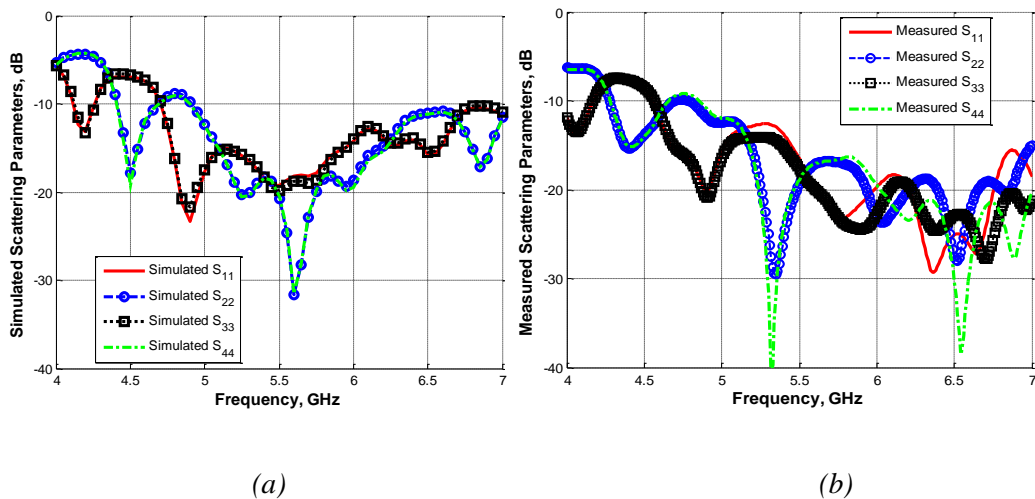


Figure 9: Comparison between simulated (a), and measured (b) result of the return loss.

The feed network composed of 90° branch-line couplers and 45° fixed differential phase shifters generates linear phase gradients ϕ_x , ϕ_y in X-direction and Y-direction at output ports. For a rectangular array of size $M \times N$ in XY-plane, to direct the beam

towards θ_0, φ_0 direction, the progressive phase shifts, between the elements must be equal to [22],

$$\varphi_x = -kd_x \sin(\theta_0) \cos(\varphi_0), \varphi_y = -kd_y \sin(\theta_0) \sin(\varphi_0) \quad (1)$$

$$\varphi_0 = \tan^{-1} \left(\frac{\varphi_y d_x}{\varphi_x d_y} \right), \theta_0 = \sin^{-1} \left(\sqrt{\left(\frac{\varphi_x}{kd_x} \right)^2 + \left(\frac{\varphi_y}{kd_y} \right)^2} \right) \quad (2)$$

Where:

θ_0, φ_0 = main beam scanning angle.

φ_x, φ_y = progressive phase shift in X- and Y- direction.

k = propagation constant in free space

d_x, d_y = distance between two neighboring antenna elements in X- and Y- direction.

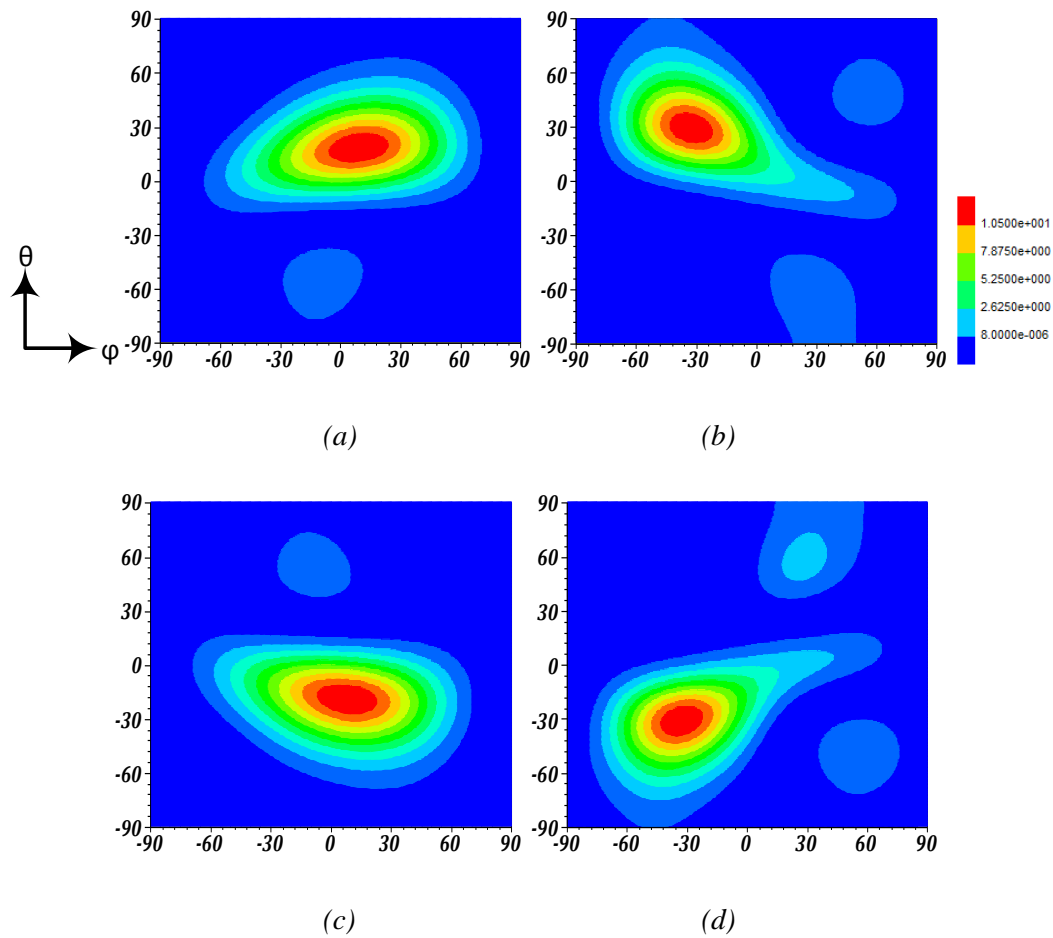


Figure 10: Simulated gain patterns corresponding to ports 1–4 at 5.5GHz. (a) port 1, (b) port 2, (c) port 3 and (d) port 4.

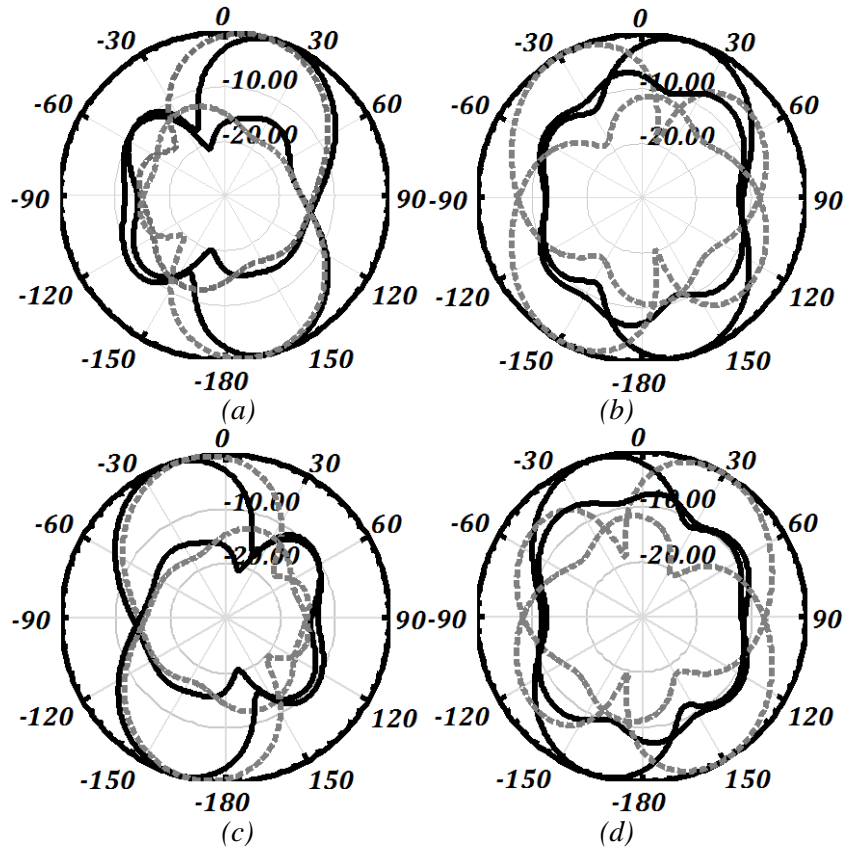


Figure 11: Measured RHCP and LHCP radiation pattern of the planar microstrip antenna array with 4×4 Butler matrix. (a) Port 1, (b) Port 2, (c) Port 3 and (d) Port 4 (Dotted line: $\phi = 90^\circ$, straight line: $\phi = 0^\circ$).

The calculated upper hemisphere gain patterns at 5.5 GHz are presented in Figure 10. The simulations suggest that the array provides four clearly defined beam forming states. The measured radiation pattern of the planar microstrip antenna array with 4×4 Butler matrix is shown in Figure 11. The planar microstrip antenna array that is fed by the 4×4 Butler matrix has four beams at four different directions. These beams have a circular polarization diversity because a beam with RHCP will be obtained when port 1 or port 2 is selected; but if port 3 or port 4 is selected a beam with LHCP will be generated. The measured gains at 5.5 GHz for port 1, port 2, port 3, and port 4 are 9.74 dBic, 8.6 dBic, 9 dBic, and 10.1 dBic, respectively. The whole triangular array grid dimension is optimized to maximize single-element performance in an array radiating environment. Figure 12 displayed the measured AR versus frequency when a different port was fed. When port 1 was fed, the measured results show that a good 3dB AR bandwidth covers 4.55–6.71 GHz. When port 2 was fed, the measured AR bandwidth is from 4.52 to 6.7 GHz.

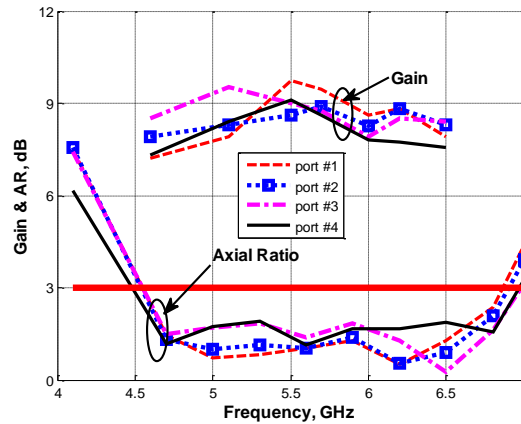


Figure 12: The measured Gain and AR versus frequency for ports 1-4

2.6.9 Conclusion

In this work, a CPW-fed CPSS antenna is designed by combining the antenna elements with the proposed Butler matrix feed network. The single antenna element is optimized for the desired broadband and circular polarization requirements. A novel feed network is design by using phase shifters and branch line couplers which are optimized to achieve a compact size and wide bandwidth performance. The obtained results give us a beam steerable antenna with an acceptable gain in the desired impedance and AR bandwidths. This antenna can be used in many applications such as mobile, Wi-Fi, RFID and WLAN/WiMAX applications.

References

- [1] Ge Tian; Jin-Ping Yang; Wen Wu, "A Novel Compact Butler Matrix Without Phase Shifter," *Microwave and Wireless Components Letters, IEEE* , vol.24, no.5, pp.306,308, May 2014
- [2] Elhefnawy, M.; Ismail, W., "A Microstrip Antenna Array for Indoor Wireless Dynamic Environments," *Antennas and Propagation, IEEE Transactions on* , vol.57, no.12, pp.3998,4002, Dec. 2009
- [3] Changrong Liu; Shaoqiu Xiao; Yong-Xin Guo; Ming-Chun Tang; Yan-Ying Bai; Bing-Zhong Wang, "Circularly Polarized Beam-Steering Antenna Array With Butler Matrix Network," *Antennas and Wireless Propagation Letters, IEEE* , vol.10, no., pp.1278,1281, 2011
- [4] Changrong Liu; Shaoqiu Xiao; Yong-Xin Guo; Yan-Ying Bai; Bing-Zhong Wang, "Broadband Circularly Polarized Beam-Steering Antenna Array," *Antennas and Propagation, IEEE Transactions on* , vol.61, no.3, pp.1475,1479, March 2013
- [5] H. Hayashi, D. A. Hitko, and C. G. Sodini, "Four-element planar butler matrix using half-wavelength open stubs," *IEEE Microw. Wireless Compon. Lett.* vol. 12, no. 3, pp. 73–75, Mar. 2002.
- [6] C. Dall’Omo, T. Monediere, B. Jecko, F. Lamour, I. Wolk, and M. Elkael, "Design and realization of a 4 4 microstrip Butler matrix without any crossing in

- millimeter waves,” *Microw. Opt. Technol. Lett.*, vol. 38, no. 6, pp. 462–465, Sep. 20, 2003.
- [7] Y. J. Cheng, W. Hong, and K. Wu, “Millimeter-wave multibeam antenna based on eight-port hybrid,” *IEEE Microw. Wireless Compon. Lett.* vol. 19, no. 4, pp. 212–214, Apr. 2009.
- [8] S. Zheng, W. S. Chan, S. H. Leung, and Q. Xue, “Broad band butler matrix with flat coupling,” *Electron. Lett.* vol. 43, pp. 576–577, May 2007.
- [9] J.Y. Sze, K.L. Wong, and C.C. Huang, “Coplanar waveguide-fed square slot antenna for broadband circularly polarized radiation,” *IEEE Trans Antennas Propag* 51, 2141–2144. 2003.
- [10] J. Y. Sze and C. C. Chang, “Circularly polarized square slot antenna with a pair of inverted-L grounded strips”, *IEEE Antennas Wireless Propag. Lett.* vol. 7, pp. 149–151, 2008.
- [11] J.-Y Sze, Chung-I. G. Hsu, Z.-W. Chen, and C.-C. Chang, “Broadband CPW-Fed Circularly Polarized Square Slot Antenna With Lightning-Shaped Feed-line and Inverted-L Grounded Strips”, *IEEE Tran. Antennas Propag.* Vol. 58, pp. 973-977, March 2010.
- [12] J.-Y. Sze and Y.-H. Ou, “Compact CPW-fed square aperture CP antenna for GPS and INMARSAT applications,” *Microwave Opt Technol Lett* 49, 427–430. 2007.
- [13] C.C. Chou, K.H. Lin, and H.L. Su, “Broadband circularly polarized cross-patch-loaded square slot antenna,” *Electron Lett* 43, 485–486. 2007.
- [14] V. Rafii, J. Nourinia, C. Ghobadi, J. Pourahmadazar, and B.S. Virdee, “Broadband circularly polarized slot antenna array using sequentially rotated technique for C-band applications,” *Antennas Wireless Propag Lett IEEE* 12, 128–131. 2013.
- [15] S. Karamzadeh, V. Rafii, M. Kartal, O.N. Ucan, and B.S. Virdee, “Circularly polarised array antenna with cascade feed network for broadband application in C-band,” *Electron Lett* 50, 1184–1186. 2014.
- [16] C. H. Tseng, and C. L. Chang, “A Rigorous Design Methodology for Compact Planar Branch-Line and Rat-Race Couplers with Asymmetrical T-Structures,” *IEEE Transactions on Microwave Theory and Techniques*, Vol. 60, No. 7, July 2012.
- [17] K. Y. Tsai, H. S. Yang, J. H. Chen, and Y. J. E. Chen “A Miniaturized 3 dB Branch-Line Hybrid Coupler with Harmonics Suppression,” *IEEE Microwave and Wireless Components Letters*, Vol. 21, No. 10, October 2011.
- [18] C. W. Tang, and M. G. Chen “Synthesizing Microstrip Branch-Line Couplers With Predetermined Compact Size and Bandwidth,” *IEEE Transactions On Microwave Theory And Techniques*, Vol. 55, No. 9, September 2007.
- [19] C. W. Tang, M. G. Chen, and J. W. Wu “Realization of Ultra-Compact Planar Microstrip Branch-Line Couplers with High-Impedance Open Stubs,” *Microwave Symposium, 2007 IEEE*.
- [20] S. S. Liao, and J. T. Peng “Compact Planar Microstrip Branch-Line Couplers Using the Quasi-Lumped Elements Approach With Nonsymmetrical and Symmetrical T-Shaped Structure,” *IEEE Transactions On Microwave Theory And Techniques*, Vol. 54, No. 9, September 2006.
- [21] C. Chen, H. Wu, and W. Wu “Design and Implementation of A Compact Planar 4×4 Microstrip Butler Matrix for Wideband Application,” *Progress in Electromagnetics Research C*, Vol. 24, 43-55, 2011.
- [22] T. Djera fi and K. Wu, “Multilayered substrate integrated waveguide 4×4 butler matrix,” *Int. J RF Microw. Compon. Aid Eng*, vol. 22, pp.336–344, 2012.

2.7 Circularly Polarized 1×4 Square Slot Array Antenna by Utilizing Compacted Modified Butler Matrix and Branch Line Coupler

Source: *International Journal of RF and Microwave Computer-Aided Engineering*, 10. 2015.

2.7.1 Abstract

Circularly polarized (CP), beam steering antennas are preferred to reduce the disruptive effects such as multi-path fading and co-channel interference in wireless communications systems. Nowadays, intensive studies have been carried out not only on the specific antenna array design but also their feeding networks to achieve circular polarization and beam steering characteristics. A compact broadband CP antenna array with a low loss feed network design is aimed in this work. In order to improve impedance and CP bandwidth, a feed network with modified Butler matrix and a compact ultra-wideband square slot antenna element are designed. With this novel design, more than 3 GHz axial ratio BW is achieved. In this study, a broadband meander line compact double box coupler with impedance bandwidth over 4.8-7 GHz frequency and the phase error less than 3° is utilized. Also the measured impedance bandwidth of the proposed beam steering array antenna is 60% (from 4.2 to 7.8 GHz). The minimum 3 dB axial ratio bandwidth between ports, support 4.6-6.8 GHz frequency range. The measured peak gain of the proposed array antenna is 8.9 dBic that could scan solid angle about ~91 degree.

Keywords: Microstrip array, square slot antenna, modified Butler matrix, coplanar waveguide feed, CP.

2.7.2 Introduction

In mobile and satellite communication, some potential problems such as multi-path fading and co-channel interference are the reason of employing circularly polarized (CP) beam steering antennas. Actually, the main beam of the CP multiple beam antenna can be well controlled and directed to the directions subject to less interference [1]. Hitherto, many techniques to provide beamforming network (BFN) such as Blass, Nolen, Butler and other multiple input networks have been reported, but among those feed networks, Butler Matrix feed network stands out with its advantages such as being theoretically lossless, able to be implemented with a minimum number of components

and beyond them, providing the circular polarization in the literature. Many different techniques to attain CP beam steering have been presented so far [1-9]. In [2], a 2×3 CP switched microstrip antenna array was presented. In the feeding network only a single-pole multi-throw microwave PIN switch was used to steer the main beam to different directions. Any directions and any number of steering beams can be realized with this structure. The main disadvantage of the reported feed network in [2] is the employed line length to attain phase delay that causes a reduction in CP bandwidth. A 4×4 Butler matrix with linearly polarized elements was presented in [3]. The impedance bandwidth and 3dB axial ratio (AR) of this antenna are 18.8% and 4.9%, respectively. In [4], a CP switched-beam patch antenna array with Butler matrix was reported.

This array has an impedance and AR bandwidth (ARBW) over a frequency range of 5.75–6.2 GHz and the main beam of the array can be scanned to any directions. A proximity-coupled L-probe feeding wideband CP antenna was exploited for wideband CP beam steering [5]. In the mentioned works [3-5], the use of low bandwidth microwave components such as 90 degree coupler, phase shifter, crossover and single element antenna is led to decrease the impedance and the CP bandwidths. Therefore, to increase the CP beam steering bandwidth, it is preferable to use broadband components in Butler matrix feed networks. A well-known technique to improve Butler matrix feed network bandwidth is to remove the cross over structures from the network. This structure is called the modified Butler matrix [6-9], and is composed of four branch-line couplers and two 45° phase shifters without any crossovers. The purpose of this article is to design a modified broadband CP beam forming array antenna by a novel technique. In order to improve the impedance and CP bandwidth, following innovations have been implemented: (i) to provide broadband feed network, the use of a new modified Butler matrix including broadband double-box slow wave branch line coupler and Schiffman phase shifter helps to demand. (ii) A CP square slot antenna element which has compact size, ultra-wide impedance BW and more than 3GHz, 3dB axial ratio BW is designed and used in the antenna array. Employing coplanar waveguide (CPW) feed line and matching it with microstrip Butler feed network by two metalized via-hole are the other distinction in our design.

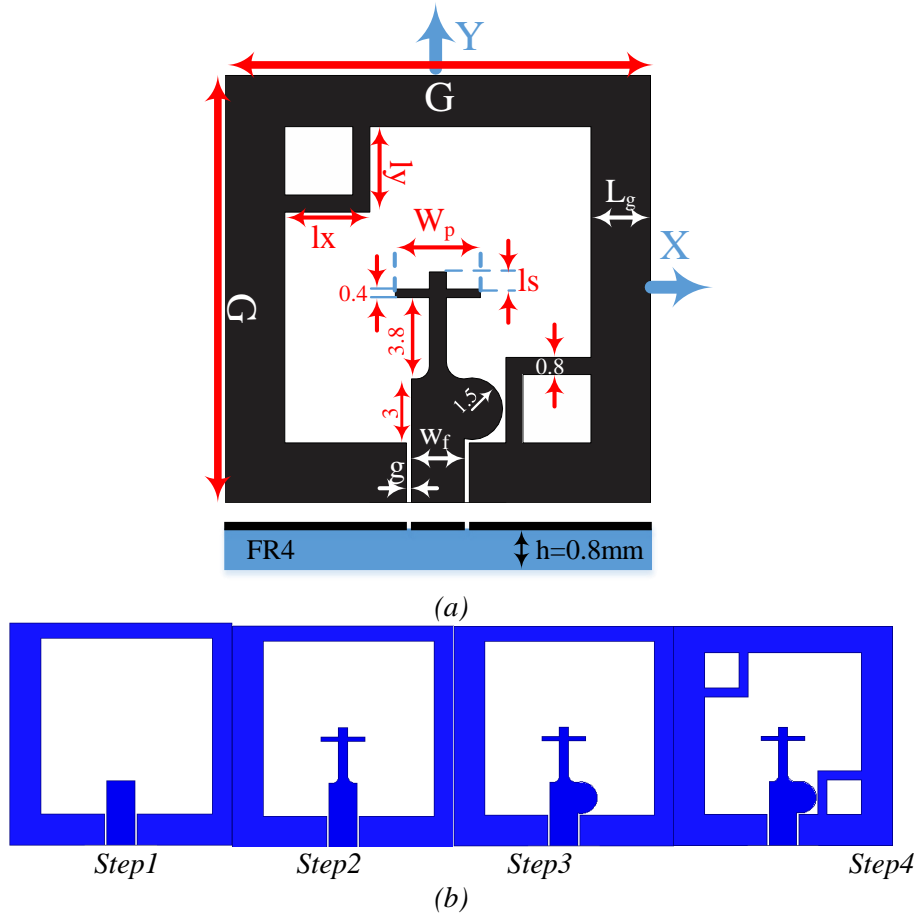


Figure 1: Configuration and design steps of the CPSSA a) Basic structure of proposed antenna, and b) Design steps ($G=20$; $L_g=1.8$; $l_x=4$; $l_y=4$, $L_s=0.8$; $W_p=4$; $g_l=0.6$; $g=0.24$; $W_f=2.48$)(all value in mm).

2.7.3 Single Element

Figure 1 displays the structure and configuration of the proposed miniaturized coplanar waveguide (CPW)-fed CP square slot antenna (CPSSA) designed in this work. The CPSSA consists of two L shape structure around two opposite corner of the ground line that is introduced in [10-11], and a circular shape stub in feeding line. Following the feed line, a cross shape patch is utilized in order to improve the bandwidth. The proposed CPSSA is printed on a FR4 substrate with relative permittivity $\epsilon_r=4.4$, loss tangent $\delta=0.02$ and compact dimension of $20 \times 20 \times 0.8 \text{ mm}^3$. To achieve 50Ω input impedance, the width W_f of the CPW feedline is fixed at 2.48 mm and the feed section is separated from the ground plane by a gap of $g = 0.24\text{mm}$. The CP excitation of the proposed CPSSA is mainly achieved by two inverted-L shape strips located around two opposite corners of the square slot with $l_x \times l_y$ dimensions [10-11]. The configuration of the CPSSA was optimized using Ansoft HFSS commercial software. The stages describing the evolution of the antenna structure are shown in Figure 1b.

A feed line is constructed within the rectangular slot in the first stage; in the second stage, in order to increase radiation resistant a cross-shape patch is embedded following the feed line; the third stage involves the feedline modification by adding a circular stub to ensure impedance matching; in final stage, two L-shape is created in two opposite of ground loop. The return loss response (S_{11}) and the 3-dB axial ratio (AR) bandwidth of the CPSSA in the four stages are displayed in Figure 2.

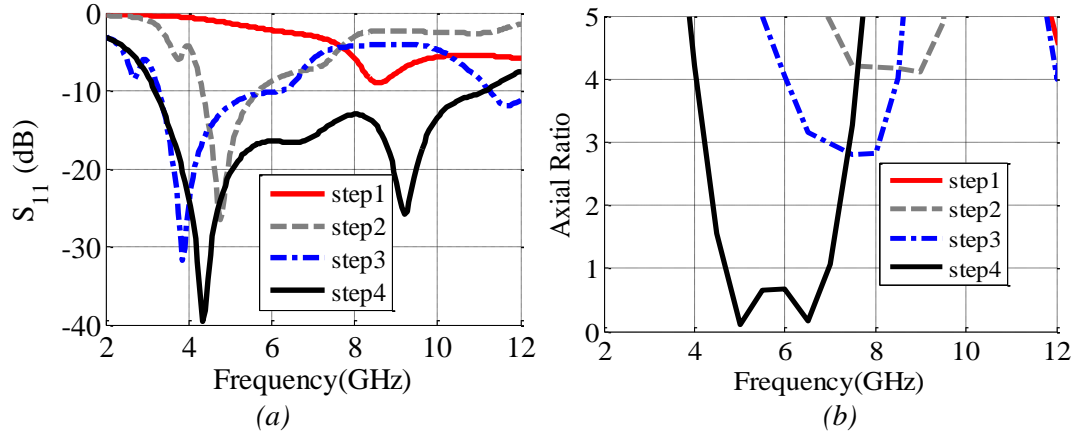


Figure 2: S_{11} and AR of antenna in four implementation steps a) S_{11} response of antenna, and b) AR curves of antenna.

Results show that sequential steps improve the impedance and 3dB AR bandwidths of the antenna. Application of L-shape strip line in the fourth step creates additional surface current paths and prevents of aggregation of current in opposite corner which significantly increase impedance band width (IBW) to 8146 MHz (3097~11243 MHz) for $S_{11} \leq -10$ dB. The addition of ground-plane strip line in the fourth step significantly enhances ARBW between 4208 and 7416 GHz for an $AR \leq 3$ dB.

The simulated results of CPSSA parameters is depicted in Figure 3. Simulated return loss and simulated frequency response of the single element for AR and gain are presented in Figure 3a and Figure 3b, respectively. Simulated LHCP and RHCP radiation patterns of the proposed CPSS antenna for $\varphi = 0^\circ$ and $\varphi = 90^\circ$ is demonstrated in Figure 3c. In Figure 3c, +z and -z directions are RHCP and LHCP, respectively. The proposed CPSSA has an area of 400mm^2 , which is considerably less than the previously published slot antennas as summarized in Table I. Compared to other similar types of CP slot antennas fabricated on the same substrate, the proposed antenna exhibits an impedance bandwidth which is significantly larger and with no reduction in the gain performance, as well as having a larger CP bandwidth. The gain is comparable to previous designs [1].

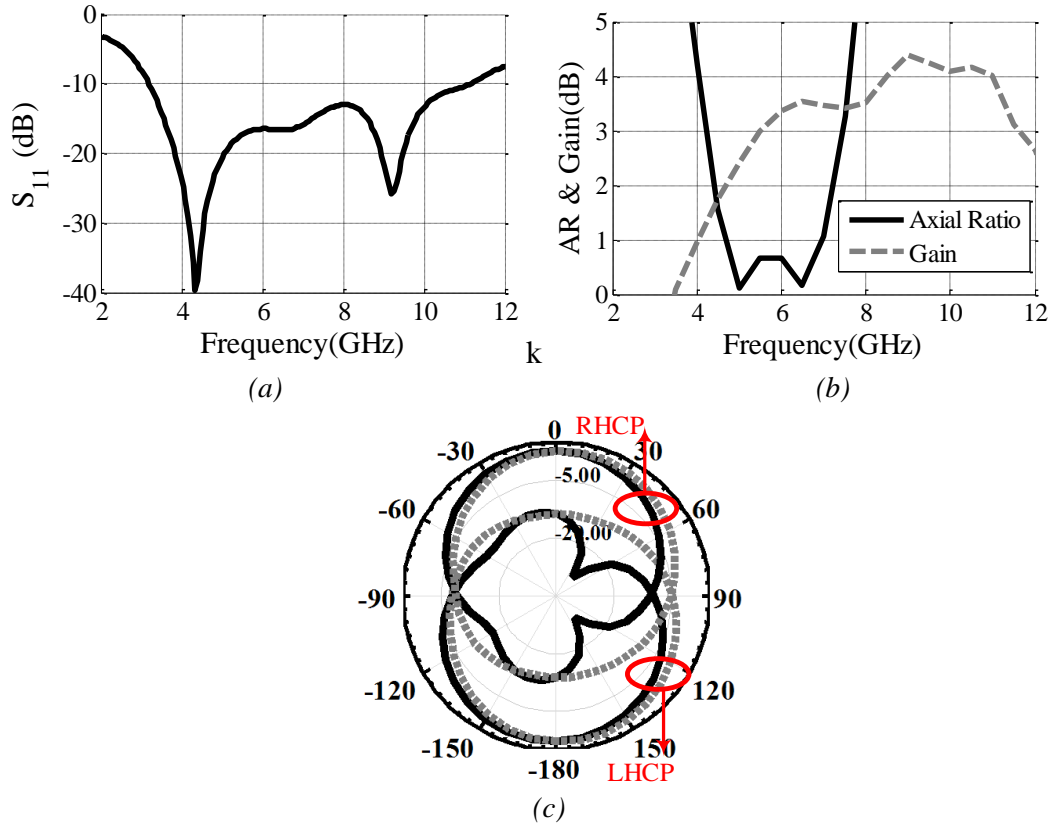


Figure 3: Simulated results of proposed single element antenna (a) return loss (b) Gain and Axial ratio (c) pattern at 5.5 GHz (Dotted line: $\phi = 90^\circ$, straight line: $\phi = 0^\circ$).

Table I: Comparison of the proposed cpssa with other references. the impedance bandwidth is for a frequency range where $vswr \leq 2$; and arbw is 3-dB axial-ratio bandwidth.

Ref.	Size (mm ³)	BW (GHz)	3dB ARBW (GHz)	Peak Gain (dBic)
[10]	70×70×1.60	0.85 (1.75-2.6)	0.4 (1.7-2.1)	3.7
[11]	25×25×0.80	1.9 (4-6.6.5)	0.8 (4.9-5.7)	3.6
[12]	25×25×0.80	7.8 (3.1-10.9)	0.7 (4.5-6.8)	3.3
[13]	60×60×1.6	3.65 (1.6-5.25)	2.45 (2.4-4.85)	3
[14]	30×30×9.5	2.2 (5.16-7.36)	1.4 (5.65-7.05)	7
[1]	25×25×0.80	7.4 (3.1-10.5)	1.7 (4.9-6.6)	4.5
This work	20×20×0.80	8.1 (3.1-11.2)	3.2 (4.2-7.4)	4.3

2.7.4 Branch Line Coupler

Figure 4 depicts the schematic of the proposed slow wave double box branch line coupler. Each section of the structure having different impedance and length consists of a meander line. The length of a unit cell of the meander line is l_i and total transverse width is W_i . The spacing between adjacent lines has the same distance and is equal to S_i . The line width of a meander line is W_{ai} . Thus, $l_i=2\times W_{ai}+2\times S_i$. The characteristic impedances of the meander line of width W_{ai} is Z_{ai} . The meander line is characterized by the characteristic impedance Z_{si} and the propagation constant β_{si} as follows [15-16]:

$$Z_{si} = \sqrt{\frac{L_{ti}}{C_{ti}}} \quad (1) \quad \beta_{si} = \frac{\omega\sqrt{L_{ti}C_{ti}}}{l_i} \quad (2)$$

Where L_{ti} and C_{ti} are the total inductance and capacitance of the unit cell, respectively. Considering the high-impedance meander line in the unit cell (Z_{ai}), as shown in Figure 4(b), the configuration of the meander line can be regarded as the parallel coupled lines where one end is connected, which forms a Schiffman section. For fixed W_{ai} and S_i , the image impedance Z_{li} and phase constant φ_i of a Schiffman section are given by [16].

$$Z_{li} = \sqrt{Z_{0ei}Z_{0oi}} \quad (3) \quad \cos\varphi_i = \frac{\frac{Z_{0ei}-\tan^2\theta_i}{Z_{0oi}}}{\frac{Z_{0ei}+\tan^2\theta_i}{Z_{0oi}}} = \frac{1-\left(\frac{Z_{0ei}\tan^2\theta_i}{Z_{0oi}}\right)}{1+\left(\frac{Z_{0ei}\tan^2\theta_i}{Z_{0oi}}\right)} \quad (4)$$

Where Z_{0ei} and Z_{0oi} are the even- and odd-mode impedances of the parallel coupled lines, respectively. θ_i is the electrical length of the transmission line. In the proposed unit cell, $\theta_i=\beta_{ai}\times W_i$, where β_{ai} is the propagation constant of the microstrip line of width W_{ai} . Since in the real situation $\theta_i\ll 2\pi$ and $\tan^2\theta_i\ll Z_{0ei}/Z_{0oi}$, (Eqn. 4) is further reduced to

$$\cos\varphi_i \approx \left(1 - \left(\frac{Z_{0ei}\tan^2\theta_i}{Z_{0oi}}\right)\right)^2 \approx 1 - \frac{2Z_{0ei}\theta_i^2}{Z_{0oi}} \quad (5)$$

Moreover, on the basis of the Taylor-series expansion of cosine function, (Eqn. 4) can also be written as

$$\cos\varphi_i \approx 1 - \frac{\varphi_i^2}{2} \quad (6)$$

The propagation constant β_{fi} of a Schiffman section is

$$\beta_{fi} = \frac{\varphi_i}{2W_i} \quad (7)$$

Comparing (5) and (6), it is easily seen that φ_i is proportional to θ_i , and consequently from (7), β_{fi} is proportional to θ_i as well as to the frequency. Consequently, the equivalent inductance and the capacitance values of the meander line in the unit cell can be calculated as follows:

$$L_{ai} = Z_{li}\beta_{fi} \times \frac{2W_i}{\omega} + Z_{ai}\beta_{ai} \times \frac{2S_i}{\omega} \quad (8) \quad C_{ai} = \beta_{fi} \times \frac{2W_i}{\omega Z_l} + \beta_{ai} \times \frac{2S_i}{\omega Z_{ai}} \quad (9)$$

The second part of the above two equations corresponds to the three short lines of length S_i in Figure 4(b). Each conventional transmission line has been replaced by a meander line structure [1].

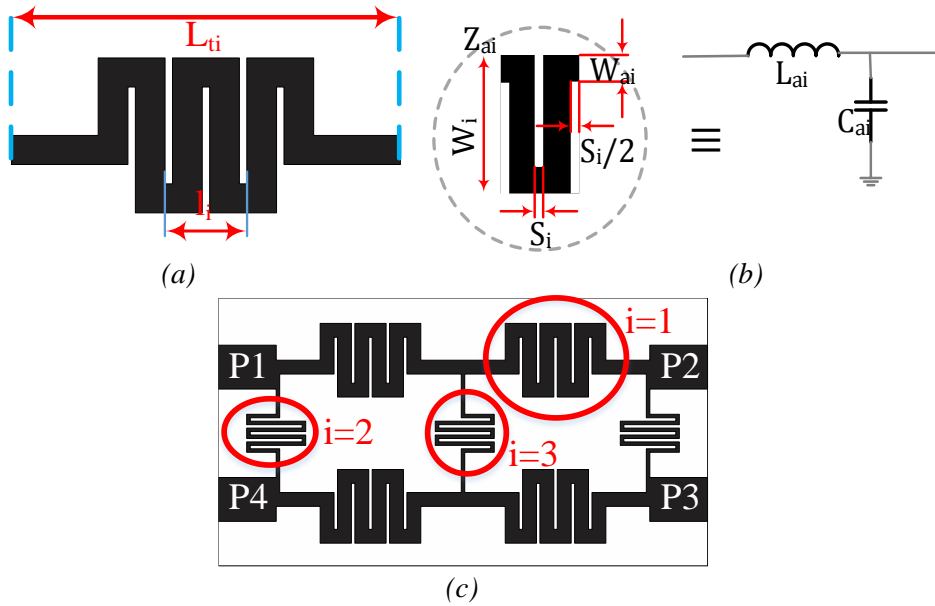


Figure4: a) Meander line structure, b) unit cell and equivalent circuit unit cell, and c) proposed 90° coupler.

The length and the width of each intersection transmission line shown in Figure 4 are listed in Table II. The simulation results of the scattering parameters of the proposed branch line coupler are shown in Figure 5(a) and the phase division is shown in Figure 5(b).

Table II. Length and width of each intersection lettered in figure 4 (mm).

	W_i	l_i	S_i	W_{ai}	L_{ti}
i=1	2.56	1.32	0.12	0.48	6.28
i=2	2.04	0.6	0.12	0.12	4.12
i=3	1.82	0.6	0.12	0.12	4.12

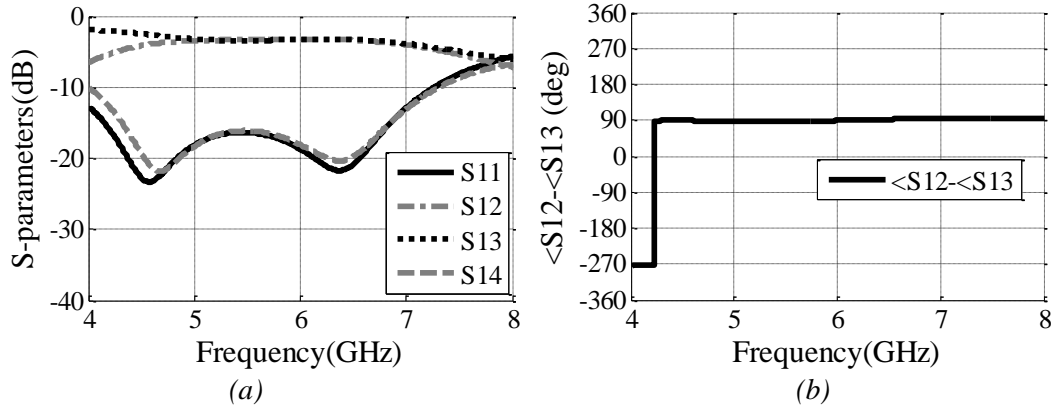


Figure 5: The simulation results of the scattering parameters of the proposed branch line coupler a) magnitude, and b) phase.

Table III: comparison of published compact branch-line couplers and this works.

Ref.	Phase Error (degree)	Substrate	f_0 (GHz)	BW (GHz)	Size Reduction Ratio
[17]	>5	FR4	2.4	0.8 (2~2.8)	0.29
[18]	~ 5	RO4003	5	2 (4~6)	0.5
[1]	~ 3	FR4	5.5	2.4 (5~7.4)	~ 0.3
This Work	~ 3	FR4	5.5	2.2 (4.8~7)	~ 0.64

At the designed frequency, 5.5 GHz, the insertion loss is -3.4 ± 0.1 dB, the isolation is about -15dB, and the phase difference is $90^\circ \pm 3$. Table III, summarizes the recently published branch-line hybrid couplers with reduced wavelength in transmission line and the results obtained in this work. It shows significant improvement in size reduction with wide bandwidth performance.

2.7.5 Butler Matrix Feed Network

The configuration of modified Butler matrix feed network consists of two slow wave double box branch line couplers and two 45 degree Schiffman phase shifters, which are printed on a FR4 substrate with 0.8mm thickness and is presented in Figure 7.

Proposed Butler matrix includes 4 input ports and 4 output ports and the distance between the output feeding lines is $0.46\lambda_{0-5.5\text{GHz}}$ (λ_0 - wavelength in free space).

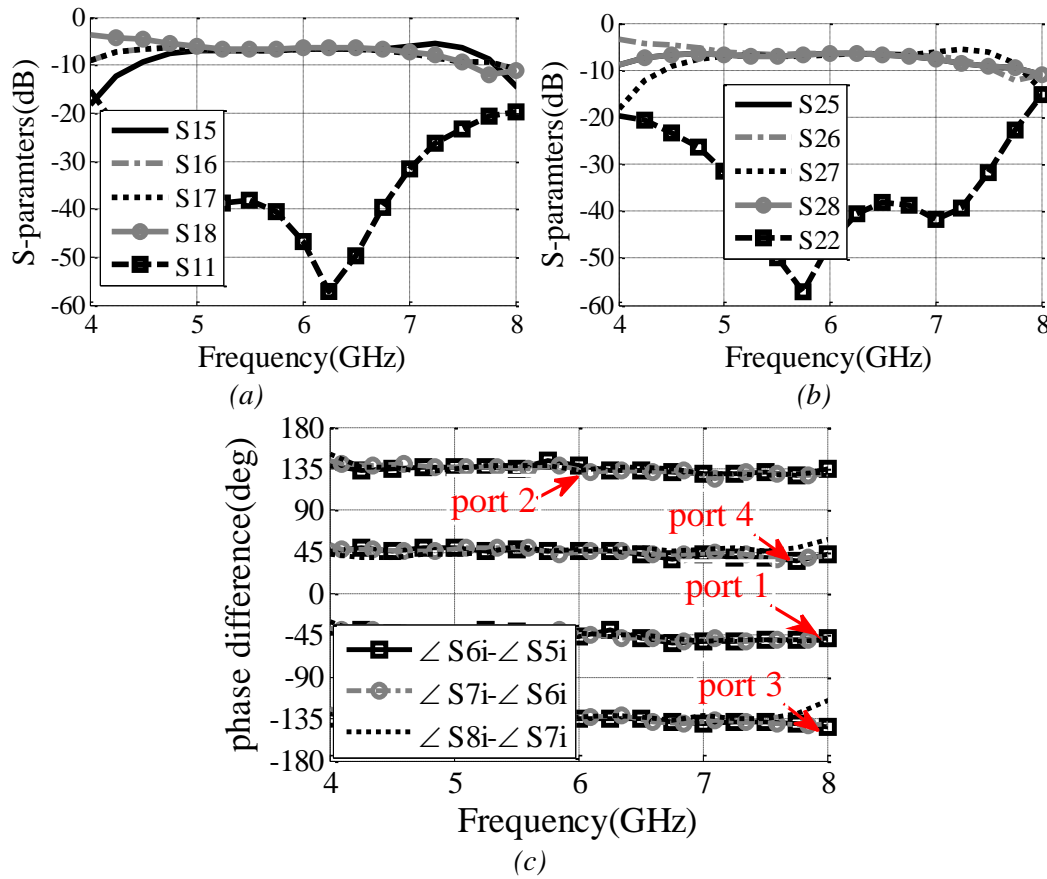


Figure 6: Magnitude results of the simulated scattering parameters of the proposed feed network for four ports. (a) Port 1, (b) Port 2 and, (c) Simulated phase difference for all port (i =input port).

By selecting each input (of four ports) as a driving input, the Butler matrix provides four output signals with equal amplitude and phase differences of 45° , 90° , 135° and 180° , respectively. As a consequence, four beams with different directions are obtained, one for each input. Proposed Butler matrix is simulated and optimized by Agilent advanced design system (ADS). Because the Butler matrix is an asymmetric feed network, therefore, just simulated results of ports 1 and 2 are presented. The simulated Magnitudes for ports 1 and 2, and simulated phase shifts for each ports are illustrated in Figure 6(a) and (b). As shown in Figure 6 (c), the maximum magnitude and phase error for all ports are $\pm 0.35\text{dB}$ and 3° , respectively.

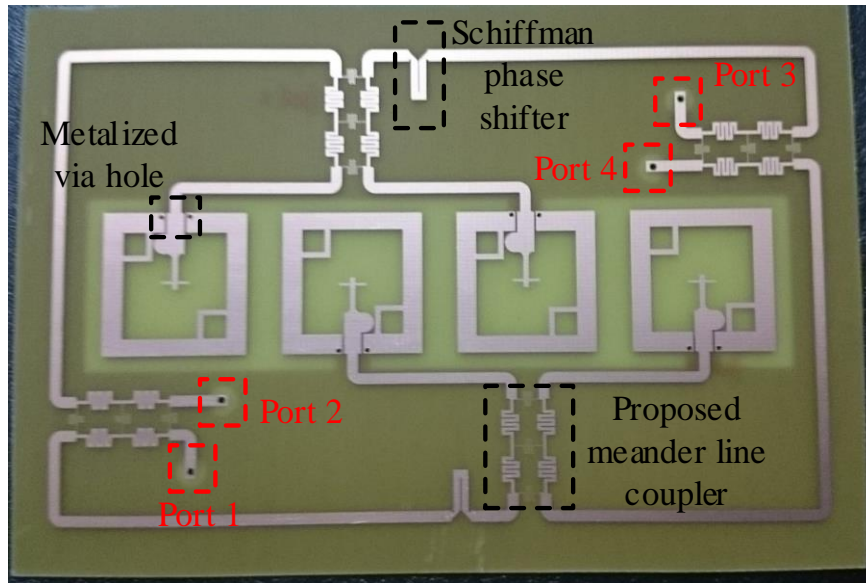


Figure 7: photograph of the fabricated modified 4×4 Butler matrix with CPSS antenna elements

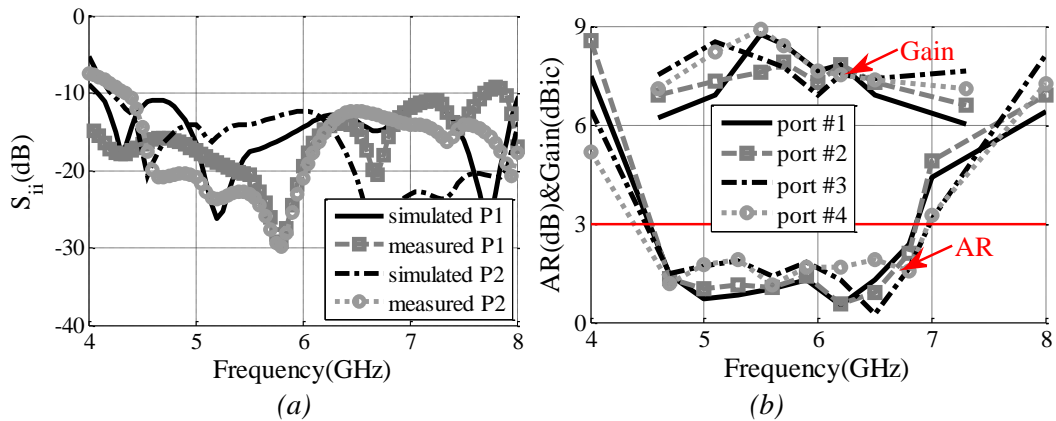


Figure 8: a) Comparison between simulated and measured result of the return loss for ports 1 and 2 ($i=P$ =port number), and b) the measured Gain and AR versus frequency for ports 1 to 4.

2.7.6 Result and Discussion

The designed array antenna elements are fed with the designed Butler feed network and a CP beam forming (CPBF) antenna is created. In the proposed beam steering array antenna structure, ground-loop of CPSSA is connected to ground of microstrip Butler matrix by using two metalized via hole. The Proposed CPBF array antenna was fabricated (Figure 7) and measured. Scattering parameters of CPBF array antenna was measured by Agilent 8722ES vector network analyzer. As seen in Figure 8a, there are a good agreement between the simulated and the measured return loss of the antenna, expect a frequency shifting which is a result of fabrication error.

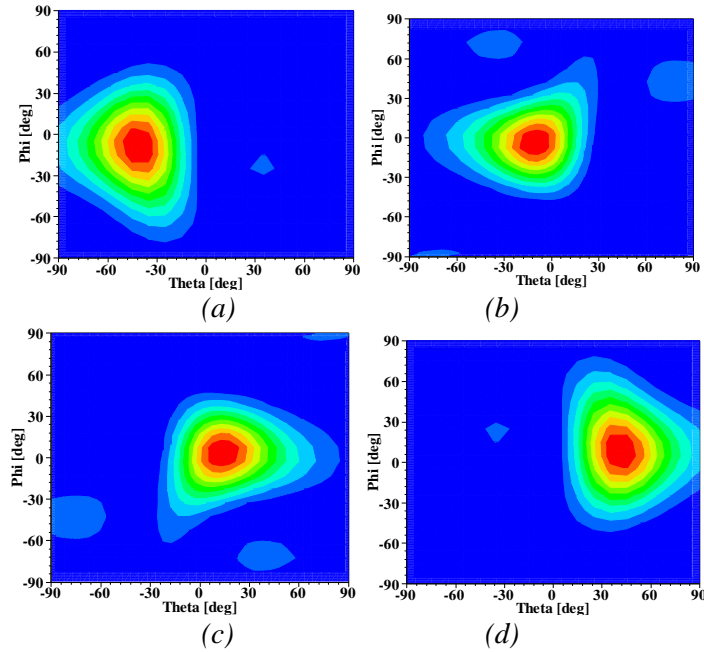


Figure 9: Simulated normalized gain patterns corresponding to ports 1–4 at 5.5GHz. (a) port 1, (b) port 2, (c) port 3 and (d) port 4

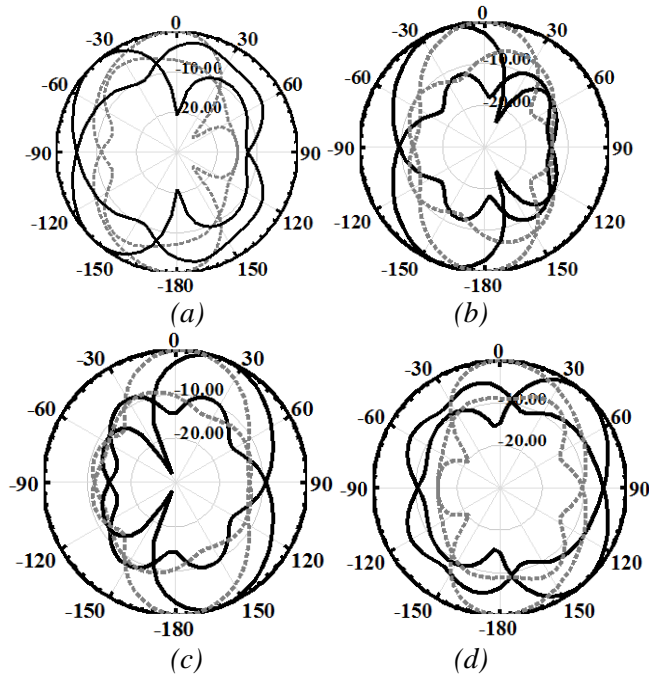


Figure 10: Measured RHCP and LHCP radiation patterns of the planar microstrip antenna array with 4×4 Butler matrix. (a) port 1, (b) port 2, (c) port 3 and (d) port 4 (Dotted line: $\phi = 90^\circ$, straight line: $\phi = 0^\circ$).

From the measured results, a good impedance bandwidth over the frequency range of 4.2–7.8 GHz can be attained. The measured gain and the axial ratio versus frequency are demonstrated in Figure 8b. As seen in Figure 8b, the measured gains at 5.5 GHz for port 1, port 2, port 3, and port 4 are 8.74 dBic, 7.6 dBic, 8 dBic, and 8.9 dBic, respectively. When to employ the antenna element by CPW fed the CPSSA gain, as

presented in Figure 3(b), is less than 4.5 dBi. By combining CPW fed with microstrip feed and matching together by metallic via, the antenna radiation resistance is increasing that is caused to enhance of radiation efficiency and Gain of single element in impedance matched range of frequency. Therefore the antenna array can provided High gain. Same article with this condition is mentioned in [1] and [12]. In addition to, Due to changes in the phase shifting between the elements of the array, the value of angle in array factor from maximum direction in uniform angle is changing which causes to reduce of gain in beam steering antenna. To study more detail of this discussion referred to [19]. The measured AR curves are given for different feeding ports. As displayed in Figure 8b, Minimum 3dB axial ratio bandwidth is covered from 4.6 to 6.8 GHz for the worst case when excited by port 2. The calculated upper hemisphere gain patterns at 5.5 GHz are presented in Figure 9. The simulations suggest that the array provides four clearly defined beam forming states. The measured radiation patterns of 1×4 CPBF array antenna with modified 4×4 Butler matrix are displayed in Figure 10. As shown in Figures 9 and 10, the proposed antenna array has four beams at four different directions. These beams have a circular polarization diversity because a beam with RHCP will be obtained when port 1 or port 3 is selected; but if port 2 or port 4 is selected a beam with LHCP will be generated. Moreover the antenna radiated in $+z$ direction with RHCP there with radiated in $-z$ direction with LHCP. Therefore the antenna diversity in $+z$ and $-z$ direction is different, that is leads to antenna with high value of front to back ratio.

2.7.7 Conclusion

A novel circularly polarized beam steering array antenna design with its compact size, good gain and broadband AR characteristics is achieved in this work. This good performance could be obtained designing both the array antenna element with CP characteristic and the feeding network with the modified Butler matrix. The measured and the simulated results are obtained in a good agreement with the expected performance. A significant improvement in size reduction with a wide bandwidth performance is obtained when comparing the other works in the literature.

References

- [1] Karamzadeh, S.; Rafii, V.; Kartal, M.; Virdee, B.S., "Modified circularly polarised beam steering array antenna by utilised broadband coupler and 4×4 butler

matrix," *Microwaves, Antennas & Propagation, IET* , vol.9, no.9, pp.975,981, 6 18 2015.

[2] Jun Ouyang, "A Circularly Polarized Switched-Beam Antenna Array," *Antennas and Wireless Propagation Letters, IEEE* , vol.10, no., pp.1325,1328, 2011.

[3] Elhefnawy, M.; Ismail, W., "A Microstrip Antenna Array for Indoor Wireless Dynamic Environments," *Antennas and Propagation, IEEE Transactions on* , vol.57, no.12, pp.3998,4002, Dec. 2009.

[4] Changrong Liu; Shaoqiu Xiao; Yong-Xin Guo; Ming-Chun Tang; Yan-Ying Bai; Bing-Zhong Wang, "Circularly Polarized Beam-Steering Antenna Array With Butler Matrix Network," *Antennas and Wireless Propagation Letters, IEEE* , vol.10, no., pp.1278,1281, 2011.

[5] Changrong Liu; Shaoqiu Xiao; Yong-Xin Guo; Yan-Ying Bai; Bing-Zhong Wang, "Broadband Circularly Polarized Beam-Steering Antenna Array," *Antennas and Propagation, IEEE Transactions on* , vol.61, no.3, pp.1475,1479, March 2013

[6] H. Hayashi, D. A. Hitko, and C. G. Sodini, "Four-element planar butler matrix using half-wavelength open stubs," *IEEE Microw. Wireless Compon. Lett.* vol. 12, no. 3, pp. 73–75, Mar. 2002.

[7] C. Dall’Omo, T. Monediere, B. Jecko, F. Lamour, I. Wolk, and M. Elkael, "Design and realization of a 4 4 microstrip Butler matrix without any crossing in millimeter waves," *Microw. Opt. Technol. Lett.* , vol. 38, no. 6, pp. 462–465, Sep. 20, 2003.

[8] Y. J. Cheng, W. Hong, and K. Wu, "Millimeter-wave multibeam antenna based on eight-port hybrid," *IEEE Microw. Wireless Compon. Lett.* vol. 19, no. 4, pp. 212–214, Apr. 2009.

[9] S. Zheng, W. S. Chan, S. H. Leung, and Q. Xue, "Broad band butler matrix with flat coupling," *Electron. Lett.* vol. 43, pp. 576–577, May 2007.

[10] J. Y. Sze and C. C. Chang, "Circularly polarized square slot antenna with a pair of inverted-L grounded strips," *IEEE Antennas Wireless Propag. Lett.* vol. 7, pp. 149–151, 2008.

[11] V. Rafii, J. Nourinia, C. Ghobadi, J. Pourahmadazar, and B.S.Virdee, Broadband circularly polarized slot antenna array using sequentially rotated technique for C-band applications, *Antennas Wireless Propag Lett IEEE* 12 (2013), 128–131.

[12] S. Karamzadeh, V. Rafii, M. Kartal, O.N. Ucan, and B.S. Virdee, Circularly polarised array antenna with cascade feed network for broadband application in C-band, *Electron Lett* 50 (2014), 1184–1186.

[13] Nasimuddin; Zhi Ning Chen; Xianming Qing, "Symmetric-Aperture Antenna for Broadband Circular Polarization," in *Antennas and Propagation, IEEE Transactions on* , vol.59, no.10, pp.3932-3936, Oct. 2011

[14] Agarwal, K.; Nasimuddin; Alphones, A., "Unidirectional wideband circularly polarised aperture antennas backed with artificial magnetic conductor reflectors," in *Microwaves, Antennas & Propagation, IET* , vol.7, no.5, pp.338-346, April 11 2013

[15] R. E. Collin, *Foundations for Microwave Engineering*, 2nd ed. New York: McGraw-Hill, 1992.

[16] B. M. Schiffman, "A new class of broadband microwave 90-degree phase shifters," *IRE Trans. Microwave Theory Tech.*, vol. MTT-6, no. 4, pp. 232–237, Apr. 1958.

[17] S. S. Liao, and J. T. Peng "Compact Planar Microstrip Branch-Line Couplers Using the Quasi-Lumped Elements Approach With Nonsymmetrical and Symmetrical T-Shaped Structure," *IEEE Transactions On Microwave Theory And Techniques*, Vol. 54, No. 9, September 2006.

3. CONCLUSIONS AND RECOMMENDATIONS

Microstrip antennas offer many benefits, including low profile, light weight, and low cost; they are fairly simple to manufacture and easy to integrate with other planar circuits. Unfortunately, microwave antennas are notoriously narrowband in nature, limiting their use for many applications. A number of approaches have been applied to overcome the inherently narrow bandwidths of microstrip antennas.

In recent years, various microstrip antenna arrays have been designed using a sequential rotation technique, with the aim of improving polarization purity, impedance matching, and pattern symmetry across wider bandwidths. These designs include the use of linearly polarized elements, circularly polarized microstrip elements, and feed networks incorporating serial or parallel feeds. Such approaches can improve the circularly polarized bandwidth, but tend not to impact the axial ratio bandwidth.

In this thesis collection of methods that accomplished result of CP antenna, have been reported. In first step by utilizing and designing two elements, have been tried to have an element with wider AR and impedance BW with acceptable gain which is the necessary condition to have an array antenna with good results. In section 2.1, a circularly polarized square slot antenna (CPSSA) fed by coplanar waveguide (CPW) with a crescent shaped patch. All of the important parameters that are determinant in antenna characteristics were depicted one by one while keeping the others fixed. The attributes of the proposed CPSSA include a relatively simple structure, low fabrication cost, and UWB operation across 3-11.1 GHz. The measured results show the impedance bandwidth is 115% for $VSWR < 2$, and axial-ratio < 3 dB is 33.3%. An antenna gain of around 3.5 dBic has been obtained. In section 2.2, A new compact broadband circularly polarized square slot antenna is designed. To improve the impedance and AR bandwidth of the antenna in a compact sized structure, impedance matching section and antenna radiation patch elements are designed and optimized. The most important improvement for the proposed antenna is performed by applying an additional current path that connects the two opposite corners of the ground layer. This technique, by preventing the current accumulation at the corners, gives us a significant enhancement for the impedance and AR bandwidths and thus allows this design to come to a challenging position among the other similar works.

In order to give a comparison between effects of CP and LP elements in results of CP array antenna, an array with sequentially rotated feed network are reported in section 2.3. This design presents circularly polarized sequentially rotated slot antenna array with seven quarter-wavelength transformers. Four quarter wavelength usage for matching impedance between 50Ω in element input impedance and array feed network. In this study by decreasing input impedance, an increase in current transmission, an increase in power, occurred. Antenna array consist of 4 elements (2×2) which each of elements have circular polarization. The measured results show the impedance bandwidth as 1.7 GHz, or 31.77%, from 4.5 to 6.2 GHz. For $VSWR < 2$, and axial-ratio < 3 dB is 4.75 to over 6.22 GHz.

But having a broadband CP element is not sufficient for designing broadband CP array antenna. To improve BW, AR and also gain and pattern in continue, novel feed network is reported, which by possessing broadband characteristics (section 2.4). In this work, a design of a CPSSA array using a two-section cascaded coupler feeding system for generating broadband circular polarization performance has been presented. The feeding network of the array is comprised of a 180-degree ring hybrid coupler connected to two branch-line couplers generating circular polarization. The proposed antenna array architecture presents a number of well-behaved attributes including the flexibility of mixed type of feeding, low parasitic radiation from the feeding network, high polarization purity (35.7% (4.6–6.6 GHz) 3dB axial-ratio bandwidth) and a very high gain (14.8dBic).

In order to design an array antenna by changing polarization diversity, having CP and broadband characteristics, in section 2.5, A novel design in circularly polarized MIMO array antenna has been reported. The antenna element is designed and optimized to satisfy the expectations for bandwidth, pattern and the gain. Then the antenna array is configured with a novel feed network design. The array antenna with the feeding network give us an improved gain and the desired CP diversity property which is very important in some applications mentioned above. Another novelty for the designed array structure is the additional gain improvement obtained by the substrates acting as a reflector for the other array elements.

in section 2.6 and 2.7, two beam steering array antenna by employing modified Butler Matrix feed network are mentioned. In section 2.6, a CPW-fed CPSS antenna is designed by combining the antenna elements with the proposed Butler matrix feed network. The single antenna element is optimized for the desired broadband and circular polarization requirements. A novel feed network is design by using phase shifters and branch line couplers which are optimized to achieve a compact size and wide bandwidth performance. The obtained results give us a beam steerable antenna with an acceptable gain in the desired impedance and AR bandwidths. This antenna can be used in many applications such as mobile, Wi-Fi, RFID and WLAN/WiMAX applications. Finally, in section 2.7, in order to improve impedance and CP bandwidth, a feed network with modified Butler matrix and a compact ultra-wideband square slot antenna element were designed. With this novel design, more than 3 GHz axial ratio BW is achieved. In this study, a broadband meander line compact double box coupler with impedance bandwidth over 4.8-7 GHz frequency and the phase error less than 3° was utilized. Also the measured impedance bandwidth of the proposed beam steering array antenna is 60% (from 4.2 to 7.8 GHz). The minimum 3 dB axial ratio bandwidth between ports, support 4.6-6.8 GHz frequency range. The measured peak gain of the proposed array antenna is 8.9 dBic that could scan solid angle about ~ 91 degree.

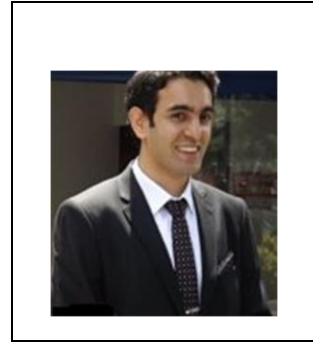
REFERENCES

- [1] **Braasch, M.S., Multipath effects**, in Global Positioning System: Theory and Applications, Edited by Parkinson, B.W. et al., American Institute of Aeronautics and Astronautics (AIAA), 1, pp. 547–568, 1996.
- [2] **Counselman, C.C.**, Multipath rejecting GPS antennas, Proceedings of IEEE, 87(1), pp. 86–91, January 1999.
- [3] **Davies, K.**, Ionospheric Radio Propagation, NBS Monograph 80, 181, US Government Printing Office, Washington, DC, 1965.
- [4] **Brookner, E., W.M. Hall, and R.H. Westlake.** Faraday loss for L-band radar and communications systems. IEEE Transactions on Aerospace and Electronic Systems, 21(4): 459–469, 1985.
- [5] **Pozar, D.M.**, Microwave Engineering, 2nd edn, John Wiley & Sons, Inc., 1997.
- [6] **Nakano, H.** Helical and Spiral Antennas: A Numerical Approach, Research Studies Press Ltd, 1987.
- [7] **Balanis, C.A.** Antenna Theory: Analysis and Design, Hoboken, NJ: John Wiley & Sons, Inc., 2005.
- [8] **Stutzman, W.L. and G.A. Thiele.** Antenna Theory and Design, 2nd edn, New York: John Wiley & Sons, Inc., 1997.
- [9] **Kraus, J.D. and R.J. Marhefka.** Antennas for all Applications, New York: McGraw-Hill, 2002.
- [10] **Toh, B.Y., R. Cahill and V.F. Fusco.** Understanding and measuring circular polarisation, IEEE Trans. Education, 46: 313–318, 2003.
- [11] **Yang, G., M. Ali and R. Dougal.** A wideband circularly polarized microstrip patch antenna for 5–6 GHz wireless LAN applications, Microwave and Optical Technology Letters, 45(4):279–285, 2005.
- [12] **Qing, X.M.** Broadband aperture-coupled circularly polarized microstrip antenna fed by a three-stub hybrid coupler, Microwave and Optical Technology Letters, 40(1):38–41, 2004.
- [13] **Guo, Y.X., K.W. Khoo and L.C. Ong.** Wideband circularly polarized patch antenna using broadband baluns, IEEE Trans. Antennas Propagat., 56(2):319–326, 2008.
- [14] **Qing, X.M. and Y.W.M. Chia.** Broadband circularly polarized slot loop antenna fed by three-stub hybrid coupler, *Electronics Letters*, 35(15):1210–1211, 1999.
- [15] **Tseng, L.Y. and T.Y. Han.** Microstrip-fed circular slot antenna for circular polarization, Microwave and Optical Technology Letters, 50(4):1056–1058, 2008.
- [16] **Sze, J.Y., K.L. Wong and C.C. Huang.** Coplanar waveguide-fed square slot antenna for broadband circularly polarized radiation, IEEE Trans. Antennas Propagat., 51(8):2141–2144, 2003.
- [17] **Deng, I.C., J.B. Chen, Q.X. Ke, J.R. Chang, W.F. Chang and Y.T. King.** A circular CPW-fed slot antenna for broadband circularly polarization

- radiation, *Microwave and Optical Technology Letters*, 49(11):2728–2733, 2007.
- [18] **Xu, R.P., X.D. Huang and C.H. Cheng.** Broadband circularly polarized wide-slot antenna, *Microwave and Optical Technology Letters*, 49(5):1005–1007, 2007.
- [19] **Sze, J.Y. and C.C. Chang** Circularly polarized square slot antenna with a pair of inverted-L grounded strips, *IEEE Antennas Wireless Propagat. Lett.*, 7:149–151, 2008.
- [20] **Sze, J.Y., G.I.G. Hsu, Z.W. Chen and C.C. Chang.** Broadband CPW-fed circularly polarized square slot antenna with lightning-shaped feedline and inverted-L grounded strips, *IEEE Trans. Antennas Propagat.*, 58(3):973–977, 2010.
- [21] **Zhou, S.W., P.H. Li, Y.Wang, W.H. Feng and Z.Q. Liu.** A CPW-fed broadband circularly polarized regular hexagonal slot antenna with L-shape monopole, *IEEE Antennas Wireless Propagat. Lett.*, 10:1182–1185, 2011.
- [22] **Pourahmadazar, J., Ch. Ghobadi, J. Nourinia, N. Felegari and H. Shirzad.** Broadband CPW-fed circularly polarized square slot antenna with inverted-L strips for UWB applications, *IEEE Antennas Wireless Propagat. Lett.*, 10:369–372, 2011.
- [23] **Chen, W.S., C.C. Huang and K.L. Wong.** Microstrip-line-fed printed shorted ring-slot antennas for circular polarization, *Microwave and Optical Technology Letters*, 31(2):137–140, 2001.
- [24] **Wong, K.L., C.C. Huang and W.S. Chen.** Printed ring slot antenna for circular polarization, *IEEE Trans. Antennas Propagat.*, 50(1):75–77, 2002.
- [25] **Jia-Yi Sze; Kin-Lu Wong; Chieh-Chin Huang,** "Coplanar waveguide-fed square slot antenna for broadband circularly polarized radiation," *Antennas and Propagation, IEEE Transactions on*, vol.51, no.8, pp.2141,2144, Aug. 2003 doi: 10.1109/TAP.2003.815421
- [26] **Garg, R., P. Bhartia, I. Bahl, A. Ittipiboon.** *Microstrip Antenna Design Handbook*. Boston, MA: Artech House, 2000.
- [27] **Huang, J.** A technique for an array to generate circular polarization with linearly polarized elements. *Antennas and Propagation, IEEE Transactions on*, 34(9):1113–1124, 1986.
- [28] **Hall, P.S.** Application of sequential feeding to wide bandwidth, circularly polarised microstrip patch arrays. *Microwaves, Antennas and Propagation, IEE Proceedings H*, 136(5):390–398, 1989.
- [29] **Kraft, U.R.** An experimental study on 2 times 2 sequential-rotation arrays with circularly polarized microstrip radiators. *Antennas and Propagation, IEEE Transactions on*, 45(10):1459–1466, 1997.
- [30] **Chung, K.L. and H.K. Kan.** Stacked quasi-elliptical patch array with circular polarisation. *Electronics Letters*, 43(10):555–556, 2007.
- [31] **Balanis, C.A.** *Antenna Theory: Analysis and Design*, 3rd edn. Chichester. John Wiley & Sons, Ltd 2005.
- [32] **Caso, R., A. Buffi, M.R. Pino, P. Nepa, and G. Manara.** A novel dual-feed slot-coupling feeding technique for circularly polarized patch arrays. *Antennas and Wireless Propagation Letters, IEEE*, 9:183–186, 2010.
- [33] **Huang, T.-J. and H.-T. Hsu.** A high-gain circularly-polarized dual-band antenna array for RFID reader applications. In *Electromagnetics; Applications*

- and Student Innovation (iWEM), 2012 IEEE International Workshop on, pp. 1–2, 2012.
- [34] **Chen, Ai., Y. Zhang, Z. Chen; C. Yang.** Development of a Ka-band wideband circularly polarized 64-element microstrip antenna array with double application of the sequential rotation feeding technique. *IEEE Antennas and Wireless Propagation Letters*, 10:1270–1273, 2011.
- [35] **Ouyang, J.** A circularly polarized switched-beam antenna array. *Antennas and Wireless Propagation Letters, IEEE*, 10:1325–1328, 2011.
- [36] **Elhefnawy, M. and W. Ismail.** A microstrip antenna array for indoor wireless dynamic environments. *Antennas and Propagation, IEEE Transactions on*, 57(12):3998–4002, 2009.
- [37] **Tseng, C.-H., C.-J. Chen, and T.-H. Chu.** A low-cost 60-GHz switched-beam patch antenna array with Butler Matrix Network. *Antennas and Wireless Propagation Letters, IEEE*, 7:432–435, 2008.
- [38] **Liu, C., S. Xiao, Y.-X. Guo, M.-C. Tang, Y.-Y. Bai, and B.-Z. Wang.** Circularly polarized beam-steering antenna array with Butler Matrix network. *Antennas and Wireless Propagation Letters, IEEE*, 10:1278–1281, 2011.

CURRICULUM VITAE



Name Surname: Saeid Karamzadeh

Place and Date of Birth: IRAN 29.06.1986

Address: ISTANBUL

E-Mail: karamzadeh@itu.edu.tr

B.Sc.: Telecommunication Engineering

M.Sc.: Satellite Communication and Remote Sensing

PUBLICATIONS/PRESENTATIONS ON THE THESIS

- **Saeid Karamzadeh**, Mesut Kartal: Circularly polarized 1×4 square slot array antenna by utilizing compacted modified butler matrix and branch line coupler. *International Journal of RF and Microwave Computer-Aided Engineering* 10/2015; DOI:10.1002/mmce.20947.
- **Saeid Karamzadeh**, Mesut Kartal: Circularly polarised MIMO tapered slot antenna array for C-band application. *Electronics Letters* 08/2015; 51(18). DOI:10.1049/el.2015.1784.
- **Saeid Karamzadeh**, Vahid Rafii, Mesut Kartal, Bal S. Virdee: Modified circularly polarised beam steering array antenna by utilised broadband coupler and 4×4 butler matrix. *IET Microwaves Antennas & Propagation* 04/2015; 9(9). DOI:10.1049/iet-map.2014.0768.
- **Saeid Karamzadeh**, Vahid Rafiei, M. Kartal, M. Dibayi: Circularly Polarized Square Slot Antenna Using Crooked T-Shape Technique. *Applied Computational Electromagnetics Society Journal* 03/2015.
- **Saeid Karamzadeh**, Bal. S. Virdee, Vahid Rafii, Mesut Kartal: Circularly polarized slot antenna array with sequentially rotated feed network for broadband application: CP Slot Antenna Array. *International Journal of RF and Microwave Computer-Aided Engineering* 05/2015; 25(4):358-363. DOI:10.1002/mmce.20869.
- **Saeid Karamzadeh**, Vahid Rafii, Mesut Kartal, Hasan Saygin: Compact UWB CP Square Slot Antenna with Two Corner Connected by a Strip Line. *Electronics Letters*, August 2015 doi: 10.1049/el.2015.2817.

- **S. Karamzadeh**, V. Rafii, M. Kartal, Bal S. Virdee, O. N. Ucan,,: Circularly polarised array antenna with cascade feed network for broadband application in C-band. *Electronics Letters* 08/2014; 50(17):1184-1186. DOI:10.1049/el.2014.1147.